UNIVERSIDAD DE CONCEPCION
ESCUELA DE GRADUADOS
CONCEPCION-CHILE

ANALISIS DE ERROR A-PRIORI Y A-POSTERIORI DE ALGUNOS METODOS DE ELEMENTOS FINITOS MIXTOS ESTABILIZADOS

Tesis para optar al grado de Doctor
en Ciencias Aplicadas con mención en Ingeniería Matemática

Tomás Patricio Barrios Faúndez

FACULTAD DE CIENCIAS FISICAS Y MATEMATICAS
DEPARTAMENTO DE INGENIERIA MATEMATICA
2006

ANALISIS DE ERROR A-PRIORI Y A-POSTERIORI DE ALGUNOS METODOS DE ELEMENTOS FINITOS MIXTOS ESTABILIZADOS

Tomás Patricio Barrios Faúndez

Director de Tesis: Gabriel N. Gatica y Freddy Paiva.

Director de Programa: Mauricio Sepúlveda.

COMISION EVALUADORA

Mark Ainsworth, The University of Strathclyde in Glasgow, Scotland.
Peter Hansbo, Chalmers University of Technology, Sweden.
Salim Meddahi, Universidad de Oviedo, España.

COMISION EXAMINADORA

Firma: _____
Mario Durán
Pontificia Universidad Católica de Chile.

Firma: _____
Gabriel N. Gatica
Universidad de Concepción, Chile.

Firma: _____
Freddy Paiva
Universidad de Concepción, Chile.

Firma: _____
Rodolfo Rodríguez
Universidad de Concepción, Chile.

Fecha Examen de Grado: _____

Calificación: _____

Concepción–Marzo 2006

AGRADECIMIENTOS

Quiero expresar mi más sincero agradecimiento a mis profesores Dr. Gabriel Gatica y Dr. Freddy Paiva. Sin lugar a dudas, toda la motivación, paciencia y constante apoyo, que han empleado antes y durante el desarrollo de esta tesis, han sido cruciales para llegar a buen término. Además de la matemática, he aprendido bastante de ustedes. Más que profesores los considero unos buenos amigos.

A la Comisión Nacional de Investigación Científica y Tecnológica (CONICYT) y la Escuela de Graduados de la Universidad de Concepción por financiar parte de esta tesis a través de sus sistemas de becas. Al programa MECESUP, que a través del proyecto UCO9907, financió mi estadía en la Technische Universität Chemnitz, Chemnitz, Alemania. A la Universidad Católica de la Santísima Concepción, de la cual formo parte del plantel docente, por todo el tiempo invertido.

A todos mis compañeros que he conocido en la Cabina 6, ha sido un placer formar parte de ese grupo. Especialmente a mis amigos Mario Mellado, Erwin Hernández, Mauricio Barrientos, Rommel Bustinza, Luis Gatica y Edwin Behrens.

A los profesores Dr. Norbert Heuer y Dr. Rodolfo Rodríguez, con quienes, en distinta etapa de mi formación, he tenido la suerte de compartir trabajo.

No puedo dejar de agradecer a los compañeros de batalla, a los más antiguos Gabriel Barrenechea, César Flores y Carlos Pérez, y a la más reciente Anahí Gajardo. Siempre ha sido grato conversar con ustedes.

Por mostrarme el camino cuando dudé en continuar en la ciencia, muchas gracias Claudia. A Galina y Teresita, al final lo consiguieron, he terminado. A la Dra. Alice Kozakevicius, ni te imaginas lo oportuno e importante que resultó todo tu apoyo, Dale Chile!!!.

Por hacerme más grato el diario vivir, muchas gracias a todo el personal administrativo de la Facultad de Ciencias Físicas y Matemáticas, en particular a los del departamento de Ingeniería Matemática, María Estrella, Cecilia, Anita, María Eugenia, Teresita y especialmente a mi amigo René Quintrel.

Finalmente, un especial agradecimiento y un fuerte abrazo a mis Padres y hermanos por todo el cariño, comprensión y sobre todo la paciencia que me han entregado.

A mis Padres y Hermanos
Por su incondicional apoyo.
A Fernando y Claudia,
Aunque no se lo esperan,
Esto es gracias a ustedes.

Resumen

En esta tesis desarrollamos el análisis de error a-priori y a-posteriori de algunos métodos de elementos finitos mixtos estabilizados. Para tal efecto consideramos los siguientes problemas modelos:

- Un problema de Poisson con condiciones de contorno mixtas.
- Un problema de Poisson con condiciones de tipo Neumann.
- Un problema de elasticidad lineal con condiciones de tipo Dirichlet.

Para el primer problema presentamos una nueva formulación mixta aumentada con multiplicador de Lagrange que nos permite analizar su resolución numérica. Específicamente, el esquema aumentado se deduce introduciendo términos residuales de mínimos cuadrados provenientes de la ecuaciones constitutiva y de equilibrio. Utilizamos la teoría clásica de Babuška-Brezzi para demostrar que la formulación mixta dual resultante y su esquema de Galerkin correspondiente son problemas bien planteados, y proporcionamos las razones de convergencia optimales. Luego, desarrollamos el análisis de error a-posteriori de dos estimadores diferentes, uno de tipo residual, que resulta ser confiable y eficiente, y otro estimador basado en la proyección de Ritz del error, que resulta ser confiable y cuasi-eficiente. Finalmente, incluimos resultados numéricos que avalan la eficiencia de ambos esquemas adaptivos.

Para el segundo problema presentamos el análisis de error a-priori y a-posteriori de un nuevo esquema estabilizado, el cual introduce la traza de la solución en la frontera como un multiplicador de Lagrange. Esto nos sugiere enriquecer la formulación con un término residual medido en la norma del espacio de Sobolev de orden 1/2. Utilizamos bases de ondelettes para construir una forma bilineal, equivalente al producto escalar respectivo, que

permite controlar este término estabilizador. Probamos que tanto la formulación variacional como el esquema de Galerkin asociado son problemas bien propuestos, y deducimos las razones de convergencia optimales correspondientes. Además, presentamos el análisis de un estimador de error a-posteriori que resulta ser confiable y cuasi-eficiente.

Finalmente, para el problema de elasticidad consideramos una nueva formulación aumentada que se origina al incluir términos de mínimos cuadrados provenientes de las ecuaciones constitutiva y de equilibrio, y de la relación que define la rotación en términos de los desplazamientos. Para esta formulación desarrollamos un estimador de error de tipo residual confiable y eficiente. Presentamos resultados numéricos que confirman las propiedades teóricas del estimador y la versatilidad del esquema adaptivo.

Contents

Chapter 1

Introducción

1.1 Motivación y discusión bibliográfica

En diversas áreas de la Física y la Ingeniería se encuentran modelos dados en términos de ecuaciones diferenciales parciales. Para resolver estos problemas, el Método de Elementos Finitos (MEF) ha demostrado ser una herramienta muy eficaz. En algunos casos, tales como el problema de Poisson con condiciones de Dirichlet homogénea, la formulación variacional asociada al MEF conduce a una forma bilineal simétrica y coerciva. Como consecuencia inmediata se tiene que la existencia y unicidad de la solución del problema variacional puede establecerse utilizando el Lema de *Lax-Milgram*. No menos importante es que, en dicho caso, cualquier discretización conforme de elementos finitos conduce a sistemas de ecuaciones simétricos y definidos positivos, propiedades favorables al momento de escoger algoritmos veloces para su resolución (ver, por ejemplo, [14, 15, 26, 31, 46]).

Los MEF que utilizan espacios diferentes para aproximar variables diferentes, reciben el nombre de Métodos de Elementos Finitos Mixtos. Generalmente, las nuevas variables que se introducen en la formulación están motivadas por algún interés físico. Este es el caso de las ecuaciones de la elasticidad, donde el tensor de esfuerzos puede introducirse como una nueva incógnita para ser aproximada simultáneamente con el vector de desplazamientos. La introducción de nuevas incógnitas transforma un problema de valores de frontera elíptico en un sistema de ecuaciones diferenciales, en cuyo caso las formulaciones variacionales asociadas corresponden generalmente a problemas de punto de silla. Esto genera una serie de dificultades tanto a nivel teórico como práctico, ya que los espacios

usados para la aproximación de diferentes incógnitas no pueden escogerse de manera independiente, y deben satisfacer la condición de *Ladyzhenskaya-Babuška-Brezzi* (LBB) o *inf-sup* (ver, por ejemplo, [3, 16]). Además, una vez satisfecha la condición *inf-sup* discreta, los sistemas de ecuaciones que se obtienen suelen ser indefinidos (ver, por ejemplo, [17, 26, 31, 39, 47]). Como resultado de ello, las formulaciones de elementos finitos mixtos que evitan este tipo de condiciones de estabilidad, han sido motivo de gran interés en las últimas décadas. Estos enfoques pueden clasificarse en dos grandes categorías principales: técnicas de estabilización para Métodos Mixtos y la aplicación de principios de Mínimos Cuadrados (ver, entre otras, [13, 18, 19, 30, 31, 32, 33, 41, 42, 44]).

Por otra parte, como consecuencia de la necesidad natural de optimizar recursos y mejorar la precisión de la solución obtenida, surgen las técnicas de adaptación de mallas. Al respecto, la aplicación de algoritmos adaptivos, basados en estimadores de error *a-posteriori*, garantizan un buen comportamiento de la solución numérica por elementos finitos de problemas de valores de contorno, sean estos lineales o no lineales (ver, por ejemplo, [1, 2, 8, 38, 50]). En general, encontramos dos tipos de estimaciones de error: estimaciones de error *a-priori* y *a-posteriori*. Las estimaciones *a-priori* se basan en el conocimiento previo de la regularidad de la solución, y entregan la velocidad de convergencia del método, es decir, cuán rápido el error tiende a cero a medida que se refina la malla. Sin embargo, estas estimaciones no dan información cuantitativa del error real para una malla fija. Esta última información es posible de obtener con el uso de los estimadores de error *a-posteriori*, a través de la información obtenida en el proceso de cálculo de la solución aproximada. Para ejemplificar lo anterior, consideremos un problema elíptico bidimensional, en un dominio con una triangulación asociada con cierto parámetro h. Si llamamos u a la solución real de nuestro problema y u_h la solución numérica calculada, las estimaciones *a-priori* tienen la forma

$$\|u - u_h\| \leq Ch^{\beta}\,,$$

donde $\|\cdot\|$ denota la norma en la cual queremos medir nuestro error, β es el orden de convergencia y C es una constante que depende de la regularidad de la solución.

Es un hecho que la calidad de la aproximación puede deteriorarse ante la aparición de singularidades locales de la solución real. Una alternativa para resolver dicha dificultad, consiste en refinar más la malla. El problema radica en que la subdivisión simultánea de todos los elementos conlleva un costo computacional demasiado elevado. Por lo tanto,

necesitamos construir mallas que tengan en cuenta la localidad de la singularidad, esto es, algoritmos que refinen principalmente en esos lugares. Este proceso se conoce como Método de Refinamiento Adaptivo o simplemente adaptividad. Por tal motivo, los estimadores de error *a-posteriori* se calculan localmente a partir de los datos del problema. Esto es, si denotamos por $\mathcal{T}_h$ la triangulación del dominio, y por T a cada elemento de $\mathcal{T}_h$, un estimador de error *a-posteriori* tiene la forma

$$\eta = \left\{ \sum_{T \in \mathcal{T}_h} \eta_T^2 \right\}^{1/2},$$

donde η_T^2 representa una estimación del error en T que se cálcula usando la solución aproximada y los datos del problema. Para que un estimador η pueda considerarse una medida adecuada del error, es deseable que existan constantes C_1, $C_2 > 0$, independientes de h, tales que

$$C_1 \eta \leq \|u - u_h\| \leq C_2 \eta \,. \tag{1.1}$$

El hecho de obtener una cota superior de la norma del error global que involucre a η (lado derecho de (1.1)), refleja que se dispone de una medida *confiable* del error cometido. Es más, sólo ésta es necesaria para asegurar que la aproximación numérica ha alcanzado alguna tolerancia prescrita. Si además se puede obtener una cota inferior de la norma del error global que involucre a η (lado izquierdo de (1.1)), entonces se dice que el estimador es *eficiente*. Esto se debe a que en las demostraciones de esta desigualdad suele probarse que η_T está localmente acotado por $\|u - u_h\|_{\Delta(T)}$, donde $\Delta(T)$ es un conjunto de elementos de la triangulación $\mathcal{T}_h$ que incluyen a T, y $\|\cdot\|_{\Delta(T)}$ denota la norma de la función restringida al conjunto $\Delta(T)$. Por ende, estas técnicas de estimaciones de error a-posteriori pueden detectar eficientemente las singularidades.

1.2 Resultados obtenidos y organización de la tesis

Esta tesis se divide en tres capítulos. En el primer capítulo presentamos un nuevo método mixto estabilizado para la resolución numérica de ecuaciones diferenciales parciales con condiciones de contorno mixtas. En el segundo capítulo análizamos una estabilización, basada en bases de ondelettes, del Método de Elementos Finitos Mixto con multiplicadores de Lagrange. Por último, en el tercer capítulo realizamos el análisis de

error a-posteriori de la formulación mixta aumentada introducida en [36] para el problema de elasticidad lineal.

Para dar una presentación más detallada de los resultados obtenidos, a continuación damos una breve descripción del Método de Elementos Finitos Mixtos con multiplicadores de Lagrange. Consideramos el problema de Poisson con condiciones mixtas en la frontera. Sea Ω un dominio acotado simplemente conexo en $\mathbb{R}^2$ con frontera poligonal Γ, tal que todos sus ángulos interiores están en $(0, 2\pi)$. Denotamos por Γ_D y Γ_N a subconjuntos disjuntos de Γ tales que $|\Gamma_D|$, $|\Gamma_N| \neq 0$ y $\Gamma = \overline{\Gamma}_D \cup \overline{\Gamma}_N$. Entonces, dados $f \in L^2(\Omega)$ y $g \in H^{-1/2}(\Gamma_N)$, el problema consiste en: Hallar $u \in H^1(\Omega)$ tal que

$$-\Delta u = f \quad \text{en } \Omega, \quad u = 0 \quad \text{en } \Gamma_D, \quad \frac{\partial u}{\partial \boldsymbol{\nu}} = g \quad \text{en } \Gamma_N \,,$$

donde $\boldsymbol{\nu}$ es el vector normal unitario exterior a Γ. Recordamos que el espacio de Sobolev $H^{-1/2}(\Gamma_N)$ denota el dual de $H^{1/2}_{00}(\Gamma_N)$, donde

$$H^{1/2}_{00}(\Gamma_N) := \{v|_{\Gamma_N} : v \in H^1(\Omega) \ \text{ con } \ v = 0 \ \text{ en } \ \Gamma_D\} \,.$$

La paridad dual correspondiente con respecto al producto interior de $L^2(\Gamma_N)$ se denota por $\langle \cdot, \cdot \rangle_{\Gamma_N}$.

Puesto que estamos interesados en utilizar Métodos Mixtos, primero definimos la incógnita adicional $\boldsymbol{\sigma} := \nabla u$ en Ω. Multiplicamos esta relación por una función test $\boldsymbol{\tau}$, e integramos por partes usando el hecho que $u = 0$ en Γ_D. Enseguida imponemos débilmente la condición de Neumann, lo cual hace necesaria la introducción del multiplicador de Lagrange $\xi := -u|_{\Gamma_N} \in H^{1/2}_{00}(\Gamma_N)$. De esta forma, vemos que la formulación variacional mixta consiste en: Hallar $(\boldsymbol{\sigma}, (u, \xi)) \in H \times Q$ tal que

$$\begin{aligned} A(\boldsymbol{\sigma}, \boldsymbol{\tau}) \ + \ B(\boldsymbol{\tau}, (u, \xi)) \ &= \ 0 \,, \\ B(\boldsymbol{\sigma}, (v, \lambda)) \ &= \ - \int_\Omega f\, v \ + \ \langle\, g, v \,\rangle_{\Gamma_N} \,, \end{aligned}$$

para todo $(\boldsymbol{\tau}, (v, \lambda)) \in H \times Q$, donde $H := H(\mathrm{div}\,, \Omega)$, $Q := L^2(\Omega) \times H^{1/2}_{00}(\Gamma_N)$, y las formas bilineales $A : H \times H \to \mathbb{R}$ y $B : H \times Q \to \mathbb{R}$ están definidas por

$$A(\boldsymbol{\zeta}, \boldsymbol{\tau}) := \int_\Omega \boldsymbol{\zeta} \cdot \boldsymbol{\tau} \qquad \forall\, \boldsymbol{\zeta}\,,\ \boldsymbol{\tau} \in H \,,$$

$$B(\boldsymbol{\tau}, (v, \lambda)) := \int_\Omega v\ \mathrm{div}\,(\boldsymbol{\tau}) \ + \ \langle\, \boldsymbol{\tau} \cdot \boldsymbol{\nu}, \lambda \,\rangle_{\Gamma_N} \quad \forall\, \boldsymbol{\tau} \in H \,, \ \ \forall\, (v, \lambda) \in Q \,.$$

Existencia y unicidad del problema anterior, además del análisis del esquema de Galerkin correspondiente, fueron establecidas en [5].

Aplicaciones de este método a la resolución de diferentes problemas de valores de contorno han sido realizadas satisfactoriamente en diferentes direcciones. Por ejemplo, podemos mencionar problemas elípticos no lineales con condiciones de contorno mixtas (ver [8]), problemas de transmisión (ver [20]), y problemas de elasticidad no lineal (ver [37]).

Inspirados en éste método, en el Capítulo 2 presentamos una formulación aumentada que se obtiene al incluir términos residuales de Mínimos Cuadrados provenientes de las ecuaciones constitutiva y de equilibrio. Usamos la teoría clásica de Babuška-Brezzi para demostrar que tanto la formulación mixta dual resultante, como su esquema de Galerkin asociado, son problemas bien planteados. Derivamos la estimación de error a-priori y su orden de convergencia correspondiente. Además, desarrollamos dos análisis diferentes de error a-posteriori, uno basado en estimadores de error de tipo residual y otro basado en la proyección de Ritz de error. Los resultados de este capítulo forman parte del artículo [7]:

- T.P. Barrios, G.N. Gatica: *An augmented mixed finite element method with Lagrange multipliers: a-priori and a-posteriori error analyses*. Journal of Computational and Applied Mathematics, to appear.

En el Capítulo 3 analizamos una estabilización, basada en términos de mínimos cuadrados y bases de ondelettes, para formulaciones mixtas de problemas elípticos con condiciones de Neumann en la frontera. En general, un análisis de multiresolución consiste de una familia de subespacios de dimensión finita S_j tales que

$$S_0 \subset \ldots \subset S_j \subset S_{j+1} \subset \ldots ,$$

donde $\cup_{j\geq 0} S_j$ es densa en $L^2(\Gamma)$. Cada espacio S_j está definido por dilatación y traslación de una función escala φ, es decir, $S_j = \mathrm{span}\{\varphi_k^j : k \in \Delta_j\}$ donde $\varphi_k^j(x) := \varphi(2^j x - k)$ y Δ_j denota un conjunto de índices con cardinalidad 2^j. La función de escala puede ser, por ejemplo, la función constante a trozos o la función lineal a trozos. Las funciones de ondelettes $\Psi^j = \{\psi_k^j : k \in \nabla_j = \Delta_{j+1} \setminus \Delta_j\}$ son las funciones base del complemento $W_j = \mathrm{span}\{\psi_k^j : k \in \nabla_j\}$ de S_j en S_{j+1}, es decir,

$$S_{j+1} = S_j \oplus W_j \,, \qquad S_j \cap W_j = 0 \,.$$

Denotando por $\psi_k^{-1} := \varphi_k^0$, $\nabla_{-1} := \Delta_0$ y por Ψ_j al vector columna cuyas entradas vienen dadas por $(\psi_k^l)_{k\in\nabla_l, -1\le l<j}$, se encuentra que Ψ_j constituye la base del espacio S_{j+1}, la cual se construye de tal manera que sea una base uniformemente estable en S_{j+1} y una base de Riesz en $L^2(\mathbb{R})$. Una condición suficiente para tener una base uniformemente estable es el disponer de una base bi-ortogonal, o dual, $\tilde{\Psi} = \{\tilde{\psi}_k^l : k \in \nabla_l, l \ge -1\}$ que genere espacios $\tilde{S}_0 \subset \ldots \subset \tilde{S}_j \subset \ldots$, tales que $\langle \tilde{\psi}_k^j, \psi_l^i \rangle_{L^2(\Gamma)} = \delta_{k,l}\delta_{i,j}$. En este caso, todo $v \in L^2(\Gamma)$ puede representarse como

$$v = \sum_{j\ge -1} \sum_{k\in\nabla_j} \langle \tilde{\psi}_k^j, v\rangle_{L^2(\Gamma)}\, \psi_k^j \;=\; \sum_{j\ge -1} \sum_{k\in\nabla_j} \langle v, \psi_k^j\rangle_{L^2(\Gamma)}\, \tilde{\psi}_k^j \,.$$

Entonces, los proyectores Q_j y Q_j^* sobre los espacios de ondelettes W_j y $\tilde{W}_j$, respectivamente, están dados por

$$Q_j\, v \;=\; \sum_{l\in\nabla_j} \langle v, \tilde{\psi}_l^j\rangle_{L^2(\Gamma)}\, \psi_l^j \,, \qquad Q_j^*\, v \;=\; \sum_{l\in\nabla_j} \langle v, \psi_l^j\rangle_{L^2(\Gamma)}\, \tilde{\psi}_l^j \,.$$

Definiendo $\gamma := \sup\{s \in \mathbb{R} : S_j \subset H^s(\Gamma)\}$ y análogamente $\tilde{\gamma}$, se tienen las siguientes equivalencias de normas para todo $v \in H^s(\Gamma)$:

$$c_1 \|v\|^2_{H^s(\Gamma)} \;\le\; \sum_{j\ge -1} 2^{-2ls} \sum_{l\in\nabla_j} |\langle v, \tilde{\psi}_l^j\rangle_{L^2(\Gamma)}|^2 \;\le\; c_2 \|v\|^2_{H^s(\Gamma)} \,,$$

$$c_1 \|v\|^2_{H^{-s}(\Gamma)} \;\le\; \sum_{j\ge -1} 2^{2ls} \sum_{l\in\nabla_j} |\langle v, \psi_l^j\rangle_{L^2(\Gamma)}|^2 \;\le\; c_2 \|v\|^2_{H^{-s}(\Gamma)} \,,$$

donde $-\tilde{\gamma} < s < \gamma$. Es importante aquí observar que las ondelettes se construyen de manera tal que ellas sean locales en sus correspondientes escalas (ver [22, 29]). Una descripción más detallada del uso de ondelettes en Análisis Numérico puede hallarse en [12, 22, 28, 43, 45].

El esquema de resolución de nuestro problema introduce la traza de la solución en la frontera Neumann como un multiplicador de Lagrange, lo cual sugiere enriquecer la formulación variacional con el término residual correspondiente medido en la norma del espacio de Sobolev de orden 1/2. Para este efecto, seguimos parcialmente [12] y utilizamos la propiedad de equivalencia de normas, descrita anteriormente, para construir una forma bilineal que permite aproximar dicha norma. El procedimiento de estabilización se completa con términos residuales de Mínimos Cuadrados provenientes de la ecuación constitutiva y de equilibrio. Mostramos que la formulación variacional resultante y su

esquema de Galerkin correspondiente están bien planteados. Además, desarrollamos un estimador de error a-posteriori de tipo residual confiable y cuasi-eficiente. Los resultados obtenidos se encuentran detallados en el Capítulo 3 y son parte de los trabajos [9, 10]:

- T.P. Barrios, G.N. Gatica and F. Paiva: *A wavelet-based stabilization of the mixed finite element method with Lagrange multipliers*. Applied Mathematics Letters, vol. 19, 3, pp. 244-250, (2006).

- T.P. Barrios, G.N. Gatica and F. Paiva: *A-priori and a-posteriori error analysis of a wavelet-based stabilization for the mixed finite element*. Preprint 2006-02, Departamento de Ingeniería Matemática, Universidad de Concepción, (2006).

Finalmente, en el Capítulo 4 consideramos el problema de elasticidad lineal con condiciones de tipo Dirichlet en la frontera. Para la resolución utilizamos la formulación aumentada estudiada recientemente en [36]. Esta formulación aumentada se obtiene al introducir términos de mínimos cuadrados provenientes de la ecuación constitutiva, de equilibrio, y de la relación que define la rotación en términos de los desplazamientos. Para ejemplificar lo anterior describimos la obtención de la formulación variacional presentada en [36]. Para ello sea Ω un dominio acotado y simplemente conexo en $\mathbb{R}^2$ con frontera Lipschitz continua Γ. Dada la fuerza volumétrica $\mathbf{f} \in [L^2(\Omega)]^2$, buscamos el tensor de esfuerzos $\boldsymbol{\sigma}$ y el vector de desplazamientos $\mathbf{u}$ tal que

$$\boldsymbol{\sigma} = \mathcal{C}\,\mathbf{e}(\mathbf{u})\,, \quad \mathbf{div}\,(\boldsymbol{\sigma}) = -\,\mathbf{f} \qquad \text{en} \quad \Omega\,, \quad \text{y} \quad \mathbf{u} = \mathbf{0} \qquad \text{en} \quad \Gamma\,, \tag{1.2}$$

donde $\mathbf{e}(\mathbf{u}) := \frac{1}{2}\,(\nabla \mathbf{u} + (\nabla \mathbf{u})^{\mathtt{t}})$ denota al tensor de deformaciones y $\mathcal{C}$ es el tensor de elasticidad determinado por la ley de Hooke, es decir,

$$\mathcal{C}\,\boldsymbol{\zeta} \;:=\; \lambda\,\mathrm{tr}(\boldsymbol{\zeta})\,\mathbf{I} \;+\; 2\,\mu\,\boldsymbol{\zeta} \qquad \forall\,\boldsymbol{\zeta} \,\in\, [L^2(\Omega)]^{2\times 2}\,,$$

donde λ, $\mu > 0$ denotan las constantes de Lamé correspondientes. El tensor de elasticidad inverso $\mathcal{C}^{-1}$ viene dado por

$$\mathcal{C}^{-1}\,\boldsymbol{\zeta} \,:=\, \frac{1}{2\,\mu}\,\boldsymbol{\zeta} \,-\, \frac{\lambda}{4\,\mu\,(\lambda+\mu)}\,\mathrm{tr}(\boldsymbol{\zeta})\,\mathbf{I} \qquad \forall\,\boldsymbol{\zeta} \,\in\, [L^2(\Omega)]^{2\times 2}\,.$$

Imponemos débilmente la simetría de $\boldsymbol{\sigma}$ a través de la rotación $\boldsymbol{\gamma} := \frac{1}{2}\,(\nabla \mathbf{u} - (\nabla \mathbf{u})^{\mathtt{t}})$, multiplicamos por funciones test convenientes e integramos la ecuación de equilibrio y

la relación $\nabla \mathbf{u} - \boldsymbol{\gamma} = \mathbf{e}(\mathbf{u}) = \mathcal{C}^{-1}\boldsymbol{\sigma}$, para obtener la siguiente formulación variacional asociada a (1.2): Hallar $(\boldsymbol{\sigma}, (\mathbf{u}, \boldsymbol{\gamma})) \in H \times Q$ tal que

$$\begin{array}{rcl} a(\boldsymbol{\sigma}, \boldsymbol{\tau}) \ + \ b(\boldsymbol{\tau}, (\mathbf{u}, \boldsymbol{\gamma})) & = & 0 \quad \forall\, \boldsymbol{\tau} \in H\,, \\ b(\boldsymbol{\sigma}, (\mathbf{v}, \boldsymbol{\eta})) & = & -\displaystyle\int_\Omega \mathbf{f} \cdot \mathbf{v} \quad \forall\, (\mathbf{v}, \boldsymbol{\eta}) \in Q\,, \end{array} \tag{1.3}$$

donde $H = H(\mathbf{div}\,;\Omega) := \{\boldsymbol{\tau} \in [L^2(\Omega)]^{2\times 2} : \quad \mathbf{div}\,(\boldsymbol{\tau}) \in [L^2(\Omega)]^2\}$, $Q := [L^2(\Omega)]^2 \times [L^2(\Omega)]^{2\times 2}_{\mathtt{skew}}$, con $[L^2(\Omega)]^{2\times 2}_{\mathtt{skew}} := \{\boldsymbol{\eta} \in [L^2(\Omega)]^{2\times 2} : \boldsymbol{\eta} + \boldsymbol{\eta}^{\mathtt{t}} = \mathbf{0}\}$, y las formas bilineales $a : H \times H \to \mathbb{R}$ y $b : H \times Q \to \mathbb{R}$ están definidas por

$$a(\boldsymbol{\zeta}, \boldsymbol{\tau}) := \int_\Omega \mathcal{C}^{-1}\,\boldsymbol{\zeta} : \boldsymbol{\tau} \,=\, \frac{1}{2\mu}\int_\Omega \boldsymbol{\zeta} : \boldsymbol{\tau} - \frac{\lambda}{4\mu(\lambda+\mu)}\int_\Omega \mathrm{tr}(\boldsymbol{\zeta})\,\mathrm{tr}(\boldsymbol{\tau})\,, \tag{1.4}$$

y

$$b(\boldsymbol{\tau}, (\mathbf{v}, \boldsymbol{\eta})) := \int_\Omega \mathbf{v} \cdot \mathbf{div}\,(\boldsymbol{\tau}) \,+\, \int_\Omega \boldsymbol{\eta} : \boldsymbol{\tau}\,, \tag{1.5}$$

para todo $\boldsymbol{\zeta},\ \boldsymbol{\tau} \in H$ y para todo $(\mathbf{v}, \boldsymbol{\eta}) \in Q$. Notamos de (1.4) y (1.5) que para todo $(\boldsymbol{\tau}, (\mathbf{v}, \boldsymbol{\eta}), c) \in [L^2(\Omega)]^{2\times 2} \times Q \times \mathbb{R}$ tenemos

$$a(c\,\mathbf{I}, \boldsymbol{\tau}) \,=\, \frac{c}{2(\lambda+\mu)}\int_\Omega \mathrm{tr}(\boldsymbol{\tau}) \quad \text{y} \quad b(c\,\mathbf{I}, (\mathbf{v}, \boldsymbol{\eta})) \,=\, 0\,. \tag{1.6}$$

Por otra parte, definimos $H_0 := \{\boldsymbol{\tau} \in H : \int_\Omega \mathrm{tr}(\boldsymbol{\tau}) = 0\}$ y vemos que $H = H_0 \oplus \mathbb{R}\,\mathbf{I}$, es decir, para todo $\boldsymbol{\tau} \in H$ existe un único $\boldsymbol{\tau}_0 \in H_0$ y $d := \frac{1}{2|\Omega|}\int_\Omega \mathrm{tr}(\boldsymbol{\tau}) \in \mathbb{R}$ tal que $\boldsymbol{\tau} = \boldsymbol{\tau}_0 + d\,\mathbf{I}$. Usamos esta descomposición y las identidades dadas en (1.6) para ver que (1.3) es equivalente a: Hallar $(\boldsymbol{\sigma}, (\mathbf{u}, \boldsymbol{\gamma})) \in H_0 \times Q$ tal que

$$\begin{array}{rcl} a(\boldsymbol{\sigma}, \boldsymbol{\tau}) \ + \ b(\boldsymbol{\tau}, (\mathbf{u}, \boldsymbol{\gamma})) & = & 0 \qquad \forall\, \boldsymbol{\tau} \in H_0\,, \\ b(\boldsymbol{\sigma}, (\mathbf{v}, \boldsymbol{\eta})) & = & -\displaystyle\int_\Omega \mathbf{f} \cdot \mathbf{v} \qquad \forall\, (\mathbf{v}, \boldsymbol{\eta}) \in Q\,. \end{array} \tag{1.7}$$

Luego, en (1.7) restamos la segunda ecuación a la primera y al resultado le sumamos los términos de mínimos cuadrados dados por

$$\kappa_1 \int_\Omega (\mathbf{e}(\mathbf{u}) - \mathcal{C}^{-1}\,\boldsymbol{\sigma}) : (\mathbf{e}(\mathbf{v}) + \mathcal{C}^{-1}\,\boldsymbol{\tau}) \,=\, 0\,,$$

$$\kappa_2 \int_\Omega \mathbf{div}\,(\boldsymbol{\sigma}) \cdot \mathbf{div}\,(\boldsymbol{\tau}) \,=\, -\,\kappa_2 \int_\Omega \mathbf{f} \cdot \mathbf{div}\,(\boldsymbol{\tau})\,,$$

y

$$\kappa_3 \int_\Omega \left(\boldsymbol{\gamma} - \frac{1}{2}(\nabla \mathbf{u} - (\nabla \mathbf{u})^{\mathtt{t}})\right) : \left(\boldsymbol{\eta} + \frac{1}{2}(\nabla \mathbf{v} - (\nabla \mathbf{v})^{\mathtt{t}})\right) \,=\, 0\,,$$

para todo $(\boldsymbol{\tau}, \mathbf{v}, \boldsymbol{\eta}) \in H_0 \times [H_0^1(\Omega)]^2 \times [L^2(\Omega)]^{2\times 2}_{\mathtt{skew}}$, donde $(\kappa_1, \kappa_2, \kappa_3)$ es un vector de parámetros positivos independientes de λ. De esta forma obtenemos la siguiente formulación variacional aumentada: Hallar $(\boldsymbol{\sigma}, \mathbf{u}, \boldsymbol{\gamma}) \in \mathbf{H}_0 := H_0 \times [H_0^1(\Omega)]^2 \times [L^2(\Omega)]^{2\times 2}_{\mathtt{skew}}$ tal que

$$A((\boldsymbol{\sigma}, \mathbf{u}, \boldsymbol{\gamma}), (\boldsymbol{\tau}, \mathbf{v}, \boldsymbol{\eta})) \;=\; F(\boldsymbol{\tau}, \mathbf{v}, \boldsymbol{\eta}) \qquad \forall\, (\boldsymbol{\tau}, \mathbf{v}, \boldsymbol{\eta}) \in \mathbf{H}_0\,, \tag{1.8}$$

donde la forma bilineal $A : \mathbf{H}_0 \times \mathbf{H}_0 \to \mathbb{R}$ y el funcional $F : \mathbf{H}_0 \to \mathbb{R}$ están definidos por

$$\begin{aligned} A((\boldsymbol{\sigma}, \mathbf{u}, \boldsymbol{\gamma}), (\boldsymbol{\tau}, \mathbf{v}, \boldsymbol{\eta})) := \int_\Omega \mathcal{C}^{-1}\boldsymbol{\sigma} : \boldsymbol{\tau} + \int_\Omega \mathbf{u}\cdot\mathbf{div}\,(\boldsymbol{\tau}) + \int_\Omega \boldsymbol{\gamma} : \boldsymbol{\tau} - \int_\Omega \mathbf{v}\cdot\mathbf{div}\,(\boldsymbol{\sigma}) - \int_\Omega \boldsymbol{\eta} : \boldsymbol{\sigma} \\ +\; \kappa_1 \int_\Omega \big(\,\mathbf{e}(\mathbf{u}) - \mathcal{C}^{-1}\,\boldsymbol{\sigma}\,\big) : \big(\,\mathbf{e}(\mathbf{v}) + \mathcal{C}^{-1}\,\boldsymbol{\tau}\,\big) \;+\; \kappa_2 \int_\Omega \mathbf{div}\,(\boldsymbol{\sigma})\cdot\mathbf{div}\,(\boldsymbol{\tau}) \\ +\; \kappa_3 \int_\Omega \left(\boldsymbol{\gamma} - \frac{1}{2}(\nabla\mathbf{u} - (\nabla\mathbf{u})^{\mathtt{t}})\right) : \left(\boldsymbol{\eta} + \frac{1}{2}(\nabla\mathbf{v} - (\nabla\mathbf{v})^{\mathtt{t}})\right)\,, \end{aligned} \tag{1.9}$$

y

$$F(\boldsymbol{\tau}, \mathbf{v}, \boldsymbol{\eta}) \;:=\; \int_\Omega \mathbf{f}\cdot(\,\mathbf{v} \;-\; \kappa_2\;\mathbf{div}\,(\boldsymbol{\tau})\,)\;. \tag{1.10}$$

Condiciones sobre el vector $(\kappa_1, \kappa_2, \kappa_3)$ para obtener existencia y unicidad, tanto a nivel continuo como discreto, fueron establecidas en [36]. Vemos que este esquema permite aproximar los desplazamientos, el tensor de esfuerzo y la rotación con funciones de base lineales a trozos, Raviart-Thomas de orden más bajo y constantes a trozos, respectivamente. Para esta formulación variacional desarrollamos el análisis de error a-posteriori, del cual obtenemos un estimador de tipo residual que resulta ser confiable y eficiente. Los resultados de este capítulo corresponden al artículo [11]:

- T.P. Barrios, G.N. Gatica, M. González, N. Heuer: *A residual-based a posteriori error estimate for an augmented mixed finite element method in linear elasticity*. Preprint 2005-20, Departamento de Ingeniería Matemática, Universidad de Concepción, (2005).

Chapter 2

An augmented mixed finite element method with Lagrange multipliers: a priori and a posteriori error analyses

In this chapter we provide a priori and a posteriori error analyses of an augmented mixed finite element method with Lagrange multipliers applied to elliptic equations in divergence form with mixed boundary conditions. The augmented scheme is obtained by including the Galerkin-least squares terms arising from the constitutive and equilibrium equations. We use the classical Babuška-Brezzi theory to show that the resulting dual-mixed variational formulation and its Galerkin scheme defined with Raviart-Thomas spaces are well-posed, and also to derive the corresponding a priori error estimates and rates of convergence. Then, we develop a reliable and efficient residual based a posteriori error estimate and a reliable and quasi-efficient Ritz projection based one, as well. Finally, several numerical results illustrating the performance of the associated adaptive schemes are reported.

2.1 Introduction

In the recent paper [5], a modified mixed finite element method solving second order elliptic equations in divergence form with mixed boundary conditions is introduced and analyzed. The approach there imposes the essential (Neumann) boundary condition in a weak sense, which yields the introduction of a further Lagrange multiplier given precisely by the trace of the solution on the Neumann boundary. Indeed, as it is well known,

the possibility of introducing auxiliary unknowns of physical interest, such as traces, fluxes, stresses, and others, constitutes one of the main advantages of applying dual-mixed variational formulations to solve diverse problems in continuum mechanics. These additional unknowns can then be approximated directly, thus avoiding the numerical post-processing that is usually employed with the solutions arising from primal formulations. Consequently, the derivation of appropriate finite element subspaces yielding well-posed Galerkin schemes and a priori error estimates has been extensively studied and several choices are already available for a large class of linear and even nonlinear boundary value problems (see, e.g. [6], [17], [21], [39], [47], and the references therein). The key issue of this analysis is certainly the verification of the discrete inf-sup conditions involved. The corresponding a posteriori error analysis of the method from [5] was provided in [38]. The results in [38] include a reliable and efficient estimate based on residuals, and a reliable and quasi-efficient Bank-Weiser type estimate based on local problems.

On the other hand, an alternative approach that has also been widely investigated is the stabilization of dual-mixed variational formulations through the application of diverse techniques. A quite general procedure to this respect is given by the Galerkin least-squares methods, also known as augmented variational formulations, which go back to [32] and [33]. These methods are certainly not restricted to dual-mixed schemes, and have already been extended in different directions. In particular, some applications to elasticity problems can be found in [34] and [19], a non-symmetric variant was considered in [30] for the Stokes problem, and a stabilized mixed finite element method for Darcy flow was recently introduced in [44]. An abstract framework concerning the stabilization of general mixed finite element methods can be seen in [18].

Consequently, the main purpose of this paper is to employ suitable Galerkin least-squares terms to augment the mixed finite element method from [5] and then derive the associated a priori and a posteriori error analyses of the resulting variational formulation. We remark that this augmented scheme allows us to approximate simultaneously the main unknown, the flux, and the Neumann trace, with Galerkin solutions in finite element subspaces of $H^1_{\Gamma_D}(\Omega)$, $H(\mathrm{div}\,;\Omega)$, and $H^{1/2}_{00}(\Gamma_N)$, respectively, where Ω is the domain under consideration, Γ_N (resp Γ_D) is the Neumann (resp. Dirichlet) boundary, $H^1_{\Gamma_D}(\Omega) := \{\, v \in H^1(\Omega) : \quad v = 0 \quad \text{on} \quad \Gamma_D \,\}$, and $H^{1/2}_{00}(\Gamma_N) := \{\, v|_{\Gamma_N} : \quad v \in H^1_{\Gamma_D}(\Omega) \,\}$. In particular, the present approach works for any subspace of $H^1_{\Gamma_D}(\Omega)$, which differs from the mixed method in [5] and [38] where the inf-sup conditions needed for the stability of the corre-

sponding Galerkin scheme only hold for some subspaces of $L^2(\Omega)$ approximating the main unknown. The rest of our work is organized as follows. In Section 2.2 we introduce the model boundary value problem, define the augmented variational formulation, and show that it is well-posed. In Section 2.3 we define the augmented mixed finite element scheme, prove its stability, and establish the corresponding a priori error estimate. In Section 2.4 we deduce a reliable and efficient residual based a posteriori error estimate. Edge and triangle bubble functions are employed there to show the corresponding efficiency. Next, a reliable and quasi-efficient Ritz projection based a posteriori error estimate is introduced and analyzed in Section 2.5. Finally, in Section 2.6 we present several numerical examples illustrating the perfomance of the augmented scheme and the associated adaptive algorithms.

Throughout this chapter, c and C, with or without subscripts, bars, tildes or hats, denote positive constants, independent of the parameters and functions involved, which may take different values at different occurrences.

2.2 The augmented mixed variational formulation

Let Ω be a simply connected domain in $\mathbb{R}^2$ with polygonal boundary Γ, and such that all its interior angles lie in $(0, 2\pi)$. Further, let Γ_D and Γ_N be disjoint open subsets of Γ, with $|\Gamma_D|\,, |\Gamma_N| \neq 0$, such that $\Gamma = \bar{\Gamma}_D \cup \bar{\Gamma}_N$. Then, given $f \in L^2(\Omega)$ and $g \in H^{-1/2}(\Gamma_N)$, we consider the model boundary value problem: Find $u \in H^1(\Omega)$ such that

$$-\Delta u \,=\, f \quad \text{in} \quad \Omega\,, \quad u \,=\, 0 \quad \text{on} \quad \Gamma_D\,, \quad \frac{\partial u}{\partial \boldsymbol{\nu}} \,=\, g \quad \text{on} \quad \Gamma_N\,, \tag{2.1}$$

where $\boldsymbol{\nu}$ is the unit outward normal vector to Γ. We recall that the Sobolev space $H^{-1/2}(\Gamma_N)$ is the dual of $H^{1/2}_{00}(\Gamma_N)$ (already defined above in Section 2.1). The corresponding duality pairing with respect to the $L^2(\Gamma_N)-$inner product is denoted by $\langle\, \cdot, \cdot \,\rangle_{\Gamma_N}$.

Since we are interested in applying mixed finite element methods to solve (2.1), we define the auxiliary unknowns $\boldsymbol{\sigma} := \nabla u$ in Ω and $\xi = -u$ on Γ_N. Hence, proceeding in the usual way (see [5] for details), we arrive to the following mixed variational formulation of (2.1): Find $((\boldsymbol{\sigma}, u), \xi) \in H \times Q$ such that

$$\begin{aligned} a((\boldsymbol{\sigma}, u), (\boldsymbol{\tau}, v)) \,+\, b((\boldsymbol{\tau}, v), \xi) \;&=\; \int_\Omega f\, v \qquad \forall\, (\boldsymbol{\tau}, v) \,\in H\,, \\ b((\boldsymbol{\sigma}, u), \lambda) \;&=\; \langle g, \lambda \rangle_{\Gamma_N} \qquad \forall\, \lambda \in Q\,, \end{aligned} \tag{2.2}$$

where $H := H(\mathrm{div}\,;\Omega) \times L^2(\Omega)$, $Q := H^{1/2}_{00}(\Gamma_N)$, and the bilinear forms $a : H \times H \to \mathbb{R}$ and $b : H \times Q \to \mathbb{R}$ are given by

$$\begin{aligned} a((\boldsymbol{\zeta}, w), (\boldsymbol{\tau}, v)) &:= \int_\Omega \boldsymbol{\zeta} \cdot \boldsymbol{\tau} \; + \int_\Omega w \,\mathrm{div}\,\boldsymbol{\tau} \; - \int_\Omega v \,\mathrm{div}\,\boldsymbol{\zeta}\,, \\ b((\boldsymbol{\tau}, v), \lambda) &:= \langle \boldsymbol{\tau} \cdot \boldsymbol{\nu}, \lambda \rangle_{\Gamma_N}\,, \end{aligned}$$

for all $(\boldsymbol{\zeta}, w)$, $(\boldsymbol{\tau}, v) \in H$ and for all $\lambda \in Q$. The well-posedness of (2.2) is established by Theorem 2.1 in [5].

Now, it is not difficult to see that u really lives in the space $H^1_{\Gamma_D}(\Omega)$. Hence, we now proceed as in [9], [36], and [44], and include the Galerkin-least squares terms given by

$$\frac{1}{2}\int_\Omega (\nabla u - \boldsymbol{\sigma}) \cdot (\nabla v + \boldsymbol{\tau}) \; = 0 \qquad \forall\, (\boldsymbol{\tau}, v) \in H(\mathrm{div}\,;\Omega) \times H^1_{\Gamma_D}(\Omega)\,, \tag{2.3}$$

and

$$\int_\Omega \mathrm{div}\,\boldsymbol{\sigma}\,\mathrm{div}\,\boldsymbol{\tau} \;=\; -\int_\Omega f\,\mathrm{div}\,\boldsymbol{\tau} \qquad \forall\, \boldsymbol{\tau} \in H(\mathrm{div}\,;\Omega)\,. \tag{2.4}$$

Thus, adding the equations (2.2), (2.3) and (2.4), we obtain the following augmented mixed variational formulation: Find $((\boldsymbol{\sigma}, u), \xi) \in \mathbf{H} \times Q$ such that

$$\begin{aligned} A((\boldsymbol{\sigma}, u), (\boldsymbol{\tau}, v)) \; + \quad B((\boldsymbol{\tau}, v), \xi) \;&=\; F(\boldsymbol{\tau}, v) \qquad \forall\, (\boldsymbol{\tau}, v) \in \mathbf{H}\,, \\ B((\boldsymbol{\sigma}, u), \lambda) \;&=\; G(\lambda) \qquad \forall\, \lambda \in Q\,, \end{aligned} \tag{2.5}$$

where $\mathbf{H} := H(\mathrm{div}\,;\Omega) \times H^1_{\Gamma_D}(\Omega)$, and the bilinear forms $A : \mathbf{H} \times \mathbf{H} \to \mathbb{R}$ and $B : \mathbf{H} \times Q \to \mathbb{R}$, and the linear functionals $F : \mathbf{H} \to \mathbb{R}$ and $G : Q \to \mathbb{R}$, are given by

$$\begin{aligned} A((\boldsymbol{\zeta}, w), (\boldsymbol{\tau}, v)) &:= \int_\Omega \boldsymbol{\zeta} \cdot \boldsymbol{\tau} \; + \int_\Omega w \,\mathrm{div}\,\boldsymbol{\tau} \; - \int_\Omega v \,\mathrm{div}\,\boldsymbol{\zeta} \\ &+ \quad \int_\Omega \mathrm{div}\,(\boldsymbol{\zeta})\,\mathrm{div}\,(\boldsymbol{\tau}) \; + \; \frac{1}{2}\int_\Omega (\nabla w - \boldsymbol{\zeta}) \cdot (\nabla v + \boldsymbol{\tau})\,, \end{aligned} \tag{2.6}$$

$$B((\boldsymbol{\tau}, v), \lambda) := \langle \boldsymbol{\tau} \cdot \boldsymbol{\nu}, \lambda \rangle_{\Gamma_N}\,, \tag{2.7}$$

$$F(\boldsymbol{\tau}, v) := \int_\Omega f\, v \; - \int_\Omega f\,\mathrm{div}\,\boldsymbol{\tau}\,, \tag{2.8}$$

and

$$G(\lambda) \;:=\; \langle g, \lambda \rangle_{\Gamma_N}\,, \tag{2.9}$$

for all $(\boldsymbol{\zeta}, w)$, $(\boldsymbol{\tau}, v) \in \mathbf{H}$ and for all $\lambda \in Q$.

We remark here that the inclusion of the factor $\frac{1}{2}$ in the definition of A will become clear from the proof of Theorem 2.2.1. Actually, it could be taken as any number in $(0,1)$. In addition, we notice that the augmented formulation (2.5) is still written in a dual-mixed structure. In fact, in order to apply below some results from [5], we need the term dealing with the Neumman boundary condition to be kept separate (in the form of B). This approach differs from the one in [9] where the dual-mixed setting is avoided by introducing an additional boundary residual term expressed in the $H^{1/2}$ Sobolev norm by means of wavelet bases.

Now, since the seminorm $|\cdot|_{H^1(\Omega)}$ and the norm $\|\cdot\|_{H^1(\Omega)}$ of the Sobolev space $H^1(\Omega)$ are equivalent in $H^1_{\Gamma_D}(\Omega)$, we can define

$$\|(\boldsymbol{\tau},v)\|^2_{\mathbf{H}} := \|\boldsymbol{\tau}\|^2_{H(\mathrm{div};\Omega)} + |v|^2_{H^1(\Omega)} \qquad \forall\,(\boldsymbol{\tau},v) \in \mathbf{H}\,.$$

Hence, A, B, F and G are all bounded with constants $\|A\|$, $\|B\|$, $\|F\|$, and $\|G\|$, respectively.

The following result establishes that (2.5) is well-posed.

Theorem 2.2.1 *There exists a unique* $((\boldsymbol{\sigma},u),\xi) \in \mathbf{H}\times Q$ *solution of the variational problem* (2.5) *and the following continuous dependence result holds*

$$\|(\boldsymbol{\sigma},u),\xi)\|_{\mathbf{H}\times Q} \leq C\,\{\,\|F\|_{\mathbf{H}'} + \|G\|_{Q'}\,\} \leq C\left\{\,\|f\|_{L^2(\Omega)} + \|g\|_{H^{-1/2}(\Gamma_N)}\,\right\}. \qquad (2.10)$$

Proof. We first recall from Theorem 2.1 in [5] that the bilinear form B satisfies the continuous inf-sup condition. More precisely, there exists $C > 0$ such that

$$\sup_{\substack{(\boldsymbol{\tau},v)\in\mathbf{H}\\(\boldsymbol{\tau},v)\neq 0}} \frac{B((\boldsymbol{\tau},v),\lambda)}{\|(\boldsymbol{\tau},v)\|_{\mathbf{H}}} \geq \sup_{\substack{\boldsymbol{\tau}\in H(\mathrm{div};\Omega)\\ \mathrm{div}\,\boldsymbol{\tau}=0,\,\boldsymbol{\tau}\neq 0}} \frac{B((\boldsymbol{\tau},0),\lambda)}{\|\boldsymbol{\tau}\|_{H(\mathrm{div};\Omega)}} = \sup_{\substack{\boldsymbol{\tau}\in H(\mathrm{div};\Omega)\\ \mathrm{div}\,\boldsymbol{\tau}=0,\,\boldsymbol{\tau}\neq 0}} \frac{\langle \boldsymbol{\tau}\cdot\boldsymbol{\nu},\lambda\rangle_{\Gamma_N}}{\|\boldsymbol{\tau}\|_{H(\mathrm{div};\Omega)}} \geq C\,\|\lambda\|_{H^{1/2}_{00}(\Gamma_N)} \qquad (2.11)$$

for all $\lambda \in Q$. Also, we easily find from the definition of A in (2.6) that

$$A((\boldsymbol{\tau},v),(\boldsymbol{\tau},v)) = \frac{1}{2}\|\boldsymbol{\tau}\|^2_{[L^2(\Omega)]^2} + \|\mathrm{div}\,\boldsymbol{\tau}\|^2_{L^2(\Omega)} + \frac{1}{2}|v|^2_{H^1(\Omega)} \geq \frac{1}{2}\,\|(\boldsymbol{\tau},v)\|^2_{\mathbf{H}} \qquad (2.12)$$

for all $(\boldsymbol{\tau},v) \in \mathbf{H}$, and hence, in particular, A is strongly coercive on the kernel of the operator associated to B. The rest of the proof is a simple application of the classical Babuška-Brezzi theory (see, e.g. Theorem 1.1 in Chapter II of [17]). □

2.3 The augmented Galerkin scheme

Let $\{\mathcal{T}_h\}_{h>0}$ be a regular family of triangulations of $\bar{\Omega}$ made of straight side triangles T of diameter h_T such that $h := \max\{\, h_T : \; T \in \mathcal{T}_h \,\}$. We assume that all the points in $\bar{\Gamma}_D \cap \bar{\Gamma}_N$ become vertices of $\mathcal{T}_h$ for all $h > 0$. Then, the finite element subspace M_h for the unknown $\boldsymbol{\sigma} \in H(\mathrm{div}\,;\Omega)$ is defined as the Raviart-Thomas space of order zero, that is

$$M_h := \{\, \boldsymbol{\tau}_h \in H(\mathrm{div}\,;\Omega) : \quad \boldsymbol{\tau}_h|_T \in \mathrm{RT}_0(T) \quad \forall\, T \in \mathcal{T}_h \,\}\,, \tag{2.13}$$

where $\mathrm{RT}_0(T) := \mathrm{span}\left\{ \begin{pmatrix} 1 \\ 0 \end{pmatrix}, \begin{pmatrix} 0 \\ 1 \end{pmatrix}, \begin{pmatrix} x_1 \\ x_2 \end{pmatrix} \right\}$ for each $T \in \mathcal{T}_h$, and $x := \begin{pmatrix} x_1 \\ x_2 \end{pmatrix}$ represents a generic vector of $\mathbb{R}^2$.

Next, we let $\{\Gamma_1, \Gamma_2, ..., \Gamma_n\}$ be the partition on Γ_N induced by the triangulation $\mathcal{T}_h$, and assume that $\{\mathcal{T}_h\}_{h>0}$ is uniformly regular near Γ_N, that is there exists $C > 0$, independent of h, such that $|\Gamma_j| \geq C\, h$ for all $j \in \{1, ..., n\}$, for all $h > 0$. In addition, we introduce an independent partition $\{\tilde{\Gamma}_1, \tilde{\Gamma}_2, ..., \tilde{\Gamma}_m\}$ of Γ_N, denote $\tilde{h} := \max\{\, |\tilde{\Gamma}_j| : \; j \in \{1, ..., m\} \,\}$, and assume that this partition is also uniformly regular, which means that there exists $C > 0$ such that $|\tilde{\Gamma}_j| \geq C\, \tilde{h}$ for all $j \in \{1, ..., m\}$, for all $\tilde{h} > 0$. Then, we define the finite element subspace $Q_{\tilde{h}}$ for the unknown $\xi \in H^{1/2}_{00}(\Gamma_N)$ as

$$Q_{\tilde{h}} := \{\, \lambda_{\tilde{h}} \in H^{1/2}_{00}(\Gamma_N) : \quad \lambda_{\tilde{h}}|_{\tilde{\Gamma}_j} \in \mathbf{P}_1(\tilde{\Gamma}_j) \quad \forall\, j \in \{1, ..., m\} \,\}\,. \tag{2.14}$$

Hereafter, given a non-negative integer k and a subset S of $\mathbb{R}^2$, $\mathbf{P}_k(S)$ stands for the space of polynomials defined on S of degree $\leq k$.

Lemma 2.3.1 *There exist C_0, $\beta^* > 0$, independent of h and $\tilde{h}$, such that for all $h \leq C_0\, \tilde{h}$ there holds*

$$\sup_{\substack{\boldsymbol{\tau}_h \in M_h \\ \boldsymbol{\tau}_h \neq 0}} \frac{B((\boldsymbol{\tau}_h, 0), \lambda_{\tilde{h}})}{\|\boldsymbol{\tau}_h\|_{H(\mathrm{div}\,;\Omega)}} = \sup_{\substack{\boldsymbol{\tau}_h \in M_h \\ \boldsymbol{\tau}_h \neq 0}} \frac{\langle \boldsymbol{\tau}_h \cdot \boldsymbol{\nu}, \lambda_{\tilde{h}} \rangle_{\Gamma_N}}{\|\boldsymbol{\tau}_h\|_{H(\mathrm{div}\,;\Omega)}} \geq \beta^* \|\lambda_{\tilde{h}}\|_{H^{1/2}_{00}(\Gamma_N)} \quad \forall\, \lambda_{\tilde{h}} \in Q_{\tilde{h}}\,. \tag{2.15}$$

Proof. It follows from Lemmata 3.2 and 3.3 in [5], which make use of the above assumptions on the partitions of Γ_N. □

We now let X_h be any finite element subspace for the unknown $u \in H^1_{\Gamma_D}(\Omega)$. In particular, we may consider the continuous piecewise linear functions, that is

$$X_h := \{\, v_h \in H^1_{\Gamma_D}(\Omega) : \quad v_h|_T \in \mathbf{P}_1(T) \quad \forall\, T \in \mathcal{T}_h \,\}\,. \tag{2.16}$$

Hence, denoting $\mathbf{H}_h := M_h \times X_h$, the mixed finite element scheme associated to the augmented formulation (2.5) reads as follows: Find $((\boldsymbol{\sigma}_h, u_h), \xi_{\tilde{h}}) \in \mathbf{H}_h \times Q_{\tilde{h}}$ such that

$$\begin{array}{rcll} A((\boldsymbol{\sigma}_h, u_h), (\boldsymbol{\tau}_h, v_h)) \, + \, B((\boldsymbol{\tau}_h, v_h), \xi_{\tilde{h}}) & = F(\boldsymbol{\tau}_h, v_h) & \forall\, (\boldsymbol{\tau}_h, v_h) \in \mathbf{H}_h \,, \\ B((\boldsymbol{\sigma}_h, u_h), \lambda_{\tilde{h}}) & = G(\lambda_{\tilde{h}}) & \forall\, \lambda_{\tilde{h}} \in Q_{\tilde{h}} \,. \end{array} \tag{2.17}$$

The following theorem establishes the unique solvability, stability, and convergence of (2.17).

Theorem 2.3.1 *For each $h \leq C_0\, \tilde{h}$ the mixed finite element scheme* (2.17) *has a unique solution $((\boldsymbol{\sigma}_h, u_h), \xi_{\tilde{h}}) \in \mathbf{H}_h \times Q_{\tilde{h}}$. Moreover, there exist C_1, $C_2 > 0$, independent of h and $\tilde{h}$, such that*

$$\|((\boldsymbol{\sigma}_h, u_h), \xi_{\tilde{h}})\|_{\mathbf{H}\times Q} \;\leq\; C_1 \left\{ \|f\|_{L^2(\Omega)} \,+\, \|g\|_{H^{-1/2}(\Gamma)} \right\},$$

and

$$\|((\boldsymbol{\sigma}, u), \xi) - ((\boldsymbol{\sigma}_h, u_h), \xi_{\tilde{h}})\|_{\mathbf{H}\times Q} \;\leq\; C_2 \inf_{((\boldsymbol{\tau}_h, v_h), \lambda_{\tilde{h}}) \in \mathbf{H}_h \times Q_{\tilde{h}}} \|((\boldsymbol{\sigma}, u), \xi) - ((\boldsymbol{\tau}_h, v_h), \lambda_{\tilde{h}})\|_{\mathbf{H}\times Q} \,.$$

Proof. The discrete inf-sup condition for B is provided by Lemma 2.3.1, independently of the choice of X_h, whereas the strong coercivity of A on the discrete kernel of B, which is a subspace of $\mathbf{H}_h$ and hence of $\mathbf{H}$, is trivially guaranteed by (2.12). Therefore, a straightforward application of the abstract Theorems 1.1 and 2.1 in Chapter II of [17] completes the proof. □

Because of the condition $h \leq C_0\, \tilde{h}$, we assume from now on, without loss of generality, that each edge Γ_i is contained in an edge $\tilde{\Gamma}_j$, for some $j \in \{1, ..., m\}$. Certainly, this requires implicitly that the end points of $\tilde{\Gamma}_j$ be vertices of $\mathcal{T}_h$, which is also assumed in what follows. This section is completed with a result on the rate of convergence of the mixed finite element scheme (2.17).

Theorem 2.3.2 *Let $((\boldsymbol{\sigma}, u), \xi)$ and $((\boldsymbol{\sigma}_h, u_h), \xi_{\tilde{h}})$ be the unique solutions of the continuous and discrete mixed formulations* (2.5) *and* (2.17)*, respectively. Assume that $f = \operatorname{div} \boldsymbol{\sigma} \in H^r(\Omega)$, $u \in H^{r+1}(\Omega)$ for some $r \in (0, 1]$. Then, there exists $C > 0$, independent of h and $\tilde{h}$, such that*

$$\begin{array}{c} \|((\boldsymbol{\sigma}, u), \xi) \,-\, ((\boldsymbol{\sigma}_h, u_h), \xi_{\tilde{h}})\|_{\mathbf{H}\times Q} \\ \leq\; C\, h^r \left\{ \|\boldsymbol{\sigma}\|_{[H^r(\Omega)]^2} \,+\, \|\operatorname{div} \boldsymbol{\sigma}\|_{H^r(\Omega)} \,+\, \|u\|_{H^{r+1}(\Omega)} \right\} \,+\, C\, \tilde{h}^r \, \|\xi\|_{H^{r+1/2}(\Gamma_N)} \,. \end{array}$$

Proof. It follows from the Céa estimate in Theorem 2.3.1 and the approximation properties of the subspaces M_h, X_h, and $Q_{\tilde{h}}$, respectively (see, e.g. [4], [17], [47]). □

2.4 A residual based a posteriori error analysis

In this section we proceed as in [38] and derive a reliable and efficient residual based a posteriori error estimate for our augmented mixed finite element method. Let us first introduce some notations. Given $T \in \mathcal{T}_h$, we denote by $E(T)$ the set of its edges, and by E_h the set of all edges of the triangulation $\mathcal{T}_h$. Then we can write $E_h = E_h(\Omega) \cup E_h(\Gamma)$ with $E_h(\Gamma) := E_h(\Gamma_D) \cup E_h(\Gamma_N)$, where $E_h(\Omega) := \{e \in E_h : \ e \subseteq \Omega\}$, $E_h(\Gamma_D) := \{e \in E_h : \ e \subseteq \Gamma_D\}$, and similarly for $E_h(\Gamma_N)$. In what follows, h_T and h_e stand for the diameter of triangle $T \in \mathcal{T}_h$ and the length of edge $e \in E_h$, respectively. Further, for each $e \subseteq E_h(\Gamma_N)$ we set $\tilde{h}_e := |\tilde{\Gamma}_j|$, where $\tilde{\Gamma}_j$ is the segment containing edge e. Also, given a vector valued function $\boldsymbol{\tau} := (\tau_1, \tau_2)^{\mathtt{t}}$ defined in Ω, an edge $e \in E(T) \cap E_h(\Omega)$, and the unit tangential vector $\mathbf{t}_T$ along e, we let $J[\boldsymbol{\tau} \cdot \mathbf{t}_T]$ be the corresponding jump across e, that is $J[\boldsymbol{\tau} \cdot \mathbf{t}_T] := (\boldsymbol{\tau}_T - \boldsymbol{\tau}_{T'})|_e \cdot \mathbf{t}_T$, where T' is the other triangle of $\mathcal{T}_h$ having e as edge. Here, the tangential vector $\mathbf{t}_T$ is given by $(-\nu_2, \nu_1)^{\mathtt{t}}$ where $\boldsymbol{\nu}_T := (\nu_1, \nu_2)^{\mathtt{t}}$ is the unit outward normal to ∂T. Finally, we let $\mathrm{curl}(\boldsymbol{\tau})$ be the scalar $\frac{\partial \tau_2}{\partial x_1} - \frac{\partial \tau_1}{\partial x_2}$.

Now, let $I_h : H^1(\Omega) \to X_h$ be the usual Clément interpolation operator (see [27]). The following lemma states the local approximation properties of I_h.

Lemma 2.4.1 *There exist positive constants C_1 and C_2, independent of h, such that for all $\varphi \in H^1(\Omega)$ there holds*

$$\|\varphi - I_h(\varphi)\|_{0,T} \ \leq \ C_1 \, h_T \, \|\varphi\|_{1,\Delta(T)} \qquad \forall \, T \ \in \ \mathcal{T}_h \, ,$$

and

$$\|\varphi - I_h(\varphi)\|_{0,e} \ \leq \ C_2 \, h_e^{1/2} \, \|\varphi\|_{1,\Delta(e)} \qquad \forall \, e \in \ E_h \, ,$$

where $\Delta(T) := \cup \{T' \in \mathcal{T}_h : \quad T' \cap T \neq \emptyset\}$ and $\Delta(e) := \cup \{T' \in \mathcal{T}_h : \quad T' \cap e \neq \emptyset\}$.

Throughout the rest of the chapter we assume that the Neumann datum $g \in L^2(\Gamma_N)$. The main result of the present section is summarized in the following theorem.

Theorem 2.4.1 *Let $((\boldsymbol{\sigma}, u), \xi) \in \mathbf{H} \times Q$ and $((\boldsymbol{\sigma}_h, u_h), \xi_{\tilde{h}}) \in \mathbf{H}_h \times Q_{\tilde{h}}$ be the unique solutions of the continuous and discrete formulations (2.5) and (2.17), respectively. Then there exist positive constants $C_{\mathtt{eff}}$, $C_{\mathtt{rel}}$, independent of h and $\tilde{h}$, such that*

$$C_{\mathtt{eff}} \ \boldsymbol{\eta}^2 \ \leq \ \|((\boldsymbol{\sigma} - \boldsymbol{\sigma}_h, u - u_h), \xi - \xi_{\tilde{h}})\|^2_{\mathbf{H} \times Q} \ \leq \ C_{\mathtt{rel}} \ \boldsymbol{\eta}^2 \, , \tag{2.18}$$

where $\boldsymbol{\eta}^2 := \sum_{T\in\mathcal{T}_h} \eta_T^2$, *and for each* $T \in \mathcal{T}_h$ *we define*

$$\eta_T^2 := \|f + \operatorname{div}\boldsymbol{\sigma}_h\|^2_{L^2(T)} + h_T^2\|\nabla u_h - \boldsymbol{\sigma}_h\|^2_{[L^2(T)]^2} + \sum_{e\in E(T)\cap E_h(\Gamma_N)} h_e \left\| \frac{du_h}{d\mathbf{t}_T} + \frac{d\xi_{\tilde{h}}}{d\mathbf{t}_T}\right\|^2_{L^2(e)}$$

$$+ \sum_{e\in E(T)\cap E_h(\Omega)} h_e\|J[(\boldsymbol{\sigma}_h - \nabla u_h)\cdot\mathbf{t}_T]\|^2_{L^2(e)} + \sum_{e\in E(T)\cap E_h(\Gamma)} h_e\|(\boldsymbol{\sigma}_h - \nabla u_h)\cdot\mathbf{t}_T\|^2_{L^2(e)}$$

$$+ \quad \log[1 + C_{\tilde{h}}(\Gamma_N)] \sum_{e\in E(T)\cap E_h(\Gamma_N)} \tilde{h}_e \|g - \boldsymbol{\sigma}_h\cdot\boldsymbol{\nu}\|^2_{L^2(e)}\,, \tag{2.19}$$

with $\quad C_{\tilde{h}}(\Gamma_N) := \max\left\{ \frac{|\tilde{\Gamma}_i|}{|\tilde{\Gamma}_j|} : \quad |i-j| = 1\,,\ i,j\in\{1,...,m\}\right\}$.

The proof of Theorem 2.4.1 is separated into the three parts given by the next subsections.

2.4.1 Estimate for $\|(\boldsymbol{\sigma} - \boldsymbol{\sigma}_h, u - u_h)\|_{\mathbf{H}}$

We first define the spaces $H_0 := \{\boldsymbol{\tau}\in H(\operatorname{div};\Omega) : \quad \operatorname{div}\boldsymbol{\tau} = 0 \quad \text{in} \quad \Omega\,, \quad \boldsymbol{\tau}\cdot\boldsymbol{\nu} = 0 \quad \text{on} \quad \Gamma_N\}$ and $\mathbf{H}_0 := H_0 \times H^1_{\Gamma_D}(\Omega)$. Then we have the following preliminary result.

Lemma 2.4.2 *There exists* $C > 0$, *independent of* h, *such that*

$$C\,\|(\boldsymbol{\sigma} - \boldsymbol{\sigma}_h, u - u_h)\|_{\mathbf{H}}$$

$$\leq \sup_{\substack{(\boldsymbol{\tau},v)\in\mathbf{H}_0\\(\boldsymbol{\tau},v)\neq 0}} \frac{A((\boldsymbol{\sigma} - \boldsymbol{\sigma}_h, u - u_h),(\boldsymbol{\tau},v))}{\|(\boldsymbol{\tau},v)\|_{\mathbf{H}}} + \|f + \operatorname{div}\boldsymbol{\sigma}_h\|_{L^2(\Omega)} + \|g - \boldsymbol{\sigma}_h\cdot\boldsymbol{\nu}\|_{H^{-1/2}(\Gamma_N)}\,.$$

Proof. Let $\boldsymbol{\sigma}^* := \nabla z \in H(\operatorname{div};\Omega)$, where $z\in H^1(\Omega)$ is the weak solution of the boundary value problem:

$$-\Delta z = f + \operatorname{div}\boldsymbol{\sigma}_h \quad \text{in} \quad \Omega\,, \quad z = 0 \quad \text{on} \quad \Gamma_D\,, \quad \frac{\partial z}{\partial\boldsymbol{\nu}} = g - \boldsymbol{\sigma}_h\cdot\boldsymbol{\nu} \quad \text{on} \quad \Gamma_N\,.$$

It follows that $\operatorname{div}\boldsymbol{\sigma}^* = -(f + \operatorname{div}\boldsymbol{\sigma}_h)$ in Ω and $\boldsymbol{\sigma}^*\cdot\boldsymbol{\nu} = g - \boldsymbol{\sigma}_h\cdot\boldsymbol{\nu}$ on Γ_N, whence $(\boldsymbol{\sigma} - \boldsymbol{\sigma}_h - \boldsymbol{\sigma}^*)$ belongs to H_0. In addition, the corresponding continuous dependence result yields the existence of a constant $C > 0$ such that

$$\|\boldsymbol{\sigma}^*\|_{H(\operatorname{div};\Omega)} \leq C\left\{ \|f + \operatorname{div}\boldsymbol{\sigma}_h\|_{L^2(\Omega)} + \|g - \boldsymbol{\sigma}_h\cdot\boldsymbol{\nu}\|_{H^{-1/2}(\Gamma_N)}\right\}. \tag{2.20}$$

Now, using the strong coercivity (cf. (2.12)) and boundedness of A, we find that

$$\frac{1}{2}\,\|(\boldsymbol{\sigma}-\boldsymbol{\sigma}_h-\boldsymbol{\sigma}^*,u-u_h)\|^2_{\mathbf{H}} \leq A((\boldsymbol{\sigma}-\boldsymbol{\sigma}-\boldsymbol{\sigma}^*,u-u_h),(\boldsymbol{\sigma}-\boldsymbol{\sigma}_h-\boldsymbol{\sigma}^*,u-u_h))$$

$$= A((\boldsymbol{\sigma}-\boldsymbol{\sigma}_h,u-u_h),(\boldsymbol{\sigma}-\boldsymbol{\sigma}_h-\boldsymbol{\sigma}^*,u-u_h)) - A((\boldsymbol{\sigma}^*,0),(\boldsymbol{\sigma}-\boldsymbol{\sigma}_h-\boldsymbol{\sigma}^*,u-u_h))$$

$$\leq A((\boldsymbol{\sigma}-\boldsymbol{\sigma}_h,u-u_h),(\boldsymbol{\sigma}-\boldsymbol{\sigma}_h-\boldsymbol{\sigma}^*,u-u_h)) + \|A\|\,\|\boldsymbol{\sigma}^*\|_{H(\mathrm{div}\,;\Omega)}\,\|(\boldsymbol{\sigma}-\boldsymbol{\sigma}_h-\boldsymbol{\sigma}^*,u-u_h)\|_{\mathbf{H}}$$

which, dividing by $\|(\boldsymbol{\sigma}-\boldsymbol{\sigma}_h-\boldsymbol{\sigma}^*,u-u_h)\|_{\mathbf{H}}$, and then taking supremum on $\mathbf{H}_0$, implies

$$C\,\|(\boldsymbol{\sigma}-\boldsymbol{\sigma}_h-\boldsymbol{\sigma}^*,u-u_h)\|_{\mathbf{H}} \leq \sup_{\substack{(\boldsymbol{\tau},v)\in\mathbf{H}_0\\(\boldsymbol{\tau},v)\neq 0}} \frac{A((\boldsymbol{\sigma}-\boldsymbol{\sigma}_h,u-u_h),(\boldsymbol{\tau},v))}{\|(\boldsymbol{\tau},v)\|_{\mathbf{H}}} + \|\boldsymbol{\sigma}^*\|_{H(\mathrm{div}\,;\Omega)}\,. \quad (2.21)$$

Finally, triangle inequality gives $\|(\boldsymbol{\sigma}-\boldsymbol{\sigma}_h,u-u_h)\|_{\mathbf{H}} \leq \|(\boldsymbol{\sigma}-\boldsymbol{\sigma}_h-\boldsymbol{\sigma}^*,u-u_h)\|_{\mathbf{H}} + \|\boldsymbol{\sigma}^*\|_{H(\mathrm{div}\,;\Omega)}$, which, together with the estimates (2.21) and (2.20), completes the proof. □

The corresponding upper bound for the supremum appearing in Lemma 2.4.2 is provided next.

Lemma 2.4.3 *There exists $C>0$, independent of h and $\tilde{h}$, such that*

$$\sup_{\substack{(\boldsymbol{\tau},v)\in\mathbf{H}_0\\(\boldsymbol{\tau},v)\neq 0}} \frac{A((\boldsymbol{\sigma}-\boldsymbol{\sigma}_h,u-u_h),(\boldsymbol{\tau},v))}{\|(\boldsymbol{\tau},v)\|_{\mathbf{H}}} \leq C\,\left\{\sum_{T\in\mathcal{T}_h}\tilde{\eta}^2_T\right\}^{1/2},$$

where for any triangle $T\in\mathcal{T}_h$ we define

$$\tilde{\eta}^2_T := h^2_T\,\|f+\mathrm{div}\,\boldsymbol{\sigma}_h\|^2_{L^2(T)} + h^2_T\,\|\nabla u_h-\boldsymbol{\sigma}_h\|^2_{[L^2(T)]^2} + \sum_{e\in E(T)\cap E_h(\Omega)} h_e\,\|J[(\boldsymbol{\sigma}_h-\nabla u_h)\cdot\mathbf{t}_T]\|^2_{L^2(e)}$$

$$+ \sum_{e\in E(T)\cap E_h(\Gamma)} h_e\,\|(\boldsymbol{\sigma}_h-\nabla u_h)\cdot\mathbf{t}_T\|^2_{L^2(e)} + \sum_{e\in E(T)\cap E_h(\Gamma_N)} h_e\,\left\|\frac{du_h}{d\mathbf{t}_T}+\frac{d\xi_{\tilde{h}}}{d\mathbf{t}_T}\right\|^2_{L^2(e)}. \quad (2.22)$$

Proof. Let $(\boldsymbol{\tau},v)\in\mathbf{H}_0$ such that $(\boldsymbol{\tau},v)\neq 0$. Since $\mathrm{div}\,(\boldsymbol{\tau})=0$ in Ω and Ω is connected, there exists a stream function $\varphi\in H^1(\Omega)$ such that $\displaystyle\int_\Omega\varphi = 0$ and $\boldsymbol{\tau}=\mathbf{curl}(\varphi) := \begin{pmatrix} -\frac{\partial\varphi}{\partial x_2}\\ \frac{\partial\varphi}{\partial x_1}\end{pmatrix}$. Then, denoting by v_h and φ_h the Clément interpolants of v and φ, respectively, and defining $\boldsymbol{\tau}_h := \mathbf{curl}\,\varphi_h$, we obtain $\boldsymbol{\tau}_h\in M_h$, $\mathrm{div}\,\boldsymbol{\tau}_h=0$ in Ω, and $\boldsymbol{\tau}-\boldsymbol{\tau}_h=\mathbf{curl}(\varphi-\varphi_h)$.

Next, from the first equations of (2.5) and (2.17) we find that

$$A((\boldsymbol{\sigma},u),(\boldsymbol{\tau}-\boldsymbol{\tau}_h,v-v_h)) \,=\, F(\boldsymbol{\tau}-\boldsymbol{\tau}_h,v-v_h)-B((\boldsymbol{\tau}-\boldsymbol{\tau}_h,v-v_h),\xi)$$

and

$$A((\boldsymbol{\sigma}-\boldsymbol{\sigma}_h,u-u_h),(\boldsymbol{\tau}_h,v_h)) \,=\, -B((\boldsymbol{\tau}_h,v_h),\xi-\xi_{\tilde{h}})\,,$$

which gives

$$A((\boldsymbol{\sigma}-\boldsymbol{\sigma}_h,u-u_h),(\boldsymbol{\tau},v)) = A((\boldsymbol{\sigma}-\boldsymbol{\sigma}_h,u-u_h),(\boldsymbol{\tau}-\boldsymbol{\tau}_h,v-v_h))+A((\boldsymbol{\sigma}-\boldsymbol{\sigma}_h,u-u_h),(\boldsymbol{\tau}_h,v_h))$$

$$= F(\boldsymbol{\tau}-\boldsymbol{\tau}_h,v-v_h)-B((\boldsymbol{\tau}-\boldsymbol{\tau}_h,v-v_h),\xi)-A((\boldsymbol{\sigma}_h,u_h),(\boldsymbol{\tau}-\boldsymbol{\tau}_h,v-v_h))-B((\boldsymbol{\tau}_h,v_h),\xi-\xi_{\tilde{h}})\,.$$

It follows, employing the definitions of F and B (cf. (2.7), (2.8)), and using that $\boldsymbol{\tau}\cdot\boldsymbol{\nu}=0$ on Γ_N, that

$$A((\boldsymbol{\sigma}-\boldsymbol{\sigma}_h,u-u_h),(\boldsymbol{\tau},v)) = \int_\Omega f(v-v_h) - \langle(\boldsymbol{\tau}-\boldsymbol{\tau}_h)\cdot\boldsymbol{\nu},\xi_{\tilde{h}}\rangle_{\Gamma_N} - A((\boldsymbol{\sigma}_h,u_h),(\boldsymbol{\tau}-\boldsymbol{\tau}_h,v-v_h))\,.$$

Next, developing $A((\boldsymbol{\sigma}_h,u_h),(\boldsymbol{\tau}-\boldsymbol{\tau}_h,v-v_h))$ (see (2.6)), integrating by parts in Ω, using that $u_h \,=\, 0$ on Γ_D and that $\mathrm{div}\,(\boldsymbol{\tau}-\boldsymbol{\tau}_h)=0$ in Ω, and reordering the resulting terms, we arrive to

$$A((\boldsymbol{\sigma}-\boldsymbol{\sigma}_h,u-u_h),(\boldsymbol{\tau},v)) \,=\, \int_\Omega (f+\mathrm{div}\,\boldsymbol{\sigma}_h)(v-v_h) \,-\, \langle\mathbf{curl}(\varphi-\varphi_h)\cdot\boldsymbol{\nu},u_h+\xi_{\tilde{h}}\rangle_{\Gamma_N}$$

$$-\frac{1}{2}\int_\Omega(\boldsymbol{\sigma}_h-\nabla u_h)\cdot\mathbf{curl}(\varphi-\varphi_h) \,-\, \frac{1}{2}\int_\Omega(\nabla u_h-\boldsymbol{\sigma}_h)\cdot\nabla(v-v_h)\,. \tag{2.23}$$

We now proceed to derive suitable bounds for each one of the terms on the right hand side of (2.23). We first observe that $\mathbf{curl}(\varphi-\varphi_h)\cdot\boldsymbol{\nu} = -\frac{d(\varphi-\varphi_h)}{d\mathbf{t}_T}$, and hence

$$\langle\mathbf{curl}(\varphi-\varphi_h)\cdot\boldsymbol{\nu},u_h\,+\,\xi_{\tilde{h}}\rangle_{\Gamma_N} \,=\, \left\langle\varphi\,-\,\varphi_h,\frac{du_h}{d\mathbf{t}_T}\,+\,\frac{d\xi_{\tilde{h}}}{d\mathbf{t}_T}\right\rangle_{\Gamma_N}$$

$$=\sum_{T\in\mathcal{T}_h}\sum_{e\in E(T)\cap E_h(\Gamma_N)}\left\langle\varphi\,-\,\varphi_h,\frac{du_h}{d\mathbf{t}_T}\,+\,\frac{d\xi_{\tilde{h}}}{d\mathbf{t}_T}\right\rangle_{L^2(e)}\,. \tag{2.24}$$

Also, using that $\displaystyle\int_\Omega=\sum_{T\in\mathcal{T}_h}\int_T$, integrating by parts, and noting that $\mathrm{curl}(\boldsymbol{\sigma}_h-\nabla u_h)=0$ in each $T\in\mathcal{T}_h$, we deduce that

$$\int_\Omega(\boldsymbol{\sigma}_h-\nabla u_h)\cdot\mathbf{curl}(\varphi-\varphi_h) \,=\, \frac{1}{2}\sum_{T\in\mathcal{T}_h}\sum_{e\in E(T)\cap E_h(\Omega)}\langle J[\boldsymbol{\sigma}_h-\nabla u_h]\cdot\mathbf{t}_T,\varphi-\varphi_h\rangle_{L^2(e)}$$

$$+ \sum_{T\in\mathcal{T}_h} \sum_{e\in E(T)\cap E_h(\Gamma)} \langle(\boldsymbol{\sigma}_h - \nabla u_h)\cdot \mathbf{t}_T, \varphi - \varphi_h\rangle_{L^2(e)}\,. \tag{2.25}$$

Then, applying Cauchy-Schwarz inequality, the estimates from Lemma 2.4.1, and the fact that the number of triangles in $\Delta(T)$ and $\Delta(e)$ are bounded, we obtain that the terms in (2.23), (2.24), and (2.25), respectively, are bounded as follows

$$\left|\int_\Omega (f + \operatorname{div}\boldsymbol{\sigma}_h)(v - v_h)\right| \leq C \left\{\sum_{T\in\mathcal{T}_h} h_T^2 \,\|f + \operatorname{div}\boldsymbol{\sigma}_h\|^2_{L^2(T)}\right\}^{1/2} \|v\|_{H^1(\Omega)}\,, \tag{2.26}$$

$$\left|\int_\Omega (\nabla u_h - \boldsymbol{\sigma}_h)\cdot\nabla(v - v_h)\right| \leq C \left\{\sum_{T\in\mathcal{T}_h} h_T^2 \|\nabla u_h - \boldsymbol{\sigma}_h\|^2_{[L^2(T)]^2}\right\}^{1/2} \|v\|_{H^1(\Omega)}\,, \tag{2.27}$$

$$|\langle \mathbf{curl}(\varphi-\varphi_h)\cdot\boldsymbol{\nu}, u_h+\xi_{\tilde{h}}\rangle_{\Gamma_N}| \leq C \Big\{ \sum_{T\in\mathcal{T}_h} \sum_{e\in E(T)\cap E_h(\Gamma_N)} h_e \left\|\frac{du_h}{d\mathbf{t}_T} + \frac{d\xi_{\tilde{h}}}{d\mathbf{t}_T}\right\|^2_{L^2(e)} \Big\}^{1/2} \|\varphi\|_{H^1(\Omega)}\,, \tag{2.28}$$

$$\left|\sum_{T\in\mathcal{T}_h} \sum_{e\in E(T)\cap E_h(\Omega)} \langle J[\boldsymbol{\sigma}_h - \nabla u_h]\cdot\mathbf{t}_T, \varphi - \varphi_h\rangle_{L^2(e)}\right|$$

$$\leq C \left\{\sum_{T\in\mathcal{T}_h} \sum_{e\in E(T)\cap E_h(\Omega)} h_e \,\|J[\boldsymbol{\sigma}_h - \nabla u_h]\cdot\mathbf{t}_T\|^2_{L^2(e)}\right\}^{1/2} \|\varphi\|_{H^1(\Omega)}\,, \tag{2.29}$$

and

$$\left|\sum_{T\in\mathcal{T}_h} \sum_{e\in E(T)\cap E_h(\Gamma)} \langle(\boldsymbol{\sigma}_h - \nabla u_h)\cdot\mathbf{t}_T, \varphi - \varphi_h\rangle_{L^2(e)}\right|$$

$$\leq C \left\{\sum_{T\in\mathcal{T}_h} \sum_{e\in E(T)\cap E_h(\Gamma)} h_e \,\|(\boldsymbol{\sigma}_h - \nabla u_h)\cdot\mathbf{t}_T\|^2_{L^2(e)}\right\}^{1/2} \|\varphi\|_{H^1(\Omega)}\,. \tag{2.30}$$

Since $\displaystyle\int_\Omega \varphi = 0$ and $\mathbf{curl}(\varphi) = \boldsymbol{\tau}$, we clearly have $\|\varphi\|_{H^1(\Omega)} \leq C\,|\varphi|_{H^1(\Omega)} = C\,\|\boldsymbol{\tau}\|_{L^2(\Omega)} = C\,\|\boldsymbol{\tau}\|_{H(\operatorname{div};\Omega)}$. Therefore, using this norm estimate in (2.28), (2.29), and (2.30), and replacing (2.26) up to (2.30) back into (2.23), we obtain the required inequality and conclude the proof. □

We can establish now our a posteriori error estimate for $\|(\boldsymbol{\sigma} - \boldsymbol{\sigma}_h, u - u_h)\|_{\mathbf{H}}$.

Theorem 2.4.2 *There exists $C > 0$, independent of h and $\tilde{h}$, such that*

$$\|(\boldsymbol{\sigma} - \boldsymbol{\sigma}_h, u - u_h)\|_{\mathbf{H}} \leq C \left\{\sum_{T\in\mathcal{T}_h} \eta_T^2\right\}^{1/2},$$

where η_T^2 is given by (2.19) *for each $T \in \mathcal{T}_h$.*

Proof. We see from Lemma 2.4.2 that it just remains to estimate the residuals $\|f + \operatorname{div}\boldsymbol{\sigma}_h\|_{L^2(\Omega)}$ and $\|g - \boldsymbol{\sigma}_h\cdot\boldsymbol{\nu}\|^2_{H^{-1/2}(\Gamma_N)}$ in terms of local quantities. For the first expression we simply write

$$\|f + \operatorname{div}\boldsymbol{\sigma}_h\|^2_{L^2(\Omega)} \,=\, \sum_{T\in\mathcal{T}_h} \|f + \operatorname{div}\boldsymbol{\sigma}_h\|^2_{L^2(T)}\,, \tag{2.31}$$

and for the second one we apply Theorem 2 in [23] to yield

$$\|g \,-\, \boldsymbol{\sigma}_h\cdot\boldsymbol{\nu}\|^2_{H^{-1/2}(\Gamma_N)} \,\leq\, C\,\log[1 + C_{\tilde{h}}(\Gamma_N)]\,\sum_{j=1}^{m} |\tilde{\Gamma}_j|\,\|g \,-\, \boldsymbol{\sigma}_h\cdot\boldsymbol{\nu}\|^2_{L^2(\tilde{\Gamma}_j)}\,, \tag{2.32}$$

where $C_{\tilde{h}}(\Gamma_N) := \max\Big\{\frac{|\tilde{\Gamma}_i|}{|\tilde{\Gamma}_j|} : \quad |i-j| = 1\,,\ i,j\in\{1,...,m\}\Big\}$. Then, since each edge of $E_h(\Gamma_N)$ is contained in a segment $\tilde{\Gamma}_j$ for some $j\in\{1,\ldots,m\}$, we deduce that

$$\sum_{j=1}^{m} |\tilde{\Gamma}_j|\,\|g - \boldsymbol{\sigma}_h\cdot\boldsymbol{\nu}\|^2_{L^2(\tilde{\Gamma}_j)} \,=\, \sum_{e\in E_h(\Gamma_N)} \tilde{h}_e\,\|g - \boldsymbol{\sigma}_h\cdot\boldsymbol{\nu}\|^2_{L^2(e)}\,, \tag{2.33}$$

which is replaced back into (2.32). The rest of the proof follows from Lemmata 2.4.2 and 2.4.3, and the estimates (2.31) and (2.32). We omit further details. □

2.4.2 Estimate for $\|\xi - \xi_{\tilde{h}}\|_Q$

The a posteriori error estimate for the Lagrange multiplier ξ is provided next.

Theorem 2.4.3 *There exists $C > 0$, independent of h and $\tilde{h}$, such that*

$$\|\xi - \xi_{\tilde{h}}\|_{H^{1/2}_{00}(\Gamma_N)} \,\leq\, C\,\left\{\sum_{T\in\mathcal{T}_h}\eta_T^2\right\}^{1/2}\,,$$

where η_T is given by (2.19).

Proof. According to the inf-sup condition (2.11), we can write

$$\|\xi - \xi_{\tilde{h}}\|_{H^{1/2}_{00}(\Gamma_N)} \,\leq\, C\,\sup_{\substack{\boldsymbol{\tau}\in H(\operatorname{div};\Omega)\\ \operatorname{div}\boldsymbol{\tau}=0,\,\boldsymbol{\tau}\neq 0}} \frac{\langle\boldsymbol{\tau}\cdot\boldsymbol{\nu},\xi\rangle_{\Gamma_N} - \langle\boldsymbol{\tau}\cdot\boldsymbol{\nu},\xi_{\tilde{h}}\rangle_{\Gamma_N}}{\|\boldsymbol{\tau}\|_{H(\operatorname{div};\Omega)}}\,. \tag{2.34}$$

Now, given $\boldsymbol{\tau}\in H(\operatorname{div};\Omega)$ with $\operatorname{div}\boldsymbol{\tau} = 0$ in Ω, we observe from the first equation of (2.5) that $\langle\boldsymbol{\tau}\cdot\boldsymbol{\nu},\xi\rangle_{\Gamma_N} = -A((\boldsymbol{\sigma},u),(\boldsymbol{\tau},0))$. Also, since Ω is connected, there exists

$\varphi \in H^1(\Omega)$ such that $\int_\Omega \varphi = 0$ and $\boldsymbol{\tau} = \mathbf{curl}\,\varphi$. Next, as in the proof of Lemma 2.4.3, we let φ_h be the Clément interpolant of φ and define $\boldsymbol{\tau}_h := \mathbf{curl}\,\varphi_h$. It is clear that $\boldsymbol{\tau}_h \in M_h$ and $\operatorname{div}\boldsymbol{\tau}_h = 0$ in Ω, and hence, the first equation of (2.17) gives $\langle \boldsymbol{\tau}_h \cdot \boldsymbol{\nu}, \xi_{\tilde{h}} \rangle_{\Gamma_N} = -A((\boldsymbol{\sigma}_h, u_h), (\boldsymbol{\tau}_h, 0))$.

It follows that

$$\langle \boldsymbol{\tau}\cdot\boldsymbol{\nu}, \xi\rangle_{\Gamma_N} - \langle \boldsymbol{\tau}\cdot\boldsymbol{\nu}, \xi_{\tilde{h}}\rangle_{\Gamma_N} = -A((\boldsymbol{\sigma}, u), (\boldsymbol{\tau}, 0)) - \langle (\boldsymbol{\tau}-\boldsymbol{\tau}_h)\cdot\boldsymbol{\nu}, \xi_{\tilde{h}}\rangle_{\Gamma_N} + A((\boldsymbol{\sigma}_h, u_h), (\boldsymbol{\tau}_h, 0))$$

$$= -A((\boldsymbol{\sigma}, u) - (\boldsymbol{\sigma}_h, u_h), (\boldsymbol{\tau}, 0)) - A((\boldsymbol{\sigma}_h, u_h), ((\boldsymbol{\tau}-\boldsymbol{\tau}_h), 0)) - \langle (\boldsymbol{\tau}-\boldsymbol{\tau}_h)\cdot\boldsymbol{\nu}, \xi_{\tilde{h}}\rangle_{\Gamma_N},$$

which, developing $A((\boldsymbol{\sigma}_h, u_h), ((\boldsymbol{\tau}-\boldsymbol{\tau}_h), 0))$ (see (2.6)), integrating by parts in Ω, using that $u_h = 0$ on Γ_D and that $\operatorname{div}(\boldsymbol{\tau}-\boldsymbol{\tau}_h) = 0$ in Ω, and finally replacing $(\boldsymbol{\tau}-\boldsymbol{\tau}_h)$ by $\mathbf{curl}(\varphi-\varphi_h)$, leads to

$$\langle \boldsymbol{\tau}\cdot\boldsymbol{\nu}, \xi\rangle_{\Gamma_N} - \langle \boldsymbol{\tau}\cdot\boldsymbol{\nu}, \xi_{\tilde{h}}\rangle_{\Gamma_N} = -A((\boldsymbol{\sigma}, u) - (\boldsymbol{\sigma}_h, u_h), (\boldsymbol{\tau}, 0))$$

$$- \langle \mathbf{curl}(\varphi-\varphi_h)\cdot\boldsymbol{\nu}, u_h + \xi_{\tilde{h}}\rangle_{\Gamma_N} - \frac{1}{2}\int_\Omega (\boldsymbol{\sigma}_h - \nabla u_h)\cdot\mathbf{curl}(\varphi-\varphi_h)\,. \tag{2.35}$$

Therefore, using the boundedness of A for the first term on the right hand side of (2.35), proceeding as in (2.25) for the third one, and then applying the upper bounds provided by (2.28), (2.29), and (2.30), we conclude that

$$\frac{|\langle \boldsymbol{\tau}\cdot\boldsymbol{\nu}, \xi\rangle_{\Gamma_N} - \langle \boldsymbol{\tau}\cdot\boldsymbol{\nu}, \xi_{\tilde{h}}\rangle_{\Gamma_N}|}{\|\boldsymbol{\tau}\|_{H(\operatorname{div};\Omega)}} \leq C \left\{ \|(\boldsymbol{\sigma}-\boldsymbol{\sigma}_h, u-u_h)\|^2_{\mathbf{H}} + \sum_{T\in\mathcal{T}_h} \bar{\eta}^2_T \right\}^{1/2}, \tag{2.36}$$

where

$$\bar{\eta}^2_T = \tilde{\eta}^2_T - h^2_T \|f + \operatorname{div}\boldsymbol{\sigma}_h\|^2_{L^2(T)} - h^2_T \|\nabla u_h - \boldsymbol{\sigma}_h\|^2_{L^2(T)},$$

with $\tilde{\eta}^2_T$ given by (2.22). In this way, (2.34), (2.36), and the a posteriori error estimate for $\|(\boldsymbol{\sigma}-\boldsymbol{\sigma}_h, u-u_h)\|_{\mathbf{H}}$ (cf. Theorem 2.4.2) complete the proof. □

Consequently, the reliability of the a posteriori error estimate, which is given by the upper bound in (2.18), follows directly from Theorems 2.4.2 and 2.4.3.

2.4.3 Efficiency of the a posteriori error estimate

In this subsection we follow the approach from [35] (see also [38]) to derive the lower bound in (2.18), which shows the efficiency of the a posteriori error estimate. We first recall from [49] that given $k \in \mathbb{N}$, $T \in \mathcal{T}_h$, and $e \in E(T)$, there exists an extension

operator $L : C(e) \to C(T)$ that satisfies $L(p) \in \mathbf{P}_k(T)$ and $L(p)|_e = p \ \forall p \in \mathbf{P}_k(e)$. In addition, we define $w_e := \cup\{T' \in \mathcal{T}_h : \quad e \in E(T')\}$ and let ψ_T and ψ_e be te usual triangle-bubble and edge-bubble functions, respectively (see (1.5) and (1.6) in [50]), which satisfy $\mathrm{supp}(\psi_T) \subseteq T$, $\psi_T \in \mathbf{P}_3(T)$, $\psi_T = 0$ on ∂T, $0 \leq \psi_T \leq 1$ in T, $\mathrm{supp}(\psi_e) \subseteq w_e$, $\psi_e|_T \in \mathbf{P}_2(T)\ \forall T \subseteq w_e$, $\psi_e = 0$ on $\partial T \backslash e$, and $0 \leq \psi_e \leq 1$ in w_e. Additional properties of ψ_T, ψ_e, and L are collected in the following lemma.

Lemma 2.4.4 *There exist positive constants c_1, c_2, c_3 and c_4, depending only on k and the shape of the triangles, such that for all $q \in \mathbf{P}_k(T)$ and $p \in \mathbf{P}_k(e)$, there hold*

$$\|\psi_T\, q\|^2_{L^2(T)} \ \leq\ \|q\|^2_{L^2(T)} \ \leq\ c_1\, \|\psi_T^{1/2}\, q\|^2_{L^2(T)}\,, \tag{2.37}$$

$$\|\psi_e\, L(p)\|^2_{L^2(e)} \ \leq\ \|p\|^2_{L^2(e)} \ \leq\ c_2\, \|\psi_e^{1/2}\, p\|^2_{L^2(e)}\,, \tag{2.38}$$

$$c_4\, h_e\, \|p\|^2_{L^2(e)} \ \leq\ \|\psi_e^{1/2}\, L(p)\|^2_{L^2(T)} \ \leq\ c_3\, h_e\, \|p\|^2_{L^2(e)}\,. \tag{2.39}$$

Proof. See Lemma 4.1 in [49]. □

For the first term in (2.19) we use that $\mathrm{div}\,\boldsymbol{\sigma} = -f$ in Ω and write

$$\sum_{T\in\mathcal{T}_h} \|f + \mathrm{div}\,\boldsymbol{\sigma}_h\|^2_{L^2(T)} \ =\ \|\mathrm{div}\,(\boldsymbol{\sigma} - \boldsymbol{\sigma}_h)\|^2_{L^2(\Omega)}\,. \tag{2.40}$$

The corresponding estimate for the second term is also easily obtained. In fact, adding and substracting $\boldsymbol{\sigma} = \nabla u$, we get

$$h_T^2\, \|\nabla u_h - \boldsymbol{\sigma}_h\|^2_{[L^2(T)]^2} \ \leq\ C\, \|\nabla u_h - \boldsymbol{\sigma}_h\|^2_{[L^2(T)]^2} \ \leq\ C\, \Big\{\, |u - u_h|^2_{H^1(T)} \ +\ \|\boldsymbol{\sigma} - \boldsymbol{\sigma}_h\|^2_{[L^2(T)]^2} \,\Big\}\,,$$

whence

$$\sum_{T\in\mathcal{T}_h} h_T^2\, \|\nabla u_h - \boldsymbol{\sigma}_h\|^2_{[L^2(T)]^2} \ \leq\ C\, \Big\{\, |u - u_h|^2_{H^1(\Omega)} \ +\ \|\boldsymbol{\sigma} - \boldsymbol{\sigma}_h\|^2_{[L^2(\Omega)]^2} \,\Big\}\,. \tag{2.41}$$

The third term in (2.19) is bounded next.

Lemma 2.4.5 *There exists $C > 0$, independent of h and $\tilde{h}$, such that*

$$\sum_{e\in E_h(\Gamma_N)} h_e\, \left\| \frac{du_h}{d\mathbf{t}_T} \ +\ \frac{d\xi_{\tilde{h}}}{d\mathbf{t}_T} \right\|^2_{L^2(e)} \ \leq\ C\, \Big\{ \|\xi - \xi_{\tilde{h}}\|^2_{H^{1/2}_{00}(\Gamma_N)} \ +\ \|u - u_h\|^2_{H^1(\Omega)} \Big\}\,. \tag{2.42}$$

Proof. Let us define $v_e := \dfrac{du_h}{d\mathbf{t}_T} + \dfrac{d\xi_{\tilde{h}}}{d\mathbf{t}_T}$ on $e \in E_h(\Gamma_N)$. Then, using that $u = -\xi$ on Γ_N, we can write $v_e = \dfrac{d}{d\mathbf{t}_T}(u_h - u) + \dfrac{d}{d\mathbf{t}_T}(\xi_{\tilde{h}} - \xi)$ on e. Hence, applying (2.38), we obtain that

$$h_e \, \|v_e\|^2_{L^2(e)} \, \leq \, c_1 \left\{ h_e \left\langle \psi_e \, v_e \, , \, \frac{d}{d\mathbf{t}_T}(u_h - u) \right\rangle_e \, + \, h_e \left\langle \psi_e \, v_e \, , \, \frac{d}{d\mathbf{t}_T}(\xi_{\tilde{h}} - \xi) \right\rangle_e \right\} . \quad (2.43)$$

We now define the function $\psi := h_e \, \psi_e \, v_e$ on each $e \in E_h(\Gamma_N)$, and introduce the trivial extensions $\hat{\psi} := \left\{ \begin{array}{lll} \psi & \text{on} & \Gamma_N \\ 0 & \text{on} & \Gamma_D \end{array} \right.$ and $\hat{\xi} := \left\{ \begin{array}{lll} \xi_{\tilde{h}} - \xi & \text{on} & \Gamma_N \\ 0 & \text{on} & \Gamma_D \end{array} \right.$. Since ψ and $(\xi_{\tilde{h}} - \xi)$ belong to $H^{1/2}_{00}(\Gamma_N)$, it follows that $\hat{\psi}$ and $\hat{\xi}$ lie in $H^{1/2}(\Gamma)$ and that $\|\hat{\psi}\|_{H^{1/2}(\Gamma)}$ and $\|\hat{\xi}\|_{H^{1/2}(\Gamma)}$ are equivalent to $\|\psi\|_{H^{1/2}_{00}(\Gamma_N)}$ and $\|\xi_{\tilde{h}} - \xi\|_{H^{1/2}_{00}(\Gamma_N)}$, respectively.

Thus, applying the inverse inequality to the piecewise polynomial $\hat{\psi}$, using the boundedness of the tangential derivative, noting that $0 \leq \psi_e \leq 1$, $h_e \leq h$, and that $u_h = u = 0$ on Γ_D, and employing the usual trace Theorem, we deduce that

$$\sum_{e \in E_h(\Gamma_N)} h_e \left\langle \psi_e \, v_e \, , \, \frac{d}{d\mathbf{t}_T}(u_h - u) \right\rangle_e \, = \left\langle \hat{\psi} \, , \, \frac{d}{d\mathbf{t}_T}(u_h - u) \right\rangle_\Gamma \, \leq \, \|\hat{\psi}\|_{H^{1/2}(\Gamma)} \left\| \frac{d}{d\mathbf{t}_T}(u_h - u) \right\|_{H^{-1/2}(\Gamma)}$$

$$\leq \, C \, h^{-1/2} \, \|\hat{\psi}\|_{L^2(\Gamma)} \, \|u - u_h\|_{H^{1/2}(\Gamma)} \, \leq \, C \left\{ \sum_{e \in E_h(\Gamma_N)} h_e \, \|v_e\|^2_{L^2(e)} \right\}^{1/2} \|u - u_h\|_{H^1(\Omega)} \, . \quad (2.44)$$

Proceeding similarly as for the above estimate (see also proof of Lemma 5.7 in [35]), using now the extension $\hat{\xi}$, we find that there exists $C > 0$, independent of h and $\tilde{h}$, such that

$$\sum_{e \in E_h(\Gamma_N)} h_e \int_e \psi_e \, v_e \, \frac{d}{d\mathbf{t}_T}(\xi_{\tilde{h}} - \xi) \, \leq \, C \left\{ \sum_{e \in E_h(\Gamma_N)} h_e \, \|v_e\|^2_{L^2(e)} \right\}^{1/2} \|\xi_{\tilde{h}} - \xi\|_{H^{1/2}_{00}(\Gamma_N)} \, . \quad (2.45)$$

Therefore, (2.42) is a consequence of (2.43), (2.44), and (2.45). □

The following technical lemma is needed to bound the fourth and fifth terms in (2.19).

Lemma 2.4.6 *There exists $c > 0$, independent of h and $\tilde{h}$, such that for each $e \in E_h$ there holds*

$$h_e \, \|\hat{J}_e[(\boldsymbol{\sigma}_h - \nabla u_h) \cdot \mathbf{t}_T]\|^2_{L^2(e)} \, \leq \, c \, \|\boldsymbol{\sigma}_h - \nabla u_h\|^2_{[L^2(w_e)]^2} \, , \quad (2.46)$$

where $\hat{J}_e[(\boldsymbol{\sigma}_h - \nabla u_h) \cdot \mathbf{t}_T] := \left\{ \begin{array}{ll} J[(\boldsymbol{\sigma}_h - \nabla u_h) \cdot \mathbf{t}_T] & \text{if } e \in E_h(\Omega) \\ (\boldsymbol{\sigma}_h - \nabla u_h) \cdot \mathbf{t}_T & \text{if } e \in E_h(\Gamma) \end{array} \right. .$

Proof. We adapt the proof of Lemma 6.2 in [24]. To this end we first define the function $v_e := \hat{J}_e[(\boldsymbol{\sigma}_h - \nabla u_h)\cdot \mathbf{t}_T]$ on each $e \in E_h$. Then, (2.38) and the fact that $L(v_e) = v_e$ on e, yield

$$c_1^{-1}\,\|v_e\|^2_{L^2(e)} \;\leq\; \|\psi_e^{1/2}\,v_e\|^2_{L^2(e)} \;=\; \int_e \psi_e\,L(v_e)\,\hat{J}_e[(\boldsymbol{\sigma}_h - \nabla u_h)\cdot \mathbf{t}_T]\,. \tag{2.47}$$

Now, integrating by parts on each triangle $T \subseteq w_e$, noting that $\mathrm{curl}(\boldsymbol{\sigma}_h - \nabla u_h) = 0$ in Ω, and employing Cauchy-Schwarz's inequality, we find that

$$\begin{aligned}\int_e \psi_e\,L(v_e)\,\hat{J}_e[(\boldsymbol{\sigma}_h - \nabla u_h)\cdot \mathbf{t}_T] \;&=\; \int_{w_e} \mathbf{curl}(\psi_e\,L(v_e))\cdot(\boldsymbol{\sigma}_h - \nabla u_h)\\ &\leq\; \|\,\mathbf{curl}(\psi_e\,L(v_e))\|_{[L^2(w_e)]^2}\;\|\boldsymbol{\sigma}_h - \nabla u_h\|_{[L^2(w_e)]^2}\,.\end{aligned} \tag{2.48}$$

On the other hand, applying the local inverse inequality to the polynomial $\psi_e\,L(v_e)$ (see Theorem 3.2.6 in [26]), and using the estimate (2.39), and the fact that $0 \leq \psi_e^{1/2} \leq 1$, we deduce that

$$\begin{aligned}\|\,\mathbf{curl}(\psi_e\,L(v_e))\|_{[L^2(w_e)]^2} \;&=\; |\psi_e\,L(v_e)|_{H^1(w_e)} \;\leq\; c\,h_e^{-1}\,\|\psi_e\,L(v_e)\|_{L^2(w_e)}\\ &\leq\; c\,h_e^{-1/2}\,\|\psi_e^{1/2}\,L(v_e)\|_{L^2(e)} \leq\; c\,h_e^{-1/2}\,\|v_e\|_{L^2(e)}\,.\end{aligned} \tag{2.49}$$

Finally, (2.46) follows from (2.47), (2.48), and (2.49). □

As a direct consequence of Lemma 2.4.6, noting that the number of triangles of each w_e is at most 2, and adding and substracting $\boldsymbol{\sigma} = \nabla u$ on the right hand side of (2.46), we deduce now that there exists $C > 0$, independent of h and $\tilde{h}$, such that

$$\sum_{e\in E_h(\Omega)} h_e\,\|J[(\boldsymbol{\sigma}_h - \nabla u_h)\cdot \mathbf{t}_T]\|^2_{L^2(e)} \;\leq\; C\left\{\|\boldsymbol{\sigma} - \boldsymbol{\sigma}_h\|^2_{[L^2(\Omega)]^2} \;+\; |u - u_h|^2_{H^1(\Omega)}\right\}, \tag{2.50}$$

and

$$\sum_{e\in E_h(\Gamma)} h_e\,\|(\boldsymbol{\sigma}_h - \nabla u_h)\cdot \mathbf{t}_T\|^2_{L^2(e)} \;\leq\; C\left\{\|\boldsymbol{\sigma} - \boldsymbol{\sigma}_h\|^2_{[L^2(\Omega)]^2} \;+\; |u - u_h|^2_{H^1(\Omega)}\right\}. \tag{2.51}$$

In order to bound the last term in (2.19) we recall the following result from [35].

Lemma 2.4.7 *There exists $c > 0$, independent of h and $\tilde{h}$, such that*

$$\log[1+C_{\tilde{h}}(\Gamma_N)]\sum_{e\in E_h(\Gamma_N)} \tilde{h}_e\,\|g - \boldsymbol{\sigma}_h\cdot\boldsymbol{\nu}\|^2_{L^2(e)} \leq\; c\left\{\|\boldsymbol{\sigma} - \boldsymbol{\sigma}_h\|^2_{[L^2(\Omega)]^2} + h^2\,\|\mathrm{div}\,(\boldsymbol{\sigma} - \boldsymbol{\sigma}_h)\|^2_{L^2(\Omega)}\right\}.$$

Proof. See Lemma 5.9 and equation (5.25) in [35]. □

It follows easily from the previous lemma that

$$\log[1 + C_{\tilde{h}}(\Gamma_N)] \sum_{e \in E_h(\Gamma_N)} \tilde{h}_e \, \|g - \boldsymbol{\sigma}_h \cdot \boldsymbol{\nu}\|^2_{L^2(e)} \leq \; C \, \|\boldsymbol{\sigma} - \boldsymbol{\sigma}_h\|^2_{H(\mathrm{div}\,;\Omega)} \,. \tag{2.52}$$

Finally, the efficiency estimate of the a posteriori error estimate is a straightforward consequence of (2.40), (2.41), (2.42), (2.50), (2.51) and (2.52).

2.5 A Ritz projection based a posteriori error analysis

In this section we introduce and analyze a second reliable a posteriori error estimate for our boundary value problem. To this end, we now define the Ritz projection of the error with respect to the inner product of $\mathbf{H}$, as the unique $(\bar{\boldsymbol{\sigma}}, \bar{u}) \in \mathbf{H}$ such that

$$\langle (\bar{\boldsymbol{\sigma}}, \bar{u}), (\boldsymbol{\tau}, v) \rangle_{\mathbf{H}} \; = \; A((\boldsymbol{\sigma} - \boldsymbol{\sigma}_h, u - u_h), (\boldsymbol{\tau}, v)) + B((\boldsymbol{\tau}, v), \xi - \xi_{\tilde{h}}) \qquad \forall \, (\boldsymbol{\tau}, v) \in \mathbf{H} \,, \tag{2.53}$$

where $\langle (\bar{\boldsymbol{\sigma}}, \bar{u}), (\boldsymbol{\tau}, v) \rangle_{\mathbf{H}} \; := \; \langle \bar{\boldsymbol{\sigma}}, \boldsymbol{\tau} \rangle_{H(\mathrm{div}\,;\Omega)} \; + \; \langle \bar{u}, v \rangle_{H^1(\Omega)}$, and $\langle \cdot, \cdot \rangle_{H(\mathrm{div}\,;\Omega)}$ and $\langle \cdot, \cdot \rangle_{H^1(\Omega)}$ denote the usual inner products of $H(\mathrm{div}\,;\Omega)$ and $H^1(\Omega)$, respectively. The existence and uniqueness of $(\bar{\boldsymbol{\sigma}}, \bar{u})$ is guaranteed by the fact that the right hand side of (2.53) is a linear and bounded functional on $\mathbf{H}$. The following lemma provides an upper bound for $\|(\bar{\boldsymbol{\sigma}}, \bar{u})\|_{\mathbf{H}}$.

Lemma 2.5.1 *There exists $C > 0$, independent of h and $\tilde{h}$, such that*

$$\|(\bar{\boldsymbol{\sigma}}, \bar{u})\|^2_{\mathbf{H}} \; \leq \; C \left\{ \|f + \mathrm{div}\, \boldsymbol{\sigma}_h\|^2_{L^2(\Omega)} \; + \; \|\boldsymbol{\sigma}_h - \nabla u_h\|^2_{[L^2(\Omega)]^2} \; + \; \|u_h + \xi_{\tilde{h}}\|^2_{H^{1/2}_{00}(\Gamma_N)} \right\} . \tag{2.54}$$

Proof. We see from the first equation in (2.5) that

$$A((\boldsymbol{\sigma}, u), (\boldsymbol{\tau}, v)) \; + \; B((\boldsymbol{\tau}, v), \xi) \; = \; F(\boldsymbol{\tau}, v) \,,$$

and thus (2.53) reduces to

$$\langle (\bar{\boldsymbol{\sigma}}, \bar{u}), (\boldsymbol{\tau}, v) \rangle_{\mathbf{H}} \; = \; F(\boldsymbol{\tau}, v) - A((\boldsymbol{\sigma}_h, u_h), (\boldsymbol{\tau}, v)) - B((\boldsymbol{\tau}, v), \xi_{\tilde{h}}) \qquad \forall \, (\boldsymbol{\tau}, v) \in \mathbf{H} \,. \tag{2.55}$$

It follows, according to the definitions of A, B, and F (cf. (2.6), (2.7), (2.8)), that (2.55) is equivalent to

$$\langle \bar{\boldsymbol{\sigma}}, \boldsymbol{\tau} \rangle_{H(\mathrm{div}\,;\Omega)} = F_1(\boldsymbol{\tau}) \qquad \forall \, \boldsymbol{\tau} \in H(\mathrm{div}\,;\Omega) \,, \tag{2.56}$$

and

$$\langle \bar{u}, v\rangle_{H^1(\Omega)} \,=\, F_2(v) \qquad \forall\, v \in H^1_{\Gamma_D}(\Omega)\,, \tag{2.57}$$

where F_1 and F_2 are the linear and bounded functionals defined by

$$F_1(\boldsymbol{\tau}) \,:=\, -\int_\Omega (f+\mathrm{div}\,\boldsymbol{\sigma}_h)\,\mathrm{div}\,\boldsymbol{\tau} - \int_\Omega \boldsymbol{\sigma}_h\cdot\boldsymbol{\tau} - \int_\Omega u_h\,\mathrm{div}\,\boldsymbol{\tau} \,-\, \frac{1}{2}\int_\Omega (\nabla u_h - \boldsymbol{\sigma}_h)\cdot\boldsymbol{\tau} \,-\, \langle \boldsymbol{\tau}\cdot\boldsymbol{\nu}, \xi_{\tilde{h}}\rangle_{\Gamma_N}\,, \tag{2.58}$$

and

$$F_2(v) \,:=\, \int_\Omega (f + \mathrm{div}\,\boldsymbol{\sigma}_h)\, v \,-\, \frac{1}{2}\int_\Omega (\nabla u_h - \boldsymbol{\sigma}_h)\cdot\nabla v\,. \tag{2.59}$$

In addition, integrating by parts $\displaystyle\int_\Omega u_h\,\mathrm{div}\,\boldsymbol{\tau}$, we observe that F_1 simplifies to

$$F_1(\boldsymbol{\tau}) \,:=\, -\int_\Omega (f + \mathrm{div}\,\boldsymbol{\sigma}_h)\,\mathrm{div}\,\boldsymbol{\tau} - \frac{1}{2}\int_\Omega (\boldsymbol{\sigma}_h - \nabla u_h)\cdot\boldsymbol{\tau} - \langle \boldsymbol{\tau}\cdot\boldsymbol{\nu}, u_h + \xi_{\tilde{h}}\rangle_{\Gamma_N}\,. \tag{2.60}$$

Finally, it is clear from the formulations (2.56) and (2.57) that $\|\bar{\boldsymbol{\sigma}}\|_{H(\mathrm{div};\Omega)} = \|F_1\|_{(H(\mathrm{div};\Omega))'}$ and $\|\bar{u}\|_{H^1(\Omega)} \,=\, \|F_2\|_{(H^1_{\Gamma_D}(\Omega))'}$, whence (2.60) and (2.59) yield, respectively,

$$\|\bar{\boldsymbol{\sigma}}\|^2_{H(\mathrm{div};\Omega)} \,\leq\, c\,\Big\{\|f + \mathrm{div}\,\boldsymbol{\sigma}_h\|^2_{L^2(\Omega)} \;+\; \|\boldsymbol{\sigma}_h - \nabla u_h\|^2_{[L^2(\Omega)]^2} \;+\; \|u_h + \xi_{\tilde{h}}\|^2_{H^{1/2}_{00}(\Gamma_N)}\Big\}\,,$$

and

$$\|\bar{u}\|^2_{H^1(\Omega)} \,\leq\, c\,\Big\{\|f + \mathrm{div}\,\boldsymbol{\sigma}_h\|^2_{L^2(\Omega)} \;+\; \|\boldsymbol{\sigma}_h - \nabla u_h\|^2_{[L^2(\Omega)]^2}\Big\}\,.$$

This provides the required estimate and completes the proof. □

The following theorem establishes a reliable and efficient *quasi-local* a posteriori error estimate $\tilde{\boldsymbol{\theta}}$ for our augmented mixed finite element scheme. It makes use of the continuous dependence result given by (2.10) (cf. Theorem 2.2.1), the Ritz projection $(\bar{\boldsymbol{\sigma}}, \bar{u})$, and the associated upper bound provided by Lemma 2.5.1. The name *quasi-local* refers to the fact that one of the terms defining $\tilde{\boldsymbol{\theta}}$ can not be decomposed into local quantities associated to each triangle $T \in \mathcal{T}_h$ (unless it is either conveniently bounded or previously modified, as we will see below).

Theorem 2.5.1 *Let $((\boldsymbol{\sigma}, u), \xi) \in \mathbf{H}\times Q$ and $((\boldsymbol{\sigma}_h, u_h), \xi_{\tilde{h}}) \in \mathbf{H}_h \times Q_{\tilde{h}}$ be the unique solutions of the continuous and discrete formulations* (2.5) *and* (2.17)*, respectively. Then, there exist positive constants $\tilde{C}_{\mathtt{eff}}$, $\tilde{C}_{\mathtt{rel}}$, independent of h and $\tilde{h}$, such that*

$$\tilde{C}_{\mathtt{eff}}\;\tilde{\boldsymbol{\theta}}^2 \;\leq\; \|((\boldsymbol{\sigma} - \boldsymbol{\sigma}_h, u - u_h), \xi - \xi_{\tilde{h}})\|^2_{\mathbf{H}\times Q} \;\leq\; \tilde{C}_{\mathtt{rel}}\;\tilde{\boldsymbol{\theta}}^2\,, \tag{2.61}$$

where $\tilde{\boldsymbol{\theta}}^2 := \sum_{T\in\mathcal{T}_h} \tilde{\theta}_T^2 \,+\, \|u_h+\xi_{\tilde{h}}\|^2_{H^{1/2}_{00}(\Gamma_N)}$, *and for each* $T\in\mathcal{T}_h$ *we define*

$$\tilde{\theta}_T^2 := \|f+\mathrm{div}\,\boldsymbol{\sigma}_h\|^2_{L^2(T)} + \|\boldsymbol{\sigma}_h-\nabla u_h\|^2_{[L^2(T)]^2} + \log[1+C_{\tilde{h}}(\Gamma_N)] \sum_{e\in E(T)\cap E_h(\Gamma_N)} \tilde{h}_e\,\|g-\boldsymbol{\sigma}_h\cdot\boldsymbol{\nu}\|^2_{L^2(e)}\,.$$

Proof. It is not difficult to see that the first inequality in the continuous dependence result given by (2.10) constitutes a global inf-sup condition for the linear operator arising after adding the two equations of the variational formulation (2.5). Then, applying this estimate to the error $((\boldsymbol{\sigma}-\boldsymbol{\sigma}_h, u-u_h), \xi-\xi_{\tilde{h}}) \in \mathbf{H}$, and using the definition of the Ritz projection (cf. (2.53)), we find that

$$\begin{aligned}
&\|((\boldsymbol{\sigma}-\boldsymbol{\sigma}_h, u-u_h), \xi-\xi_{\tilde{h}})\|_{\mathbf{H}\times Q} \\
\leq\, C \sup_{\substack{((\boldsymbol{\tau},v),\lambda)\in\mathbf{H}\times Q \\ ((\boldsymbol{\tau},v),\lambda)\neq 0}} &\frac{A((\boldsymbol{\sigma}-\boldsymbol{\sigma}_h, u-u_h),(\boldsymbol{\tau},v)) \,+\, B((\boldsymbol{\tau},v),\xi-\xi_{\tilde{h}}) \,+\, B((\boldsymbol{\sigma}-\boldsymbol{\sigma}_h, u-u_h),\lambda)}{\|((\boldsymbol{\tau},v),\lambda)\|_{\mathbf{H}\times Q}} \\
= \, C \sup_{\substack{((\boldsymbol{\tau},v),\lambda)\in\mathbf{H}\times Q \\ ((\boldsymbol{\tau},v),\lambda)\neq 0}} &\frac{\langle(\bar{\boldsymbol{\sigma}},\bar{u}),(\boldsymbol{\tau},v)\rangle_{\mathbf{H}} \,+\, \langle g-\boldsymbol{\sigma}_h\cdot\boldsymbol{\nu},\lambda\rangle_{\Gamma_N}}{\|((\boldsymbol{\tau},v),\lambda)\|_{\mathbf{H}\times Q}}\,,
\end{aligned}$$

which yields

$$\|((\boldsymbol{\sigma}-\boldsymbol{\sigma}_h, u-u_h), \xi-\xi_{\tilde{h}})\|^2_{\mathbf{H}\times Q} \,\leq\, C\left\{\,\|(\bar{\boldsymbol{\sigma}},\bar{u})\|^2_{\mathbf{H}} \,+\, \|g-\boldsymbol{\sigma}_h\cdot\boldsymbol{\nu}\|^2_{H^{-1/2}(\Gamma_N)}\right\}. \quad (2.62)$$

In this way, the reliability of $\tilde{\boldsymbol{\theta}}$, which is given by the right hand side of (2.61), follows from the upper bound (2.54) for the Ritz projection, together with the estimates (2.32) and (2.33) bounding the Neumann residual.

Now, for the efficiency of $\tilde{\boldsymbol{\theta}}$ we proceed as follow. The terms defining $\tilde{\theta}_T^2$ are bounded as in (2.40), (2.41), and (2.52), which gives

$$\sum_{T\in\mathcal{T}} \tilde{\theta}_T^2 \,\leq\, C\left\{\,|u-u_h|^2_{H^1(\Omega)} \,+\, \|\boldsymbol{\sigma}-\boldsymbol{\sigma}_h\|^2_{H(\mathrm{div};\Omega)}\right\}, \quad (2.63)$$

whereas for the second term defining $\tilde{\boldsymbol{\theta}}^2$ we add and substract $\xi = -u|_{\Gamma_N}$, and then apply the trace theorem, to obtain:

$$\|u_h+\xi_{\tilde{h}}\|^2_{H^{1/2}_{00}(\Gamma_N)} \,\leq\, C\left\{\,\|u-u_h\|^2_{H^1(\Omega)} \,+\, \|\xi-\xi_{\tilde{h}}\|^2_{H^{1/2}_{00}(\Gamma_N)}\right\}. \quad (2.64)$$

In this way, (2.63) and (2.64) imply the left hand side of (2.61) and finish the proof. □

At this point we remark that the eventual use of $\tilde{\boldsymbol{\theta}}$ in an adaptive algorithm solving (2.17) would be discouraged by the non-local character of the expression $\|u_h+\xi_{\tilde{h}}\|^2_{H^{1/2}_{00}(\Gamma_N)}$. In order to circumvent this, as mentioned before, we now apply an interpolation argument and replace this term by a suitable upper bound, which yields a reliable and fully local a posteriori error estimate.

Theorem 2.5.2 *There exists a positive constant $\hat{C}_{\mathtt{rel}}$, independent of h and $\tilde{h}$, such that*

$$\|((\boldsymbol{\sigma}-\boldsymbol{\sigma}_h,u-u_h),\xi-\xi_{\tilde{h}})\|^2_{\mathbf{H}\times Q} \leq \hat{C}_{\mathtt{rel}}\,\hat{\boldsymbol{\theta}}^2\,, \tag{2.65}$$

where $\hat{\boldsymbol{\theta}}^2 := \sum_{T\in\mathcal{T}_h}\hat{\theta}^2_T$, *and for each $T\in\mathcal{T}_h$ we define*

$$\hat{\theta}^2_T := \|f+\operatorname{div}\boldsymbol{\sigma}_h\|^2_{L^2(T)} + \|\boldsymbol{\sigma}_h-\nabla u_h\|^2_{[L^2(T)]^2} + \sum_{e\in E(T)\cap E_h(\Gamma_N)}\|u_h+\xi_{\tilde{h}}\|^2_{H^1(e)}$$

$$+ \quad \log[1+C_{\tilde{h}}(\Gamma_N)]\sum_{e\in E(T)\cap E_h(\Gamma_N)}\tilde{h}_e\,\|g-\boldsymbol{\sigma}_h\cdot\boldsymbol{\nu}\|^2_{L^2(e)}\,.$$

Proof. Since $H^{1/2}_{00}(\Gamma_N)$ is the interpolation space with index $1/2$ between $H^1_0(\Gamma_N)$ and $L^2(\Gamma_N)$, there holds

$$\|u_h+\xi_{\tilde{h}}\|^2_{H^{1/2}_{00}(\Gamma_N)} \leq C\left\{\|u_h+\xi_{\tilde{h}}\|_{L^2(\Gamma_N)}\,|u_h+\xi_{\tilde{h}}|_{H^1(\Gamma_N)}\right\}$$

$$\leq C\,\|u_h+\xi_{\tilde{h}}\|^2_{H^1(\Gamma_N)} = C\sum_{e\in E_h(\Gamma_N)}\|u_h+\xi_{\tilde{h}}\|^2_{H^1(e)}\,.$$

This estimate and the upper bound in (2.61) provide (2.65) and complete the proof. □

On the other hand, we now deal differently with the original expression of the functional F_1 in (2.58) and derive an alternative upper bound for the Ritz projection, which can be entirely decomposed into local terms. More precisely, we have the following result.

Lemma 2.5.2 *Let $\bar{u}_h$ be the unique function in a Lagrange finite element subspace X_h of $H^1_{\Gamma_D}(\Omega)$ such that $\bar{u}_h(\mathbf{x})=u_h(\mathbf{x})$ for each node $\mathbf{x}\in\Omega\cup\Gamma_D$, and $\bar{u}_h(\mathbf{x})=-\xi_{\tilde{h}}(\mathbf{x})$ for each node $\mathbf{x}\in\Gamma_N$. Then, there exists $C>0$, independent of h and $\tilde{h}$, such that*

$$\begin{aligned}\|(\bar{\boldsymbol{\sigma}},\bar{u})\|^2_{\mathbf{H}} \leq C\,\Big\{&\|f+\operatorname{div}\boldsymbol{\sigma}_h\|^2_{L^2(\Omega)} + \|\boldsymbol{\sigma}_h-\nabla u_h\|^2_{[L^2(\Omega)]^2}\\ &+\|\boldsymbol{\sigma}_h-\nabla\bar{u}_h\|^2_{[L^2(\Omega)]^2} + \|u_h-\bar{u}_h\|^2_{L^2(\Omega)} + \|\bar{u}_h+\xi_{\tilde{h}}\|^2_{H^{1/2}_{00}(\Gamma_N)}\Big\}\,.\end{aligned} \tag{2.66}$$

Proof. Adding and substrating $\bar{u}_h$ in the term $\displaystyle\int_\Omega u_h \,\mathrm{div}\,\boldsymbol{\tau}$ appearing in the definition of the functional F_1 (cf. (2.58)), and then integrating by parts $\displaystyle\int_\Omega \bar{u}_h \,\mathrm{div}\,\boldsymbol{\tau}$, gives

$$F_1(\boldsymbol{\tau}) := -\int_\Omega (f + \mathrm{div}\,\boldsymbol{\sigma}_h)\,\mathrm{div}\,\boldsymbol{\tau} + \int_\Omega (\nabla \bar{u}_h - \boldsymbol{\sigma}_h)\cdot\boldsymbol{\tau} - \int_\Omega (u_h - \bar{u}_h)\,\mathrm{div}\,\boldsymbol{\tau}$$
$$- \frac{1}{2}\int_\Omega (\nabla u_h - \boldsymbol{\sigma}_h)\cdot\boldsymbol{\tau} - \langle \boldsymbol{\tau}\cdot\boldsymbol{\nu}, \bar{u}_h + \xi_{\tilde{h}}\rangle_{\Gamma_N} \qquad \forall\, \boldsymbol{\tau} \in H(\mathrm{div}\,;\Omega)\,.$$

The rest of the proof proceeds as in Lemma 2.5.1 bounding now $\|F_1\|_{H(\mathrm{div}\,;\Omega)'}$ from the above expression. We omit further details. □

At first glance, the new upper bound (2.66) looks more complicated than (2.54) and yet it does not get rid, apparently, of the non-local term $\|\bar{u}_h + \xi_{\tilde{h}}\|^2_{H^{1/2}_{00}(\Gamma_N)}$. Nevertheless, the fact that the function $\bar{u}_h + \xi_{\tilde{h}}$ now vanishes at the nodes of Γ_N (which was not necessarily the case with u_h) allows us to estimate its $H^{1/2}_{00}(\Gamma_N)$-norm in terms of L^2-local norms on the edges of Γ_N. More precisely, according to Theorem 1 in [23], there holds

$$\|\bar{u}_h + \xi_{\tilde{h}}\|^2_{H^{1/2}_{00}(\Gamma_N)} \le C\,\log[1 + C_h(\Gamma_N)] \sum_{e\in E_h(\Gamma_N)} h_e \left\| \frac{d\bar{u}_h}{d\mathbf{t}_T} + \frac{d\xi_{\tilde{h}}}{d\mathbf{t}_T}\right\|^2_{L^2(e)}, \tag{2.67}$$

where $C_h(\Gamma_N) := \max\left\{\frac{|\Gamma_i|}{|\Gamma_j|} : \quad |i-j| = 1\,,\ i,j \in \{1,...,n\}\right\}$ and $\{\Gamma_1, \Gamma_2, ..., \Gamma_n\}$ is the partition on Γ_N induced by $\mathcal{T}_h$.

In addition, in the particular case in which the finite element subspace X_h is given by (2.16), we easily deduce that $\bar{u}_h + \xi_{\tilde{h}}$ vanishes identically on Γ_N. Indeed, since each edge Γ_i is contained in an edge $\tilde{\Gamma}_j$ and the end points of each $\tilde{\Gamma}_j$ are nodes of $\mathcal{T}_h$, the above statement follows from the fact that $Q_{\tilde{h}}$ (cf. (2.14)) is also piecewise linear on the independent partition $\{\tilde{\Gamma}_1, ..., \tilde{\Gamma}_m\}$ of Γ_N.

On the other hand, since $u_h = \bar{u}_h$ on each $T \in \mathcal{T}_h$ not touching the Neumann boundary Γ_N, we see that $\|u_h - \bar{u}_h\|_{L^2(T)}$ vanishes and $\|\boldsymbol{\sigma}_h - \nabla\bar{u}_h\|^2_{[L^2(T)]^2}$ becomes $\|\boldsymbol{\sigma}_h - \nabla u_h\|^2_{[L^2(T)]^2}$ on these triangles. This property of the auxiliary function $\bar{u}_h$ induces the definition of the following parameter associated to each $T \in \mathcal{T}_h$:

$$\kappa(T) := \begin{cases} 1 & \text{if} \quad \partial T \cap \bar{\Gamma}_N \neq \phi\,, \\ 0 & \text{otherwise}\,. \end{cases} \tag{2.68}$$

Consequently, we are now in a position to establish a reliable and *quasi-efficient* fully local a posteriori error estimate. Here, the *quasi-efficiency* refers to the extra term appearing below on the right hand side of (2.70).

Theorem 2.5.3 *There exist positive constants $C_{\mathtt{rel}}$, $C_{\mathtt{eff}}$, independent of h and $\tilde{h}$, such that*

$$\|((\boldsymbol{\sigma}-\boldsymbol{\sigma}_h,u-u_h),\xi-\xi_{\tilde{h}})\|^2_{\mathbf{H}\times Q} \,\leq\, C_{\mathtt{rel}}\,\boldsymbol{\theta}^2\,, \tag{2.69}$$

and

$$C_{\mathtt{eff}}\,\boldsymbol{\theta}^2 \,\leq\, \|((\boldsymbol{\sigma}-\boldsymbol{\sigma}_h,u-u_h),\xi-\xi_{\tilde{h}})\|^2_{\mathbf{H}\times Q} \,+\, \sum_{T\in\mathcal{T}_h}\kappa(T)\,\|u-\bar{u}_h\|^2_{H^1(T)}\,, \tag{2.70}$$

where $\boldsymbol{\theta}^2 := \displaystyle\sum_{T\in\mathcal{T}_h}\theta^2_T$, *and for each* $T\in\mathcal{T}_h$ *we define*

$$\begin{aligned}\theta^2_T \,:=\, &\|f+\operatorname{div}\boldsymbol{\sigma}_h\|^2_{L^2(T)} \,+\, \|\boldsymbol{\sigma}_h-\nabla u_h\|^2_{[L^2(T)]^2} \,+\, \kappa(T)\,\|\boldsymbol{\sigma}_h-\nabla\bar{u}_h\|^2_{[L^2(T)]^2}\\ &+\,\kappa(T)\,\|u_h-\bar{u}_h\|^2_{L^2(T)} \,+\, \log[1+C_{\tilde{h}}(\Gamma_N)]\sum_{e\in E(T)\cap E_h(\Gamma_N)}\tilde{h}_e\,\|g-\boldsymbol{\sigma}_h\cdot\boldsymbol{\nu}\|^2_{L^2(e)}\\ &+\,\log[1+C_h(\Gamma_N)]\sum_{e\in E(T)\cap E_h(\Gamma_N)}h_e\left\|\frac{d\bar{u}_h}{d\mathbf{t}_T}+\frac{d\xi_{\tilde{h}}}{d\mathbf{t}_T}\right\|^2_{L^2(e)}\,.\end{aligned}$$

In particular, if the finite element subspace X_h is given by (2.16), *θ^2_T simplifies to*

$$\begin{aligned}\theta^2_T \,:=\, &\|f+\operatorname{div}\boldsymbol{\sigma}_h\|^2_{L^2(T)} \,+\, \|\boldsymbol{\sigma}_h-\nabla u_h\|^2_{[L^2(T)]^2} \,+\, \kappa(T)\,\|\boldsymbol{\sigma}_h-\nabla\bar{u}_h\|^2_{[L^2(T)]^2}\\ &+\,\kappa(T)\,\|u_h-\bar{u}_h\|^2_{L^2(T)} \,+\, \log[1+C_{\tilde{h}}(\Gamma_N)]\sum_{e\in E(T)\cap E_h(\Gamma_N)}\tilde{h}_e\,\|g-\boldsymbol{\sigma}_h\cdot\boldsymbol{\nu}\|^2_{L^2(e)}\,.\end{aligned} \tag{2.71}$$

Proof. The reliability of $\boldsymbol{\theta}$ follows easily from (2.62), the estimate for the Neumann residual given by (2.32) and (2.33), the upper bound for the Ritz projection provided by Lemma 2.5.2, and the previous analysis yielding (2.67) and (2.68).

On the other hand, for the quasi-efficiency we first observe, after adding and substrating $\boldsymbol{\sigma}=\nabla u$ in the second and third term defining $\boldsymbol{\theta}_T$, and u in the fourth one, that

$$\begin{aligned}&\|f+\operatorname{div}\boldsymbol{\sigma}_h\|^2_{L^2(T)} \,+\, \|\boldsymbol{\sigma}_h-\nabla u_h\|^2_{[L^2(T)]^2} \,+\, \kappa(T)\,\|\boldsymbol{\sigma}_h-\nabla\bar{u}_h\|^2_{[L^2(T)]^2} \,+\, \kappa(T)\,\|u_h-\bar{u}_h\|^2_{L^2(T)}\\ &\qquad\leq\, C\left\{\,\|\boldsymbol{\sigma}-\boldsymbol{\sigma}_h\|^2_{H(\operatorname{div};T)} \,+\, \|u-u_h\|^2_{H^1(T)} \,+\, \kappa(T)\,\|u-\bar{u}_h\|^2_{H^1(T)}\,\right\}.\end{aligned} \tag{2.72}$$

Next, we know from (2.52) that

$$\log[1+C_{\tilde{h}}(\Gamma_N)]\sum_{e\in E_h(\Gamma_N)}\tilde{h}_e\,\|g-\boldsymbol{\sigma}_h\cdot\boldsymbol{\nu}\|^2_{L^2(e)} \,\leq\, C\,\|\boldsymbol{\sigma}-\boldsymbol{\sigma}_h\|^2_{H(\operatorname{div};\Omega)}\,, \tag{2.73}$$

and applying the same arguments of Lemma 2.4.5 we find that

$$\log[1+C_h(\Gamma_N)]\sum_{e\in E_h(\Gamma_N)} h_e\left\|\frac{d\bar{u}_h}{d\mathbf{t}_T}+\frac{d\xi_{\tilde{h}}}{d\mathbf{t}_T}\right\|^2_{L^2(e)} \leq C\left\{\|\xi-\xi_{\tilde{h}}\|^2_{H_{00}^{1/2}(\Gamma_N)} + \|u-\bar{u}_h\|^2_{H^1(\Omega)}\right\}. \tag{2.74}$$

In this way, (2.70) is a straightforward consequence of (2.72), (2.73), and (2.74). □

2.6 Numerical results

In this section we present several examples illustrating the perfomance of the augmented mixed finite element method (2.17) and the associated adaptive algorithms using the a-posteriori error estimates $\boldsymbol{\eta}$ and $\boldsymbol{\theta}$ (cf. Theorems 2.4.1 and 2.5.3). All the numerical results given below were obtained in a *Compaq Alpha ES40 Parallel Computer* using a Fortran 90 code. The nonsymmetric scheme (2.17) is solved by using a LU factorization method for sparse matrices. In addition, the errors on each triangle are calculated using a 7 points quadrature rule (see p. 314 in [48]).

We begin with some further notations. In what follows, N denotes the number of degrees of freedom defining the subspaces $\mathbf{H}_h$ and $Q_{\tilde{h}}$, that is N:= number of edges of $\mathcal{T}_h$ + number of nodes in $(\bar{\Omega}-\bar{\Gamma}_D)$ + $(m-1)$. We recall here that $\{\tilde{\Gamma}_1,\tilde{\Gamma}_2,...,\tilde{\Gamma}_m\}$ is the independent partition of Γ_N, and, according to the stability condition required in Theorem 2.3.1, we now set a vertex of it every two vertices of the partition on Γ_N inherited from $\mathcal{T}_h$.

On the other hand, the individual and total errors are defined by

$$\mathbf{e}(\boldsymbol{\sigma}) := \|\boldsymbol{\sigma}-\boldsymbol{\sigma}_h\|_{H(\mathrm{div};\Omega)}, \quad \mathbf{e}_0(u) := \|u-u_h\|_{L^2(\Omega)}, \quad \mathbf{e}_1(u) := |u-u_h|_{H^1(\Omega)},$$

$$\mathbf{e}(u) := \|u-u_h\|_{H^1(\Omega)}, \qquad \mathbf{e}(\xi) := \|\xi-\xi_{\tilde{h}}\|_{H_{00}^{1/2}(\Gamma_N)},$$

and

$$\mathbf{e} := \left\{ [\mathbf{e}(\boldsymbol{\sigma})]^2 + [\mathbf{e}(u)]^2 + [\mathbf{e}(\xi)]^2 \right\}^{1/2},$$

where $((\boldsymbol{\sigma},u),\xi)\in\mathbf{H}\times Q$ and $((\boldsymbol{\sigma}_h,u_h),\xi_{\tilde{h}})\in\mathbf{H}_h\times Q_{\tilde{h}}$ are the unique solutions of (2.5) and (2.17), respectively. In addition, we introduce the experimental rates of convergence

$$\mathbf{r}(\boldsymbol{\sigma}) := \frac{\log(\mathbf{e}(\boldsymbol{\sigma})/\mathbf{e}'(\boldsymbol{\sigma}))}{\log(h/h')}, \quad \mathbf{r}_0(u) := \frac{\log(\mathbf{e}_0(u)/\mathbf{e}'_0(u))}{\log(h/h')}, \quad \mathbf{r}_1(u) := \frac{\log(\mathbf{e}_1(u)/\mathbf{e}'_1(u))}{\log(h/h')}.$$

$$\mathbf{r}(u) := \frac{\log(\mathbf{e}(u)/\mathbf{e}'(u))}{\log(h/h')}, \quad \mathbf{r}(\xi) := \frac{\log(\mathbf{e}(\xi)/\mathbf{e}'(\xi))}{\log(h/h')}, \quad \text{and} \quad \mathbf{r}(\mathbf{e}) := \frac{\log(\mathbf{e}/\mathbf{e}')}{\log(h/h')},$$

where $\mathbf{e}(\cdot)$ and $\mathbf{e}'(\cdot)$ (resp. $\mathbf{e}$ and $\mathbf{e}'$ or $\mathbf{e}_j(u)$ and $\mathbf{e}'_j(u)$, $j \in \{0,1\}$) denote the corresponding errors at two consecutive triangulations with mesh sizes h and h', respectively.

We first illustrate the performance of our augmented mixed finite element method (2.17) when a uniform refinement is employed. To this end, we consider three examples of boundary value problems with smooth solutions on the square $\Omega :=]0,1[^2$ with $\Gamma_D := [0,1] \times \{0\} \cup \{0\} \times [0,1]$ and $\Gamma_N := \Gamma - \bar{\Gamma}_D$. We chose the data f and g so that the exact solutions are given by

$$u(\mathbf{x}) := \sin(x_1)\,\sin(x_2)\,, \quad u(\mathbf{x}) := x_1\,x_2\,\sin(x_1^2 + x_2^2)\,, \quad \text{and} \quad u(\mathbf{x}) := \frac{x_1^2\,x_2^2}{x_1^2 + x_2^2 + 5}$$

for each $\mathbf{x} := (x_1, x_2) \in \Omega$, in the Examples 1, 2, and 3, respectively. In Tables 6.1 throughout 6.3 we provide the individual errors, the total error, and the experimental rates of convergence on a sequence of uniform meshes. Given a coarse uniform initial triangulation, each subsequent mesh is obtained from the previous one by dividing each triangle into the four ones arising when connecting the midpoints of its sides. We observe that the rate of convergence $O(h)$ predicted by Theorem 2.3.2 (when $r = 1$) is attained in all the examples, which confirms the a priori error estimate provided by that theorem. Moreover, we also notice a quadratic order of convergence for the error $\mathbf{e}_0(u)$, whose theoretical proof should follow from usual duality arguments.

We now show the performance of the associated adaptive algorithms using the a-posteriori error estimates $\boldsymbol{\eta}$ and $\boldsymbol{\theta}$. In this case, the experimental rate of convergence $\mathbf{r}(\mathbf{e})$ is defined by $\mathbf{r}(\mathbf{e}) := -2\,\dfrac{\log(\mathbf{e}/\mathbf{e}')}{\log(N/N')}$, where $\mathbf{e}$ and $\mathbf{e}'$ denote the total errors at two consecutive triangulations with N and N' degrees of freedom, respectively. In addition, the mesh refinement process follows a standard approach from [50], which considers a parameter $\gamma \in (0,1)$ and reads as follows:

1. Start with a coarse mesh $\mathcal{T}_h$.
2. Solve the discrete problem (2.17) for the actual mesh $\mathcal{T}_h$.
3. Compute η_T (θ_T) for each triangle $T \in \mathcal{T}_h$.
4. Evaluate stopping criterion and decide to finish or go to next step.
5. Use *blue-green* procedure to refine each $T' \in \mathcal{T}_h$ whose indicator $\eta_{T'}$ ($\theta_{T'}$) is greater than or equal to γ times the maximum value of the indicators η_T (θ_T), $T \in \mathcal{T}_h$.

6. Define resulting mesh as actual mesh $\mathcal{T}_h$ and go to step 2.

The examples to be considered for the adaptive algorithms are described as follows. In Example 4 we take $\Omega :=]0,1[^2$, with $\Gamma_D := [0,1]\times\{0\} \cup \{0\}\times[0,1]$ and $\Gamma_N := \Gamma - \bar{\Gamma}_D$, and chose the data f and g so that the exact solution is

$$u(\mathbf{x}) := \frac{x_1 x_2}{(x_1-1)^2+(x_2-1)^2+0.01} \qquad \forall\, \mathbf{x} := (x_1,x_2) \in \Omega\,.$$

We observe that u vanishes at Γ_D and has a boundary layer around the point $(1,1)$.

Next, in Example 5 we consider the L-shaped domain $\Omega :=]-1,1[^2 - [0,1]^2$, with $\Gamma_D := [0,1]\times\{0\} \cup \{0\}\times[0,1]$ and $\Gamma_N := \Gamma - \bar{\Gamma}_D$, and chose the data f and g so that the exact solution, in polar coordinates (r,ϑ), is given by

$$u(r,\vartheta) := r^{2/3}\,\sin\Big(\frac{2\vartheta-\pi}{3}\Big) \qquad \forall\,(r,\vartheta) \in \Omega\,.$$

It is easy to see that u vanishes at Γ_D, which holds for $\vartheta = \pi/2$ and $\vartheta = 2\,\pi$. In addition, because of the power of r, the partial derivatives of u are singular at the origin. According to this singularity, Theorem 2.3.2 yields a rate of convergence of $O(h^{2/3})$ for the augmented mixed finite element scheme (2.17).

In Tables 6.4 throughout 6.7 we provide the errors for each unknown, the total error, the experimental rates of convergence, the a posteriori error estimates $\boldsymbol{\eta}$ and $\boldsymbol{\theta}$, and the corresponding effectivity indices $\mathbf{e}/\boldsymbol{\eta}$ and $\mathbf{e}/\boldsymbol{\theta}$ for the uniform and adaptive refinements. We use $\gamma = 0.5$ and $\gamma = 0.3$ for Examples 4 and 5, respectively. We observe here that the indices $\mathbf{e}/\boldsymbol{\eta}$ and $\mathbf{e}/\boldsymbol{\theta}$ remain always bounded above and below, which confirms the reliability of $\boldsymbol{\eta}$ and $\boldsymbol{\theta}$, and the efficiency of $\boldsymbol{\eta}$. Moreover, this fact provides also numerical evidences for the eventual efficiency of $\boldsymbol{\theta}$. Next, Figures 6.1 and 6.4 show $\mathbf{e}$ versus the degrees of freedom N. As expected, the total error $\mathbf{e}$ of each adaptive algorithm decreases much faster than that of the uniform one. This property is particularly notorious in Example 5 where the experimental rates of convergence of the adaptive algorithms (see Table 6.7) recover the quasi-optimal order h, thus improving the rate $2/3$ obtained with the uniform refinement (see Table 6.6). Finally, Figures 6.2, 6.3, 6.5, and 6.6 display some intermediate meshes obtained with the adaptive refinements. It is important to verify that both algorithms are able to recognize the singularities of the solution u. In particular, this is observed in Example 4 (cf. Figures 6.2 and 6.3) where the adapted meshes are highly refined around $(1,1)$. Similarly, the adapted meshes obtained in Example 5 (cf. Figures

6.5 and 6.6) concentrate the corresponding refinements around the origin. In addition, we notice in Example 5 (see Figure 6.6) that the adaptive algorithm based on $\boldsymbol{\theta}$ also tends to slightly refine in a neighborhood of the Neumann boundary, which should be explained by the terms $\kappa(T)\,\|\boldsymbol{\sigma}_h - \nabla \bar{u}_h\|^2_{[L^2(T)]^2}$ and $\kappa(T)\,\|u_h - \bar{u}_h\|^2_{L^2(T)}$ appearing in the definition of the local indicator θ_T (cf. (2.71)). However, this effect is not observed explicitly in Example 4 (see Figure 6.3) since the point $(1,1)$ (around which the boundary layer holds) lies precisely on the Neumann boundary of the problem.

Table 6.1: Individual errors, total errors, and experimental rates of convergence for a sequence of uniform refinements (Example 1).

h	$\mathbf{e}_0(u)$	$\mathbf{r}_0(u)$	$\mathbf{e}_1(u)$	$\mathbf{r}_1(u)$	$\mathbf{e}(u)$	$\mathbf{r}(u)$
0.5190E+0	0.5623E-1	—	0.2081E+0	—	0.2155E+0	—
0.2595E+0	0.1321E-1	2.0897	0.7601E-1	1.4530	0.7714E-1	1.4821
0.1297E+0	0.3191E-2	2.0484	0.3312E-1	1.1978	0.3327E-1	1.2125
0.6488E-1	0.7880E-3	2.0190	0.1581E-1	1.0675	0.1583E-1	1.0722
0.3244E-1	0.1961E-3	2.0066	0.7801E-2	1.0191	0.7803E-2	1.0205
0.1622E-1	0.4897E-4	2.0016	0.3885E-2	1.0057	0.3885E-2	1.0061
0.8110E-2	0.1252E-4	1.9676	0.1941E-2	1.0011	0.1940E-2	1.0018
h	$\mathbf{e}(\boldsymbol{\sigma})$	$\mathbf{r}(\boldsymbol{\sigma})$	$\mathbf{e}(\xi)$	$\mathbf{r}(\xi)$	$\mathbf{e}$	$\mathbf{r}(\mathbf{e})$
0.5190E+0	0.2519E+0	—	0.2834E+0	—	0.4362E+0	—
0.2595E+0	0.9847E-1	1.3550	0.9987E-1	1.5047	0.1601E+0	1.4460
0.1297E+0	0.4490E-1	1.1323	0.4108E-1	1.2809	0.6936E-1	1.2061
0.6488E-1	0.2178E-1	1.0444	0.1859E-1	1.1446	0.3273E-1	1.0842
0.3244E-1	0.1079E-1	1.0133	0.8786E-2	1.0812	0.1595E-1	1.0370
0.1622E-1	0.5386E-2	1.0024	0.4234E-2	1.0531	0.7876E-2	1.0180
0.8110E-2	0.2691E-2	1.0010	0.2081E-2	1.0247	0.3916E-2	1.0080

Table 6.2: Individual errors, total errors, and experimental rates of convergence for a sequence of uniform refinements (Example 2).

h	$\mathbf{e}_0(u)$	$\mathbf{r}_0(u)$	$\mathbf{e}_1(u)$	$\mathbf{r}_1(u)$	$\mathbf{e}(u)$	$\mathbf{r}(u)$
0.5190E+0	0.2715E+0	—	0.6502E+0	—	0.7946E+0	—
0.2595E+0	0.7662E-1	1.8251	0.3029E+0	1.1020	0.3125E+0	1.3463
0.1297E+0	0.1826E-1	2.0678	0.1109E+0	1.4487	0.1124E+0	1.4743
0.6488E-1	0.4417E-2	2.0489	0.4202E-1	1.4365	0.4225E-1	1.4125
0.3244E-1	0.1089E-2	2.0201	0.1785E-1	1.2351	0.1789E-1	1.2398
0.1622E-1	0.2709E-3	2.0072	0.8334E-2	1.0988	0.8338E-2	1.1013
0.8110E-2	0.6876E-4	1.9781	0.4069E-2	1.0343	0.4070E-2	1.0346
h	$\mathbf{e}(\boldsymbol{\sigma})$	$\mathbf{r}(\boldsymbol{\sigma})$	$\mathbf{e}(\xi)$	$\mathbf{r}(\xi)$	$\mathbf{e}$	$\mathbf{r}(\mathbf{e})$
0.5190E+0	0.1520E+1	—	0.8945E+0	—	0.1899E+1	—
0.2595E+0	0.7674E+0	0.9860	0.4095E+0	1.1272	0.9243E+0	1.0388
0.1297E+0	0.3583E+0	1.0982	0.1504E+0	1.4442	0.4045E+0	1.1915
0.6488E-1	0.1724E+0	1.0561	0.5657E-1	1.4116	0.1863E+0	1.1193
0.3244E-1	0.8503E-1	1.0197	0.2290E-1	1.3046	0.8986E-1	1.0519
0.1622E-1	0.4232E-1	1.0066	0.1009E-1	1.1824	0.4430E-1	1.0203
0.8110E-2	0.2135E-1	0.9871	0.4811E-2	1.0685	0.2205E-1	1.0065

Table 6.3: Individual errors, total errors, and experimental rates of convergence for a sequence of uniform refinements (Example 3).

h	$\mathbf{e}_0(u)$	$\mathbf{r}_0(u)$	$\mathbf{e}_1(u)$	$\mathbf{r}_1(u)$	$\mathbf{e}(u)$	$\mathbf{r}(u)$
0.5190E+0	0.5994E-1	—	0.1489E+0	—	0.1606E+0	—
0.2595E+0	0.1244E-1	2.2685	0.4699E-1	1.6639	0.4861E-1	1.7241
0.1297E+0	0.2956E-2	2.0721	0.1579E-1	1.5724	0.1606E-1	1.5968
0.6488E-1	0.7229E-3	2.0331	0.6021E-2	1.3918	0.6064E-2	1.4060
0.3244E-1	0.1793E-3	2.0114	0.2650E-2	1.1840	0.2656E-2	1.1910
0.1622E-1	0.4472E-4	2.0033	0.1266E-2	1.0657	0.1266E-2	1.0689
0.8110E-2	0.8827E-5	2.3409	0.6237E-3	1.0213	0.6238E-3	1.0211
h	$\mathbf{e}(\boldsymbol{\sigma})$	$\mathbf{r}(\boldsymbol{\sigma})$	$\mathbf{e}(\xi)$	$\mathbf{r}(\xi)$	$\mathbf{e}$	$\mathbf{r}(\mathbf{e})$
0.5190E+0	0.1609E+0	—	0.1751E+0	—	0.2869E+0	—
0.2595E+0	0.5859E-1	1.4574	0.6883E-1	1.3470	0.1026E+0	1.4835
0.1297E+0	0.1881E-1	1.6382	0.2188E-1	1.6525	0.3302E-1	1.6347
0.6488E-1	0.7023E-2	1.4222	0.7924E-2	1.4662	0.1220E-1	1.4374
0.3244E-1	0.3062E-2	1.1976	0.3285E-2	1.2703	0.5218E-2	1.2253
0.1622E-1	0.1459E-2	1.0694	0.1484E-2	1.1464	0.2436E-2	1.0989
0.8110E-2	0.7186E-3	1.0217	0.7162E-3	1.0510	0.1191E-2	1.0323

Table 6.4: Individual errors, total errors, experimental rates of convergence, a posteriori error estimates, and effectivity indices for the uniform refinement (Example 4).

N	$\mathbf{e}(u)$	$\mathbf{e}(\boldsymbol{\sigma})$	$\mathbf{e}(\xi)$	$\mathbf{e}$	$\mathbf{r}(\mathbf{e})$	$\boldsymbol{\eta}$	$\mathbf{e}/\boldsymbol{\eta}$	$\boldsymbol{\theta}$	$\mathbf{e}/\boldsymbol{\theta}$
33	0.86E+2	0.14E+3	0.11E+2	0.20E+3	—	0.17E+3	1.182	0.15E+3	1.282
123	0.94E+2	0.12E+4	0.11E+3	0.12E+4	—	0.12E+4	1.007	0.12E+4	1.008
471	0.26E+2	0.11E+4	0.45E+2	0.11E+4	0.171	0.11E+4	0.998	0.10E+4	1.000
1839	0.19E+2	0.51E+3	0.26E+2	0.51E+3	1.097	0.51E+3	0.992	0.51E+3	0.999
7263	0.93E+1	0.24E+3	0.14E+2	0.24E+3	1.069	0.25E+3	0.990	0.25E+3	0.999
28863	0.45E+1	0.12E+3	0.68E+1	0.12E+3	0.999	0.12E+3	0.991	0.12E+3	1.000
115071	0.22E+1	0.61E+2	0.32E+1	0.61E+2	1.001	0.62E+2	0.992	0.61E+2	1.001

Table 6.5: Individual errors, total errors, experimental rates of convergence, a posteriori error estimates, and effectivity indices for the corresponding adaptive refinements (Example 4).

N	$\mathbf{e}(u)$	$\mathbf{e}(\boldsymbol{\sigma})$	$\mathbf{e}(\xi)$	$\mathbf{e}$	$\mathbf{r}(\mathbf{e})$	$\boldsymbol{\eta}$	$\mathbf{e}/\boldsymbol{\eta}$
33	0.862E+2	0.139E+3	0.107E+3	0.195E+3	——	0.165E+3	1.1824
53	0.114E+3	0.120E+4	0.127E+3	0.121E+4	——	0.120E+4	1.0115
79	0.251E+2	0.107E+4	0.436E+2	0.108E+4	0.5968	0.108E+4	0.9976
107	0.235E+2	0.512E+3	0.447E+2	0.514E+3	4.8641	0.519E+3	0.9901
133	0.221E+2	0.267E+3	0.390E+2	0.271E+3	5.8820	0.279E+3	0.9703
297	0.133E+2	0.145E+3	0.222E+2	0.147E+3	1.5169	0.151E+3	0.9741
746	0.987E+1	0.804E+2	0.163E+2	0.826E+2	1.2576	0.873E+2	0.9461
1102	0.758E+1	0.693E+2	0.114E+2	0.707E+2	0.8003	0.734E+2	0.9623
2731	0.486E+1	0.399E+2	0.770E+1	0.409E+2	1.2016	0.431E+2	0.9494
4691	0.326E+1	0.335E+2	0.468E+1	0.340E+2	0.6863	0.353E+2	0.9631
10592	0.250E+1	0.203E+2	0.348E+1	0.207E+2	1.2152	0.219E+2	0.9471
19711	0.166E+1	0.162E+2	0.226E+1	0.165E+2	0.7423	0.172E+2	0.9562
42671	0.125E+1	0.101E+2	0.161E+1	0.104E+2	1.2029	0.110E+2	0.9406
N	$\mathbf{e}(u)$	$\mathbf{e}(\boldsymbol{\sigma})$	$\mathbf{e}(\xi)$	$\mathbf{e}$	$\mathbf{r}(\mathbf{e})$	$\boldsymbol{\theta}$	$\mathbf{e}/\boldsymbol{\theta}$
33	0.862E+2	0.139E+3	0.107E+2	0.195E+3	——	0.152E+3	1.2821
53	0.114E+3	0.120E+4	0.127E+3	0.121E+4	——	0.119E+4	1.0125
79	0.251E+2	0.107E+4	0.436E+2	0.108E+4	0.5968	0.107E+4	0.9999
107	0.235E+2	0.512E+3	0.447E+2	0.514E+3	4.8641	0.514E+3	0.9988
133	0.221E+2	0.267E+3	0.390E+2	0.271E+3	5.8820	0.273E+3	0.9921
297	0.133E+2	0.145E+3	0.222E+2	0.147E+3	1.5169	0.147E+3	0.9978
649	0.124E+2	0.845E+2	0.209E+2	0.879E+2	1.3217	0.895E+2	0.9812
1140	0.775E+1	0.671E+2	0.112E+2	0.685E+2	0.8875	0.685E+2	0.9995
2605	0.551E+1	0.403E+2	0.864E+1	0.416E+2	1.2092	0.414E+2	1.0016
4939	0.384E+1	0.310E+2	0.566E+1	0.317E+2	0.8419	0.317E+2	0.9986
10486	0.279E+1	0.201E+2	0.379E+1	0.207E+2	1.1393	0.205E+2	1.0045
19592	0.194E+1	0.156E+2	0.255E+1	0.160E+2	0.8294	0.158E+2	1.0044
40545	0.144E+1	0.103E+2	0.185E+1	0.105E+2	1.1444	0.104E+2	1.0066

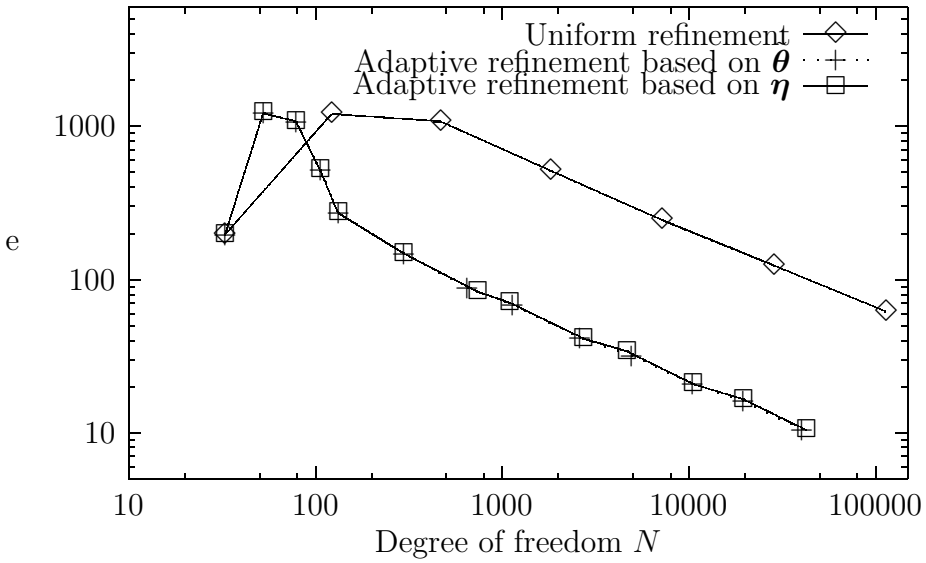

Figure 6.1: $\mathbf{e}$ vs. N for the uniform and adaptive refinements (Example 4).

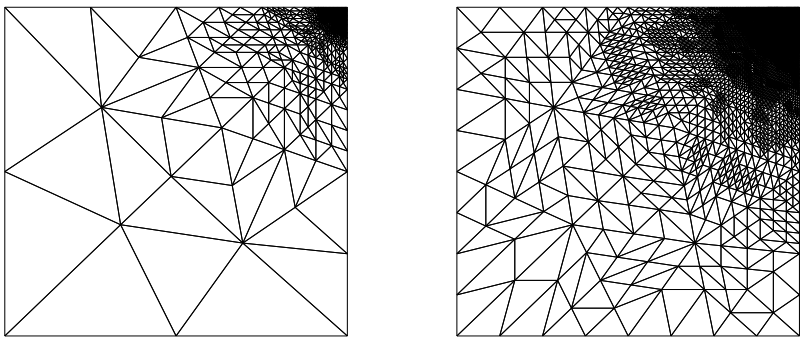

Figure 6.2: Adapted intermediate meshes with 2731 and 42671 degrees of freedom for the adaptive refinement based on $\boldsymbol{\eta}$ (Example 4).

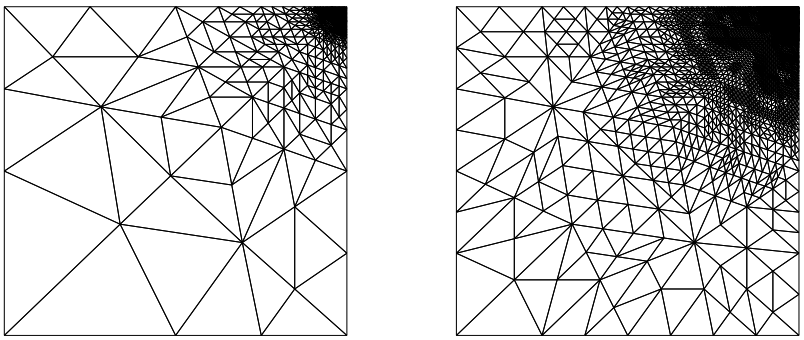

Figure 6.3: Adapted intermediate meshes with 2605 and 40545 degrees of freedom for the adaptive refinement based on $\boldsymbol{\theta}$ (Example 4).

Table 6.6: Individual errors, total errors, experimental rates of convergence, a posteriori error estimates, and effectivity indices for the uniform refinement (Example 5).

N	$\mathbf{e}(u)$	$\mathbf{e}(\boldsymbol{\sigma})$	$\mathbf{e}(\xi)$	$\mathbf{e}$	$\mathbf{r}(\mathbf{e})$	$\boldsymbol{\eta}$	$\mathbf{e}/\boldsymbol{\eta}$	$\boldsymbol{\theta}$	$\mathbf{e}/\boldsymbol{\theta}$
65	0.30E+0	0.28E+0	0.36E+0	0.55E+0	—	0.94E+0	0.585	0.49E+0	1.123
227	0.18E+0	0.18E+0	0.21E+0	0.34E+0	0.767	0.66E+0	0.519	0.28E+0	1.196
839	0.12E+0	0.11E+0	0.13E+0	0.21E+0	0.703	0.43E+0	0.498	0.17E+0	1.207
3215	0.77E-1	0.76E-1	0.83E-1	0.13E+0	0.683	0.28E+0	0.487	0.11E+0	1.205
12575	0.49E-1	0.48E-1	0.51E-1	0.86E-1	0.675	0.18E+0	0.481	0.71E-1	1.202
49727	0.31E-1	0.30E-1	0.32E-1	0.54E-1	0.671	0.11E+0	0.477	0.45E-1	1.199

Table 6.7: Individual errors, total errors, experimental rates of convergence, a posteriori error estimates, and effectivity indices for the corresponding adaptive refinements (Example 5).

N	$\mathbf{e}(u)$	$\mathbf{e}(\boldsymbol{\sigma})$	$\mathbf{e}(\xi)$	$\mathbf{e}$	$\mathbf{r}(\mathbf{e})$	$\boldsymbol{\eta}$	$\mathbf{e}/\boldsymbol{\eta}$
65	0.305E+0	0.288E+0	0.360E+0	0.554E+0	——	0.947E+0	0.5845
196	0.194E+0	0.188E+0	0.232E+0	0.357E+0	0.7962	0.662E+0	0.5385
292	0.141E+0	0.138E+0	0.171E+0	0.261E+0	1.5618	0.487E+0	0.5364
407	0.112E+0	0.110E+0	0.138E+0	0.209E+0	1.3353	0.391E+0	0.5354
821	0.745E-1	0.751E-1	0.894E-1	0.138E+0	1.1795	0.275E+0	0.5038
1117	0.619E-1	0.624E-1	0.744E-1	0.115E+0	1.1965	0.226E+0	0.5091
1740	0.482E-1	0.478E-1	0.558E-1	0.879E-1	1.2158	0.178E+0	0.4924
3066	0.350E-1	0.353E-1	0.408E-1	0.643E-1	1.1052	0.133E+0	0.4821
4569	0.280E-1	0.280E-1	0.317E-1	0.508E-1	1.1816	0.107E+0	0.4713
7347	0.221E-1	0.220E-1	0.250E-1	0.400E-1	1.0025	0.853E-1	0.4692
11772	0.171E-1	0.171E-1	0.193E-1	0.310E-1	1.0877	0.669E-1	0.4630
18062	0.138E-1	0.137E-1	0.152E-1	0.247E-1	1.0519	0.542E-1	0.4566
29069	0.110E-1	0.108E-1	0.121E-1	0.196E-1	0.9655	0.430E-1	0.4570
N	$\mathbf{e}(u)$	$\mathbf{e}(\boldsymbol{\sigma})$	$\mathbf{e}(\xi)$	$\mathbf{e}$	$\mathbf{r}(\mathbf{e})$	$\boldsymbol{\theta}$	$\mathbf{e}/\boldsymbol{\theta}$
65	0.305E+0	0.288E+0	0.3609E+0	0.554E+0	——	0.493E+0	1.1232
218	0.190E+0	0.186E+0	0.2222E+0	0.346E+0	0.7733	0.289E+0	1.1998
278	0.140E+0	0.138E+0	0.1635E+0	0.256E+0	2.4982	0.219E+0	1.1648
443	0.105E+0	0.103E+0	0.1204E+0	0.190E+0	1.2667	0.168E+0	1.1322
721	0.852E-1	0.834E-1	0.9541E-1	0.152E+0	0.9098	0.126E+0	1.2032
1227	0.591E-1	0.586E-1	0.6717E-1	0.107E+0	1.3392	0.907E-1	1.1790
1512	0.521E-1	0.520E-1	0.5788E-1	0.937E-1	1.2689	0.787E-1	1.1894
2571	0.389E-1	0.391E-1	0.4266E-1	0.697E-1	1.1118	0.574E-1	1.2146
3660	0.317E-1	0.317E-1	0.3481E-1	0.568E-1	1.1607	0.468E-1	1.2129
5707	0.249E-1	0.250E-1	0.2683E-1	0.443E-1	1.1171	0.366E-1	1.2099
8721	0.201E-1	0.201E-1	0.2159E-1	0.357E-1	1.0180	0.291E-1	1.2258
13312	0.160E-1	0.162E-1	0.1722E-1	0.286E-1	1.0522	0.233E-1	1.2251
21517	0.125E-1	0.126E-1	0.1329E-1	0.222E-1	1.0527	0.181E-1	1.2249
32613	0.101E-1	0.102E-1	0.1069E-1	0.179E-1	1.0289	0.145E-1	1.2295

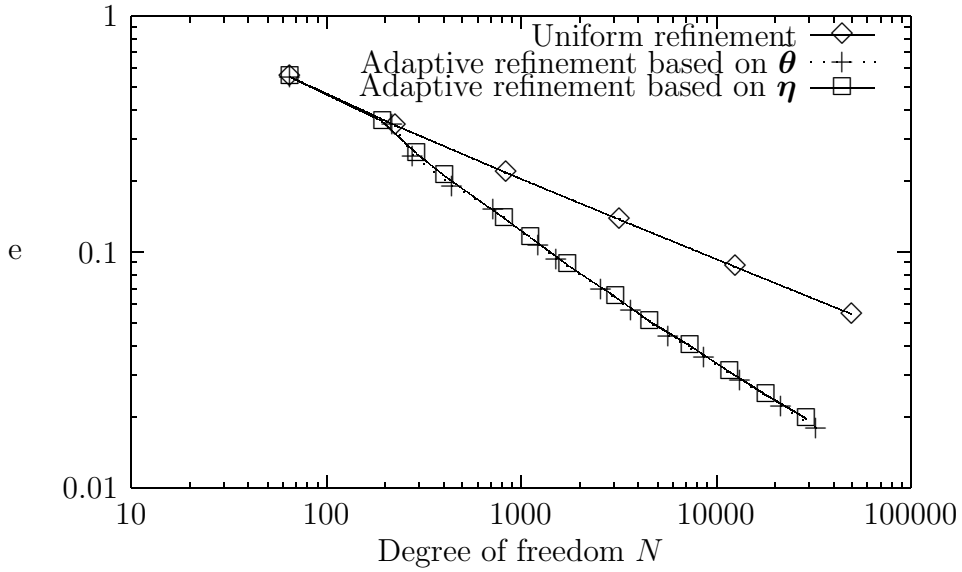

Figure 6.4: **e** vs. N for the uniform and adaptive refinements (Example 5).

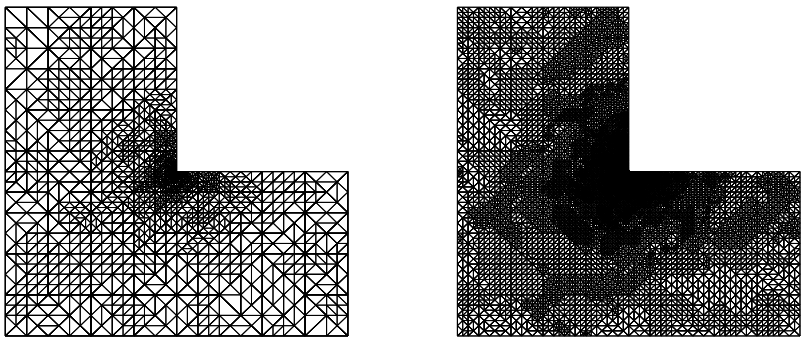

Figure 6.5: Adapted intermediate meshes with 4569 and 29069 degrees of freedom for the adaptive refinement based on $\boldsymbol{\eta}$ (Example 5).

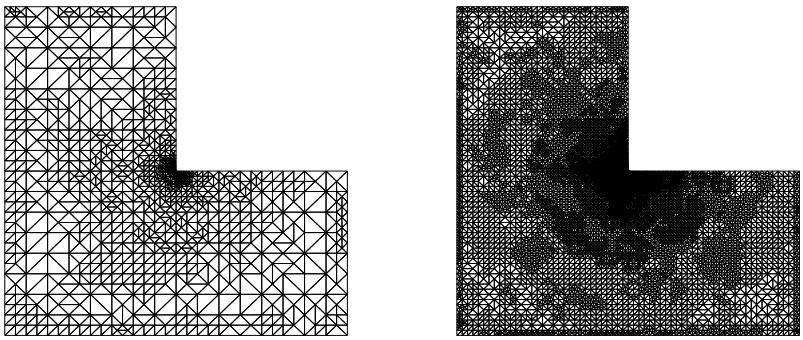

Figure 6.6: Adapted intermediate meshes with 3660 and 32613 degrees of freedom for the adaptive refinement based on $\boldsymbol{\theta}$ (Example 5).

Summarizing, the numerical results presented in this section constitute enough support for the adaptive algorithms being much more efficient than a uniform discretization when solving our augmented mixed finite element scheme.

Chapter 3

A priori and a posteriori error analysis of a wavelet-based stabilization for the mixed finite element method

We use Galerkin least-squares terms and biorthogonal wavelet bases to develop a new stabilized dual-mixed finite element method for second order elliptic equations in divergence form with Neumann boundary conditions. The approach introduces the trace of the solution on the boundary as a new unknown that acts also as a Lagrange multiplier. We show that the resulting stabilized dual-mixed variational formulation and the associated discrete scheme defined with Raviart-Thomas spaces are well posed, and derive the usual a priori error estimates and the corresponding rate of convergence. Furthermore, a reliable and efficient residual based a-posteriori error estimator and a reliable and quasi-efficient one are provided.

3.1 Introduction

In the recent paper [7], the a priori and a posteriori error analysis of an augmented mixed finite element method with Lagrange multipliers, as applied to elliptic equations in divergence form with mixed boundary conditions, is introduced and analyzed. Following [5], the approach in [7] imposes first the essential (Neumann) boundary condition in a weak

sense, which motivates the introduction of a further Lagrange multiplier given precisely by the trace of the solution on the Neumann boundary. Then, the augmented scheme is obtained by including Galerkin-least squares terms arising from the constitutive and equilibrium equations, which, however, still yields a saddle point operator equation as the resulting variational formulation. Hence, the classical Babuška-Brezzi theory is applied to show that the continuous formulation and its associated Galerkin scheme defined with Raviart-Thomas spaces are well-posed. The corresponding a priori error estimates and rates of convergence are also derived. In addition, a reliable and efficient residual based a posteriori error estimator and a reliable and quasi-efficient Ritz projection based one are provided in [7]. It is important to emphasize that the application of the Babuška-Brezzi theory to saddle point variational formulations usually restricts the possible choices of the finite element subspaces and imposes certain assumptions on the corresponding mesh sizes. This is particularly necessary for the verification of the discrete inf-sup conditions, which are the main ingredients of the corresponding analysis.

The purpose of the present chapter, which is an extended and completed version of our previous paper [9], is to modify the method from [7] so that the resulting variational formulation becomes a bounded and elliptic operator equation. In this way, it just suffices to apply the well known Lax-Milgram theorem to prove the well-posedness of the continuous and discrete schemes, and hence no additional conditions on the subspaces or the meshsizes are required. In order to achieve the above, we propose here to further augment the dual-mixed formulation from [7] by incorporating the residual associated to the boundary trace. More precisely, the new feature of our approach lies in the fact that this boundary residual is measured in terms of the equivalent Sobolev norm of order $1/2$ introduced in [12], which is computed by means of biorthogonal wavelet bases. In addition, we also develop here an a posteriori error analysis yielding a reliable and efficient residual based estimator and a reliable and quasi-efficient one. The outline of the chapter is as follows. In Section 3.2 we introduce the stabilized dual-mixed variational formulation and establish its unique solvability and stability. Next, in Section 3.3 we introduce the stabilized mixed finite element scheme and prove that it is also well-posed. We remark here that this scheme makes use of a discrete version of the above mentioned equivalent Sobolev norm, which arises after a suitable finite truncation of the wavelet bases. Finally, in Section 3.4 we provide the a posteriori error analysis of our agumented scheme.

Throughout the rest of the chapter we utilize the standard terminology for Sobolev

spaces, norms, and seminorms, and use C and c, with or without subscripts, bars, tildes or hats, to denote generic positive constants independent of the discretization parameters, which may take different values at different places.

3.2 The stabilized dual-mixed variational formulation

We first describe the model boundary value problem and introduce the corresponding dual-mixed variational formulation. Let Ω be a simply connected and bounded domain in $\mathbb{R}^2$ with polygonal boundary Γ. Then, given $f \in L^2(\Omega)$, $g \in H^{-1/2}(\Gamma)$, and a matrix valued function $\boldsymbol{\kappa} \in C(\overline{\Omega})$, we seek $u \in H^1(\Omega)$ such that

$$-\mathrm{div}\,(\boldsymbol{\kappa}\nabla u) \,=\, f \quad \text{in} \quad \Omega\,, \quad \boldsymbol{\kappa}\nabla u\cdot\boldsymbol{\nu} \,=\, g \quad \text{on} \quad \Gamma\,, \tag{3.1}$$

where $\boldsymbol{\nu}$ is the unit outward normal vector to Γ. We assume that $\boldsymbol{\kappa}$ is symmetric and uniformly positive definite, that is, there exists $\alpha > 0$ such that

$$(\boldsymbol{\kappa}(\mathbf{x})\,\mathbf{z})\cdot\mathbf{z} \geq \alpha\|\mathbf{z}\|^2 \qquad \forall\,\mathbf{x}\in\Omega \qquad \forall\,\mathbf{z}\in\mathbb{R}^2\,, \tag{3.2}$$

which implies the following inequalities

$$(\boldsymbol{\kappa}^{-1}(\mathbf{x})\,\mathbf{z})\cdot\mathbf{z} \geq \alpha\|\boldsymbol{\kappa}^{-1}(\mathbf{x})\,\mathbf{z}\|^2 \quad \text{and} \quad \|\boldsymbol{\kappa}^{-1}(\mathbf{x})\,\mathbf{z}\| \leq \frac{1}{\alpha}\|\mathbf{z}\| \quad \forall\,\mathbf{x}\in\Omega,\ \ \forall\,\mathbf{z}\in\mathbb{R}^2. \tag{3.3}$$

Moreover, since $\boldsymbol{\kappa} \in C(\overline{\Omega})$ we deduce the existence of $M > 0$ such that

$$\|\boldsymbol{\kappa}(\mathbf{x})\,\mathbf{z}\| \leq M\|\mathbf{z}\| \quad \text{and} \quad \frac{1}{M}\|\mathbf{z}\| \leq \|\boldsymbol{\kappa}^{-1}(\mathbf{x})\,\mathbf{z}\| \quad \forall\,\mathbf{x}\in\Omega,\ \ \forall\,\mathbf{z}\in\mathbb{R}^2, \tag{3.4}$$

which, together with the first inequality of (3.3), implies that

$$(\boldsymbol{\kappa}^{-1}(\mathbf{x})\,\mathbf{z})\cdot\mathbf{z} \geq \frac{\alpha}{M^2}\|\mathbf{z}\|^2 \quad \forall\,\mathbf{x}\in\Omega,\ \ \forall\,\mathbf{z}\in\mathbb{R}^2. \tag{3.5}$$

In what follows, we assume that the data f and g satisfy the usual compatibility condition $\displaystyle\int_\Omega f \,+\, \int_\Gamma g \,=\, 0$. Furthermore, since the solution of (3.1) is not unique, we introduce the additional condition $\displaystyle\int_\Omega u \,=\, 0$, and define the space $L^2_0(\Omega) := \left\{ q \in L^2(\Omega) \,:\, \int_\Omega q \,=\, 0 \right\}$. Next, we define the unknowns $\boldsymbol{\sigma} := \boldsymbol{\kappa}\nabla u \quad \text{in} \quad \Omega$ and $\xi := u|_\Gamma \quad \text{on} \quad \Gamma$, and proceeding in

the usual way (see [5] for details) we arrive at the following mixed variational formulation of (3.1): Find $(\boldsymbol{\sigma}, (u, \xi)) \in H \times Q$ such that

$$\begin{aligned} a(\boldsymbol{\sigma}, \boldsymbol{\tau}) + b(\boldsymbol{\tau}, (u, \xi)) &= 0 \qquad \forall\, \boldsymbol{\tau} \in H\,, \\ -b(\boldsymbol{\sigma}, (v, \lambda)) &= \int_\Omega f\, v \,+\, \langle g, \lambda \rangle \qquad \forall\, (v, \lambda) \in Q\,, \end{aligned} \tag{3.6}$$

where $H := H(\mathrm{div}\,; \Omega)$, $Q := L^2_0(\Omega) \times H^{1/2}(\Gamma)$, and the bilinear forms $a : H \times H \to \mathbb{R}$ and $b : H \times Q \to \mathbb{R}$ are given by

$$a(\boldsymbol{\zeta}, \boldsymbol{\tau}) := \int_\Omega (\boldsymbol{\kappa}^{-1} \boldsymbol{\zeta}) \cdot \boldsymbol{\tau} \quad \text{and} \quad b(\boldsymbol{\tau}, (v, \lambda)) := \int_\Omega v\, \mathrm{div}\,(\boldsymbol{\tau}) \,-\, \langle \boldsymbol{\tau} \cdot \boldsymbol{\nu}, \lambda \rangle\,, \tag{3.7}$$

for all $\boldsymbol{\zeta}$, $\boldsymbol{\tau} \in H$ and for all $(v, \lambda) \in Q$. Concerning the solvability of (3.6) we have the following result, which is a slight variation of Theorem 2.1 in [5].

Theorem 3.2.1 *There exists a unique solution $(\boldsymbol{\sigma}, (u, \xi)) \in H \times Q$ to the Problem (3.6), and the following continuous dependence result holds*

$$\|(\boldsymbol{\sigma}, (u, \xi))\|_{H \times Q} \leq C \Big\{ \|f\|_{L^2(\Omega)} + \|g\|_{H^{-1/2}(\Gamma)} \Big\}\,.$$

Proof. It follows similarly to the proof of Theorem 2.1 in [5]. We omit further details. □

We now proceed as in [9, 12] and define an equivalent inner product in $H^{1/2}(\Gamma)$. To this end, let $\mathbf{I} = \cup_{j \geq 0} I_j$ be the countable union of finite sets I_j and consider a couple of biorthogonal wavelet bases for $L^2(\Gamma)$, denoted by $\{\psi_i\}_{i \in \mathbf{I}}$ and $\{\tilde{\psi}_i\}_{i \in \mathbf{I}}$, satisfying the following properties:

i) Any function $\lambda \in L^2(\Gamma)$ can be expended in terms of both bases as follows:

$$\lambda \,=\, \sum_{i \in \mathbf{I}} \langle \lambda, \tilde{\psi}_i \rangle_{L^2(\Gamma)}\, \psi_i \,=\, \sum_{i \in \mathbf{I}} \langle \lambda, \psi_i \rangle_{L^2(\Gamma)}\, \tilde{\psi}_i\,.$$

ii) There exist positive constants c_1 and c_2 such that for any $\lambda \in H^{1/2}(\Gamma)$ there holds:

$$c_1\, \|\lambda\|^2_{H^{1/2}(\Gamma)} \,\leq\, \sum_{j \geq 0} 2^j \sum_{i \in I_j} |\langle \lambda, \psi_i \rangle_{L^2(\Gamma)}|^2 \,\leq\, c_2\, \|\lambda\|^2_{H^{1/2}(\Gamma)}\,. \tag{3.8}$$

At this point we refer to [22, 29, 43] for the description and construction of such bases. Then, we introduce the bilinear form $(\cdot, \cdot)_{1/2} : H^{1/2}(\Gamma) \times H^{1/2}(\Gamma) \to \mathbb{R}$ defined by

$$(\lambda, \mu)_{1/2} \,=\, \sum_{j \geq 0} 2^j \sum_{i \in I_j} \langle \lambda, \psi_i \rangle_{L^2(\Gamma)}\, \langle \mu, \psi_i \rangle_{L^2(\Gamma)} \qquad \forall\, \lambda,\, \mu \in H^{1/2}(\Gamma)\,, \tag{3.9}$$

which, from (3.8), constitutes an inner product in $H^{1/2}(\Gamma)$ with induced norm $|||\cdot|||_{1/2}$ equivalent to the usual norm $\|\cdot\|_{H^{1/2}(\Gamma)}$.

In what follows we let $\mathbf{H} := H(\mathrm{div}\,;\Omega) \times M \times H^{1/2}(\Gamma)$, where $M := H^1(\Omega) \cap L^2_0(\Omega)$. Then, we consider positive parameters $(\delta_1, \delta_2, \delta_3)$, to be determined, and propose the following augmented variational formulation: Find $(\boldsymbol{\sigma}, u, \xi) \in \mathbf{H}$ such that

$$A((\boldsymbol{\sigma}, u, \xi), (\boldsymbol{\tau}, v, \lambda)) \,=\, F(\boldsymbol{\tau}, v, \lambda) \qquad \forall\, (\boldsymbol{\tau}, v, \lambda) \in \mathbf{H}\,, \tag{3.10}$$

where the bilinear form $A : \mathbf{H} \times \mathbf{H} \to \mathbb{R}$ and the functional $F : \mathbf{H} \to \mathbb{R}$ are defined as follows

$$\begin{aligned} A((\boldsymbol{\zeta}, w, \mu), (\boldsymbol{\tau}, v, \lambda)) \,:=\, & \int_\Omega (\boldsymbol{\kappa}^{-1}\boldsymbol{\zeta}) \cdot \boldsymbol{\tau} \,+\, \int_\Omega w\, \mathrm{div}\,(\boldsymbol{\tau}) \,-\, \langle \boldsymbol{\tau}\cdot\boldsymbol{\nu}, \mu\rangle \\ & - \int_\Omega v\, \mathrm{div}\,(\boldsymbol{\zeta}) \,+\, \langle \boldsymbol{\zeta}\cdot\boldsymbol{\nu}, \lambda\rangle \,+\, \delta_1\, (\mu - w, \lambda - v)_{1/2} \\ & + \delta_2 \int_\Omega (\boldsymbol{\kappa}\nabla w - \boldsymbol{\zeta}) \cdot (\nabla v + \boldsymbol{\kappa}^{-1}\boldsymbol{\tau}) \,+\, \delta_3 \int_\Omega \mathrm{div}\,(\boldsymbol{\zeta})\, \mathrm{div}\,(\boldsymbol{\tau})\,, \end{aligned} \tag{3.11}$$

and

$$F(\boldsymbol{\tau}, v, \lambda) \,=\, \int_\Omega f\, v\, dx \,-\, \delta_3 \int_\Omega f\, \mathrm{div}\,(\boldsymbol{\tau})\, dx \,+\, \langle g, \lambda\rangle\,, \tag{3.12}$$

for all $(\boldsymbol{\zeta}, w, \mu)$, $(\boldsymbol{\tau}, v, \lambda) \in \mathbf{H}$. The idea is to choose $(\delta_1, \delta_2, \delta_3)$ so that (3.10) satisfies the hypotheses of the Lax-Milgram Lemma. To this end, we now let $\|\cdot\|_{\mathbf{H}}$ be the product norm on $\mathbf{H}$, denote by c_t the norm of the usual trace operator acting from $H^1(\Omega)$ onto $H^{1/2}(\Gamma)$, and let $\overline{c} > 0$ such that $|v|^2_{H^1(\Omega)} \geq \overline{c}\, \|v\|^2_{H^1(\Omega)}$ for all $v \in M$. The following lemma establishes the $\mathbf{H}$-ellipticity of A.

Lemma 3.2.1 *Let $(\delta_1, \delta_2, \delta_3) \in \mathbb{R}^3$ such that $0 < \delta_1 < \frac{\delta_2 \alpha \overline{c}}{c_1 c_t^2}$, $0 < \delta_2 < 1$ and $0 < \delta_3$. Then, there exists $C_1 > 0$, depending only on α, M, $\overline{c}$, δ_1, δ_2, δ_3, c_t, and c_1, such that*

$$A((\boldsymbol{\tau}, v, \lambda), (\boldsymbol{\tau}, v, \lambda)) \,\geq C_1 \|(\boldsymbol{\tau}, v, \lambda)\|^2_{\mathbf{H}} \qquad \forall\, (\boldsymbol{\tau}, v, \lambda) \,\in\, \mathbf{H}\,. \tag{3.13}$$

Proof. According to the definition of A (cf. (3.11)) and the symmetry of $\boldsymbol{\kappa}$, we obtain

$$\begin{aligned} A((\boldsymbol{\tau}, v, \lambda), (\boldsymbol{\tau}, v, \lambda)) = \, & (1 - \delta_2) \int_\Omega (\boldsymbol{\kappa}^{-1}\boldsymbol{\tau}) \cdot \boldsymbol{\tau} \,+\, \delta_1\, |||\lambda - v|||^2_{1/2} \\ & + \delta_3\, \|\mathrm{div}\,(\boldsymbol{\tau})\|^2_{L^2(\Omega)} \,+\, \delta_2 \int_\Omega (\boldsymbol{\kappa}\nabla v) \cdot \nabla v\,, \end{aligned}$$

which, using (3.8), (3.5) and (3.2), yields

$$A((\boldsymbol{\tau},v,\lambda),(\boldsymbol{\tau},v,\lambda)) \geq (1-\delta_2)\frac{\alpha}{M^2}\|\boldsymbol{\tau}\|^2_{L^2(\Omega)} + \delta_3\,\|\mathrm{div}\,(\boldsymbol{\tau})\|^2_{L^2(\Omega)}$$
$$+\ \delta_2\,\alpha\,|v|^2_{H^1(\Omega)} + c_1\,\delta_1\,\|\lambda - v\|^2_{H^{1/2}(\Gamma)}\,.$$

On the other hand, using that $\|\lambda - v\|^2_{H^{1/2}(\Gamma)} \geq \frac{1}{2}\|\lambda\|^2_{H^{1/2}(\Gamma)} - \|v\|^2_{H^{1/2}(\Gamma)}$, the trace theorem, and the above mentioned equivalence between $|\cdot|_{H^1(\Omega)}$ and $\|\cdot\|_{H^1(\Omega)}$, we deduce that

$$A((\boldsymbol{\tau},v,\lambda),(\boldsymbol{\tau},v,\lambda)) \ \geq\ (1-\delta_2)\,\frac{\alpha}{M^2}\|\boldsymbol{\tau}\|^2_{L^2(\Omega)} + \delta_3\,\|\mathrm{div}\,(\boldsymbol{\tau})\|^2_{L^2(\Omega)}$$
$$+\,(\delta_2\,\alpha\,\overline{c} - c_1\,\delta_1\,c_t^2)\,\|v\|^2_{H^1(\Omega)} \ +\ \frac{c_1\delta_1}{2}\|\lambda\|^2_{H^{1/2}(\Gamma)}\,.$$

Thus, defining $\alpha_1 := (1-\delta_2)\,\frac{\alpha}{M^2}$ and $\alpha_2 := \delta_2\alpha\overline{c} - c_1\delta_1 c_t^2$, we complete the proof by taking $C_1 = \min\{\alpha_1,\ \alpha_2,\ \frac{\delta_1 c_1}{2},\ \delta_3\}$. □

Theorem 3.2.2 *Assume the same hypotheses of Lemma* 3.2.1. *Then, the Problem* (3.10) *has a unique solution* $(\boldsymbol{\sigma},u,\xi)\in\mathbf{H}$*, and there exists* $C>0$ *such that*

$$\|(\boldsymbol{\sigma},u,\xi)\|_{\mathbf{H}} \leq C\Big\{\|f\|_{L^2(\Omega)} + \|g\|_{H^{-1/2}(\Gamma)}\Big\}\,.$$

Proof. From Lemma 2.1 in [9] we know that the bilinear form A and the functional F are bounded. Then, the proof follows straightforwardly from Lemma 3.2.1 and the Lax-Milgram Theorem. □

3.3 The stabilized mixed finite element scheme

Let $\{\mathcal{T}_h\}_{h>0}$ be a regular family of triangulations of $\bar{\Omega}$ made of straight side triangles T of diameter h_T such that $h := \max\{\,h_T :\ T\in\mathcal{T}_h\,\}$. For each $T\in\mathcal{T}_h$ we let $\mathrm{RT}_0(T)$ be the local Raviart-Thomas space of lowest order (cf. Section 2.3). Then, the finite element subspace $H_h^{\boldsymbol{\sigma}}$ for the unknown $\boldsymbol{\sigma}\in H(\mathrm{div}\,;\Omega)$ is defined as

$$H_h^{\boldsymbol{\sigma}} := \{\,\boldsymbol{\tau}_h\in H(\mathrm{div}\,;\Omega) :\quad \boldsymbol{\tau}_h|_T\in\mathrm{RT}_0(T)\quad\forall\,T\in\mathcal{T}_h\,\}\,. \tag{3.14}$$

Hereafter, given a non-negative integer k and a subset S of $\mathbb{R}^2$, $\mathbf{P}_k(S)$ stands for the space of polynomials defined on S of degree $\leq k$.

Next, we introduce the space of continuous piecewise linear functions

$$H_h^u := \{v_h\in C(\overline{\Omega}) :\quad v_h|_T\in\mathbf{P}_1(T)\quad\forall\,T\in\mathcal{T}_h\,\}\,, \tag{3.15}$$

and define the finite element subspace of M as $M_h := H_h^u \cap L_0^2(\Omega)$.

For the unknown $\xi \in H^{1/2}(\Gamma)$, we consider the finite element subspace H_h^ξ defined by

$$H_h^\xi := \{\, \lambda_h \in C(\Gamma) : \quad \lambda_h|_{\Gamma_j} \in \mathbf{P}_1(\Gamma_j) \quad \forall\, j \in \{1, \ldots, m\}\}\,, \tag{3.16}$$

where $\{\Gamma_1, \ldots, \Gamma_m\}$ is the partition on Γ induced by the triangulation $\mathcal{T}_h$.

On the other hand, we need to approximate the bilinear form $(\cdot,\cdot)_{1/2}$ (cf. (3.9)) by a suitable finite sum. For this purpose, we introduce the bilinear form $(\cdot,\cdot)_{1/2,N} : H^{1/2}(\Gamma) \times H^{1/2}(\Gamma) \to \mathbb{R}$ defined as follows

$$(\lambda,\mu)_{1/2,N} := \sum_{j=0}^{N} 2^j \sum_{i\in I_j} \langle \lambda, \psi_i\rangle_{L^2(\Gamma)}\, \langle \mu, \psi_i\rangle_{L^2(\Gamma)} \quad \forall\, \lambda,\ \mu \in H^{1/2}(\Gamma)\,, \tag{3.17}$$

and observe from (3.8) that for any $\lambda \in H^{1/2}(\Gamma)$ there holds

$$(\lambda,\lambda)_{1/2,N} = \sum_{j=0}^{N} 2^j \sum_{i\in I_j} |\, \langle \lambda, \psi_i\rangle_{L^2(\Gamma)}|^2 \;\le\; c_2\, \|\lambda\|^2_{H^{1/2}(\Gamma)}\,.$$

Hence, the following lemma completes the equivalence between $(\cdot,\cdot)_{1/2,N}$ and $\|\cdot\|_{H^{1/2}(\Gamma)}$ in the finite element subspace H_h^ξ.

Lemma 3.3.1 *There exists $N = N(h) \in \mathbb{N}$ and a positive constant $\tilde{C}$, independent of h, such that*

$$(\lambda_h,\lambda_h)_{1/2,N} \;=\; \sum_{j=0}^{N} 2^j \sum_{i\in I_j} |\langle \lambda_h, \psi_i\rangle_{L^2(\Gamma)}|^2 \;\ge\; \tilde{C}\, \|\lambda_h\|^2_{H^{1/2}(\Gamma)} \quad \forall\, \lambda_h \in H_h^\xi\,. \tag{3.18}$$

Proof. Since $H_h^\xi \subset H^1(\Gamma)$, there holds the following inverse inequality

$$\|\lambda_h\|_{H^1(\Gamma)} \;\le\; C\, h^{-1/2}\, \|\lambda_h\|_{H^{1/2}(\Gamma)} \quad \forall\, \lambda_h \in H_h^\xi\,.$$

Therefore, (3.18) follows from a straightforward application of Lemma 6 in [12]. □

We now define $\mathbf{H}_h := H_h^{\boldsymbol{\sigma}} \times M_h \times H_h^\xi$ and introduce a nonconforming Galerkin formulation of (3.10): Find $(\boldsymbol{\sigma}_h, u_h, \xi_h) \in \mathbf{H}_h$ such that

$$A_h((\boldsymbol{\sigma}_h, u_h, \xi_h), (\boldsymbol{\tau}_h, v_h, \lambda_h)) \;=\; F(\boldsymbol{\tau}_h, v_h, \lambda_h) \qquad \forall\, (\boldsymbol{\tau}_h, v_h, \lambda_h) \in \mathbf{H}_h\,, \tag{3.19}$$

where $A_h : \mathbf{H} \times \mathbf{H} \to \mathbb{R}$ is the bilinear form resulting from A when $(\cdot,\cdot)_{1/2}$ is replaced by $(\cdot,\cdot)_{1/2,N(h)}$, that is

$$\begin{aligned} A_h((\boldsymbol{\zeta}, w, \mu), (\boldsymbol{\tau}, v, \lambda)) \,:=\, & \int_\Omega (\boldsymbol{\kappa}^{-1}\boldsymbol{\zeta}) \cdot \boldsymbol{\tau} \,+\, \int_\Omega w \,\mathrm{div}\,(\boldsymbol{\tau}) \,-\, \langle \boldsymbol{\tau}\cdot\boldsymbol{\nu}, \mu\rangle \\ & - \int_\Omega v \,\mathrm{div}\,(\boldsymbol{\zeta}) \,+\, \langle \boldsymbol{\zeta}\cdot\boldsymbol{\nu}, \lambda\rangle \,+\, \delta_1\,(\mu - w, \lambda - v)_{1/2,N(h)} \\ & + \,\delta_2 \int_\Omega (\boldsymbol{\kappa}\nabla w - \boldsymbol{\zeta}) \cdot (\nabla v + \boldsymbol{\kappa}^{-1}\boldsymbol{\tau}) \,+\, \delta_3 \int_\Omega \mathrm{div}\,(\boldsymbol{\zeta})\,\mathrm{div}\,(\boldsymbol{\tau})\,, \end{aligned} \tag{3.20}$$

for all $(\boldsymbol{\zeta}, w, \mu)$, $(\boldsymbol{\tau}, v, \lambda)) \in \mathbf{H}$.

Theorem 3.3.1 *Problem* (3.19) *has a unique solution* $(\boldsymbol{\sigma}_h, u_h, \xi_h) \in \mathbf{H}_h$ *and there exists* $C > 0$*, independent of* h*, such that*

$$\|(\boldsymbol{\sigma}_h, u_h, \xi_h)\|_{\mathbf{H}} \,\leq\, C \left\{ \|f\|_{L^2(\Omega)} + \|g\|_{H^{-1/2}(\Gamma)} \right\}. \tag{3.21}$$

Proof. The boundedness of A_h follows easily from that of A. In addition, the estimate (3.18) (cf. Lemma 3.3.1) yields the $\mathbf{H}_h$-ellipticity of A_h. Hence, the proof is also a consequence of the Lax-Milgram Theorem. □

Theorem 3.3.2 *Let* $(\boldsymbol{\sigma}, u, \xi) \in \mathbf{H}$ *and* $(\boldsymbol{\sigma}_h, u_h, \xi_h) \in \mathbf{H}_h$ *be the solutions of* (3.10) *and* (3.19)*, respectively. Then there exists a constant* $C > 0$*, independent of* h*, such that*

$$\|(\boldsymbol{\sigma} - \boldsymbol{\sigma}_h, u - u_h, \xi - \xi_h)\|_{\mathbf{H}} \,\leq\, C \inf_{(\boldsymbol{\tau}_h, v_h, \lambda_h) \in \mathbf{H}_h} \|(\boldsymbol{\sigma} - \boldsymbol{\tau}_h, u - v_h, \xi - \lambda_h)\|_{\mathbf{H}}\,. \tag{3.22}$$

Proof. Since the assumptions of the Second Strang Lemma are fullfilled, we have that there exists $C > 0$, independent of h, such that

$$\begin{aligned} C\,\|(\boldsymbol{\sigma} - \boldsymbol{\sigma}_h, u - u_h, \xi - \xi_h)\|_{\mathbf{H}} \,\leq\, & \inf_{(\boldsymbol{\tau}_h, v_h, \lambda_h) \in \mathbf{H}_h} \|(\boldsymbol{\sigma} - \boldsymbol{\tau}_h, u - v_h, \xi - \lambda_h)\|_{\mathbf{H}} \\ & + \sup_{\substack{(\boldsymbol{\tau}_h, v_h, \lambda_h) \in \mathbf{H}_h \\ (\boldsymbol{\tau}_h, v_h, \lambda_h) \neq 0}} \frac{A_h((\boldsymbol{\sigma}, u, \xi), (\boldsymbol{\tau}_h, v_h, \lambda_h)) - F(\boldsymbol{\tau}_h, v_h, \lambda_h)}{\|(\boldsymbol{\tau}_h, v_h, \lambda_h)\|_{\mathbf{H}}}\,. \end{aligned} \tag{3.23}$$

But, inspecting the functional F (cf. (3.12)) and making use of the properties of the exact solution $(\boldsymbol{\sigma}, u, \xi) \in \mathbf{H}$, we easily find that

$$A_h((\boldsymbol{\sigma}, u, \xi), (\boldsymbol{\tau}_h, v_h, \lambda_h)) \,=\, F(\boldsymbol{\tau}_h, v_h, \lambda_h)\,,$$

which finishes the proof. □

The analysis of the Galerkin scheme is completed with the following result on the rate of convergence.

Theorem 3.3.3 *Let* $(\boldsymbol{\sigma}, u, \xi)$ *and* $(\boldsymbol{\sigma}_h, u_h, \xi_h)$ *be the unique solutions of the continuous and discrete stabilized formulations* (3.10) *and* (3.19)*, respectively. Assume that* $f = \operatorname{div}\boldsymbol{\sigma} \in H^r(\Omega)$*,* $u \in H^{1+r}(\Omega)$*. Then there exists* $C > 0$*, independent of* h*, such that*

$$\|(\boldsymbol{\sigma}, u, \xi) - (\boldsymbol{\sigma}_h, u_h, \xi_h)\|_{\mathbf{H}}$$

$$\leq C\, h^r \left\{ \|\boldsymbol{\sigma}\|_{[H^r(\Omega)]^2} + \|\operatorname{div}\boldsymbol{\sigma}\|_{H^r(\Omega)} + \|u\|_{H^{1+r}(\Omega)} + \|\xi\|_{H^{1/2+r}(\Gamma)} \right\}.$$

Proof. It follows from Theorem 3.3.2, the standard approximation properties of the subspaces involved, and suitable interpolation theorems in the corresponding Sobolev spaces. □

We end this section by remarking that, for implementation purposes, the vanishing average condition required by the elements of M_h can be imposed as a Lagrange multiplier. In other words, we consider the following modified discrete scheme: Find $(\boldsymbol{\sigma}_h, u_h, \xi_h, \varphi_h) \in H_h^{\boldsymbol{\sigma}} \times H_h^u \times H_h^\xi \times \mathbb{R}$ such that

$$\begin{aligned} A_h((\boldsymbol{\sigma}_h, u_h, \xi_h), (\boldsymbol{\tau}_h, v_h, \lambda_h)) + \varphi_h \int_\Omega v_h\, dx &= F(\boldsymbol{\tau}_h, v_h, \gamma_h)\,, \\ \psi_h \int_\Omega u_h\, dx &= 0\,, \end{aligned} \tag{3.24}$$

for all $(\boldsymbol{\tau}_h, v_h, \lambda_h, \psi_h) \in H_h^{\boldsymbol{\sigma}} \times H_h^u \times H_h^\xi \times \mathbb{R}$. The next theorem establishes the equivalence between the variational problems (3.19) and (3.24).

Theorem 3.3.4

i) Let $(\boldsymbol{\sigma}_h, u_h, \xi_h) \in \mathbf{H}_h$ *be the solution of* (3.19)*. Then* $(\boldsymbol{\sigma}_h, u_h, \xi_h, 0)$ *is a solution of* (3.24)*.*

ii) Let $(\boldsymbol{\sigma}_h, u_h, \xi_h, \varphi_h) \in H_h^{\boldsymbol{\sigma}} \times H_h^u \times H_h^\xi \times \mathbb{R}$ *be a solution of* (3.24)*. Then* $\varphi_h = 0$ *and* $(\boldsymbol{\sigma}_h, u_h, \xi_h)$ *is the solution of* (3.19)*.*

Proof. We first observe, according to the definition of A_h (cf. (3.20)), that for each $(\boldsymbol{\tau}, v, \lambda) \in H(\mathrm{div}\,;\Omega) \times H^1(\Omega) \times H^{1/2}(\Gamma)$ there holds

$$A_h((\boldsymbol{\tau}, v, \lambda), (0, 1, 1)) = 0 \qquad \forall\, (\boldsymbol{\tau}, v, \lambda) \in H(\mathrm{div}\,;\Omega) \times H^1(\Omega) \times H^{1/2}(\Gamma)\,. \tag{3.25}$$

Now, let $(\boldsymbol{\sigma}_h, u_h, \xi_h) \in \mathbf{H}_h$ be the solution of (3.19), and let $(\boldsymbol{\tau}_h, v_h, \lambda_h) \in H_h^{\boldsymbol{\sigma}} \times H_h^u \times H_h^\xi$. We write $v_h = v_{0h} + d_h$, $\lambda_h = \lambda_{0h} + d_h$, with $v_{0h} \in M_h$, $\lambda_{0h} \in H_h^\xi$ and $d_h \in \mathbb{R}$, and observe that $(\boldsymbol{\tau}_h, v_{0h}, \lambda_{0h}) \in H_h$, whence (3.12), (3.19) and (3.25) yield

$$F(\boldsymbol{\tau}_h, v_h, \lambda_h) = F(\boldsymbol{\tau}_h, v_{0h}, \lambda_{0h}) = A_h((\boldsymbol{\sigma}_h, u_h, \xi_h), (\boldsymbol{\tau}_h, v_{0h}, \lambda_{0h})) = A_h((\boldsymbol{\sigma}_h, u_h, \xi_h), (\boldsymbol{\tau}_h, v_h, \lambda_h))$$

This identity and the fact that u_h clearly satisfies the second equation of (3.24), show that $(\boldsymbol{\sigma}, u_h, \xi_h, 0)$ is indeed a solution of (3.24).

Conversely, let $(\boldsymbol{\sigma}_h, u_h, \xi_h, \varphi_h) \in H_h^{\boldsymbol{\sigma}} \times H_h^u \times H_h^\xi \times \mathbb{R}$ be a solution of (3.24). Then taking $(\boldsymbol{\tau}_h, v_h, \lambda_h) = (0, 1, 1)$ in the first equation of (3.24) and using (3.12) and (3.25), we find that $\varphi_h = 0$, whence $(\boldsymbol{\sigma}_h, u_h, \lambda_h)$ becomes the solution of (3.24). □

3.4 The a posteriori error analysis

In this section we develop a residual based a posteriori error analysis for (3.10)-(3.19). Let us first introduce some notations. We let $E(T)$ be the set of edges of $T \in \mathcal{T}_h$, and let E_h be the set of all edges of the triangulation $\mathcal{T}_h$. Then we can write $E_h = E_h(\Omega) \cup E_h(\Gamma)$, where $E_h(\Omega) := \{e \in E_h :\ e \subseteq \Omega\}$, $E_h(\Gamma) := \{e \in E_h :\ e \subseteq \Gamma\}$. In what follows, h_T and h_e stand for the diameters of triangle $T \in \mathcal{T}_h$ and edge $e \in E_h$, respectively. Also, given a vector valued function $\boldsymbol{\tau} := (\tau_1, \tau_2)^{\mathtt{t}}$ defined in Ω, an edge $e \in E(T) \cap E_h(\Omega)$, and the unit tangential vector $\mathbf{t}_T$ along e, we let $J[\boldsymbol{\tau} \cdot \mathbf{t}_T]$ be the corresponding jump across e, that is $J[\boldsymbol{\tau} \cdot \mathbf{t}_T] := (\boldsymbol{\tau}_T - \boldsymbol{\tau}_{T'})|_e \cdot \mathbf{t}_T$, where T' is the other triangle of $\mathcal{T}_h$ having e as edge. Here, the tangential vector $\mathbf{t}_T$ is given by $(-\nu_2, \nu_1)^{\mathtt{t}}$ where $\boldsymbol{\nu}_T := (\nu_1, \nu_2)^{\mathtt{t}}$ is the unit outward normal to ∂T. Finally, we let $\mathrm{curl}(\boldsymbol{\tau})$ be the scalar $\frac{\partial \tau_2}{\partial x_1} - \frac{\partial \tau_1}{\partial x_2}$.

Now, let $I_h : H^1(\Omega) \to H_h^u$ be the usual Clément interpolation operator (see [27]). The local approximation properties of I_h are collected in Lemma 2.4.1.

The following theorem establishes a reliable and efficient *quasi-local* a posteriori error estimator for our stabilized mixed finite element scheme. The name *quasi-local* refers to the fact that one of the terms defining the estimator can not be decomposed into local quantities associated to each triangle $T \in \mathcal{T}_h$. However, it can be either conveniently bounded, or previously modified, as we will show below.

Theorem 3.4.1 *Let $(\boldsymbol{\sigma}, u, \xi) \in \mathbf{H}$ and $(\boldsymbol{\sigma}_h, u_h, \xi_h) \in \mathbf{H}_h$ be the unique solutions of the continuous and discrete formulations* (3.10) *and* (3.19)*. Assume that $\boldsymbol{\kappa} \in C^1(\Omega)$ and the Neumann data $g \in L^2(\Gamma)$. Then there exists $C_{\mathtt{eff}}$, $C_{\mathtt{rel}} > 0$, independent of h, such that*

$$C_{\mathtt{eff}}\, \tilde{\boldsymbol{\theta}}^2 \leq \|(\boldsymbol{\sigma} - \boldsymbol{\sigma}_h, u - u_h, \xi - \xi_h)\|^2_{\mathbf{H}} \leq C_{\mathtt{rel}}\, \tilde{\boldsymbol{\theta}}^2\,, \tag{3.26}$$

where $\tilde{\boldsymbol{\theta}}^2 := \displaystyle\sum_{T \in \mathcal{T}_h} \tilde{\theta}_T^2 + \|\xi_h - u_h\|^2_{H^{1/2}(\Gamma)}$ *and*

$$\tilde{\theta}_T^2 := \|f + \operatorname{div} \boldsymbol{\sigma}_h\|^2_{L^2(T)} + \|\boldsymbol{\kappa}\, \nabla u_h - \boldsymbol{\sigma}_h\|^2_{L^2(T)} + \sum_{e \in E(T) \cap E_h(\Gamma)} h_e \left\| \frac{du_h}{d\mathbf{t}_T} - \frac{d\xi_h}{d\mathbf{t}_T} \right\|^2_{L^2(e)}$$

$$+ \sum_{e \in E(T) \cap E_h(\Omega)} h_e \|J[(\nabla u_h - \boldsymbol{\kappa}^{-1}\boldsymbol{\sigma}_h) \cdot \mathbf{t}_T]\|^2_{L^2(e)} + \sum_{e \in E(T) \cap E_h(\Gamma)} h_e \|(\nabla u_h - \boldsymbol{\kappa}^{-1}\boldsymbol{\sigma}_h) \cdot \mathbf{t}_T\|^2_{L^2(e)}$$

$$+ h_T^2\, \|\operatorname{curl}(\boldsymbol{\kappa}^{-1}\boldsymbol{\sigma}_h)\|^2_{L^2(T)} + \log[1 + C_h(\Gamma)]\, h \sum_{e \in E(T) \cap E_h(\Gamma)} \|g - \boldsymbol{\sigma}_h \cdot \boldsymbol{\nu}\|^2_{L^2(e)}\,, \tag{3.27}$$

with $C_h(\Gamma) := \max\left\{ \frac{|\Gamma_i|}{|\Gamma_j|} : \quad |i-j| = 1\,,\ i,j \in \{1,...,m\} \right\}$.

The proof of Theorem 3.4.1 is separated into the two parts given by the next subsections.

3.4.1 Reliability of the a posteriori error estimate $\tilde{\boldsymbol{\theta}}$

We first define the spaces

$$H_0 := \{\boldsymbol{\tau} \in H(\operatorname{div}; \Omega) : \quad \operatorname{div} \boldsymbol{\tau} = 0 \quad \text{in} \quad \Omega\,, \quad \boldsymbol{\tau} \cdot \boldsymbol{\nu} = 0 \quad \text{on} \quad \Gamma\}\,,$$

and $\mathbf{H}_0 := H_0 \times H^1(\Omega) \times H^{1/2}(\Gamma)$. Then we have the following technical result.

Lemma 3.4.1 *There exists $C > 0$, independent of h, such that*

$$C\|(\boldsymbol{\sigma} - \boldsymbol{\sigma}_h, u - u_h, \xi - \xi_h)\|_{\mathbf{H}} \leq \sup_{\substack{(\boldsymbol{\tau}, v, \lambda) \in \mathbf{H}_0 \\ (\boldsymbol{\tau}, v, \lambda) \neq 0}} \frac{A((\boldsymbol{\sigma} - \boldsymbol{\sigma}_h, u - u_h, \xi - \xi_h), (\boldsymbol{\tau}, v, \lambda))}{\|(\boldsymbol{\tau}, v, \lambda)\|_{\mathbf{H}}}$$

$$+ \quad \|f + \operatorname{div} \boldsymbol{\sigma}_h\|_{L^2(\Omega)} + \|g - \boldsymbol{\sigma}_h \cdot \boldsymbol{\nu}\|_{H^{-1/2}(\Gamma)}\,.$$

Proof. Let $\boldsymbol{\sigma}^* := \nabla z \in H(\operatorname{div}; \Omega)$, where $z \in H^1(\Omega)$ is the unique weak solution of the boundary value problem

$$-\Delta z = f + \operatorname{div} \boldsymbol{\sigma}_h \quad \text{in} \quad \Omega\,, \quad \frac{\partial z}{\partial \boldsymbol{\nu}} = g - \boldsymbol{\sigma}_h \cdot \boldsymbol{\nu} \quad \text{on} \quad \Gamma\,, \quad \int_\Omega z = 0\,. \tag{3.28}$$

Note that there holds $\int_\Gamma (g - \boldsymbol{\sigma}_h \cdot \boldsymbol{\nu}) + \int_\Omega (f + \operatorname{div} \boldsymbol{\sigma}_h) = 0$, which is the compatibility condition required for the well-posedness of (3.28). It is not difficult to see that $(\boldsymbol{\sigma} - \boldsymbol{\sigma}_h - \boldsymbol{\sigma}^*)$ belongs to $\mathbf{H}_0$ and the corresponding continuous dependence result establishes the existence of a constant $C > 0$ such that

$$\|\boldsymbol{\sigma}^*\|_{H(\operatorname{div};\Omega)} \leq C \Big\{ \|f + \operatorname{div} \boldsymbol{\sigma}_h\|_{L^2(\Omega)} + \|g - \boldsymbol{\sigma}_h \cdot \boldsymbol{\nu}\|_{H^{-1/2}(\Gamma)} \Big\} . \tag{3.29}$$

Now, the strong coercivity and boundedness of A yield

$$\begin{aligned}
& C_1 \, \|(\boldsymbol{\sigma} - \boldsymbol{\sigma}_h - \boldsymbol{\sigma}^*, u - u_h, \xi - \xi_h)\|^2_{\mathbf{H}} \\
& \leq A((\boldsymbol{\sigma} - \boldsymbol{\sigma}_h - \boldsymbol{\sigma}^*, u - u_h, \xi - \xi_h), (\boldsymbol{\sigma} - \boldsymbol{\sigma}_h - \boldsymbol{\sigma}^*, u - u_h, \xi - \xi_h)) \\
& = A((\boldsymbol{\sigma} - \boldsymbol{\sigma}_h, u - u_h, \xi - \xi_h), (\boldsymbol{\sigma} - \boldsymbol{\sigma}_h - \boldsymbol{\sigma}^*, u - u_h, \xi - \xi_h)) \\
& \qquad - A((\boldsymbol{\sigma}^*, 0, 0), (\boldsymbol{\sigma} - \boldsymbol{\sigma}_h - \boldsymbol{\sigma}^*, u - u_h, \xi - \xi_h)) \\
& \leq A((\boldsymbol{\sigma} - \boldsymbol{\sigma}_h, u - u_h, \xi - \xi_h), (\boldsymbol{\sigma} - \boldsymbol{\sigma}_h - \boldsymbol{\sigma}^*, u - u_h, \xi - \xi_h)) \\
& \qquad + \|A\| \, \|\boldsymbol{\sigma}^*\|_{H(\operatorname{div};\Omega)} \, \|(\boldsymbol{\sigma} - \boldsymbol{\sigma}_h - \boldsymbol{\sigma}^*, u - u_h, \xi - \xi_h)\|_{\mathbf{H}} ,
\end{aligned}$$

which, dividing by $\|(\boldsymbol{\sigma} - \boldsymbol{\sigma}_h - \boldsymbol{\sigma}^*, u - u_h, \xi - \xi_h)\|_{\mathbf{H}}$, and then taking supremum on $\mathbf{H}_0$, implies that

$$\begin{aligned}
& C \, \|(\boldsymbol{\sigma} - \boldsymbol{\sigma}_h - \boldsymbol{\sigma}^*, u - u_h, \xi - \xi_h)\|_{\mathbf{H}} \\
& \leq \sup_{\substack{(\boldsymbol{\tau}, v, \lambda) \in \mathbf{H}_0 \\ (\boldsymbol{\tau}, v, \lambda) \neq 0}} \frac{A((\boldsymbol{\sigma} - \boldsymbol{\sigma}_h, u - u_h, \xi - \xi_h), (\boldsymbol{\tau}, v, \lambda))}{\|(\boldsymbol{\tau}, v, \lambda)\|_{\mathbf{H}}} + \|\boldsymbol{\sigma}^*\|_{H(\operatorname{div};\Omega)} .
\end{aligned} \tag{3.30}$$

Finally, noting that

$$\|(\boldsymbol{\sigma} - \boldsymbol{\sigma}_h, u - u_h, \xi - \xi_h)\|_{\mathbf{H}} \leq \|(\boldsymbol{\sigma} - \boldsymbol{\sigma}_h - \boldsymbol{\sigma}^*, u - u_h, \xi - \xi_h)\|_{\mathbf{H}} + \|\boldsymbol{\sigma}^*\|_{H(\operatorname{div};\Omega)} ,$$

and applying the estimates (3.29) and (3.30), we complete the proof. □

The next lemma gives an upper bound for the supremum appearing in Lemma 3.4.1.

Lemma 3.4.2 *Assume that $\boldsymbol{\kappa} \in C^1(\Omega)$. Then there exists $C > 0$, independent of h, such that*

$$\begin{aligned}
& \sup_{\substack{(\boldsymbol{\tau}, v, \lambda) \in \mathbf{H}_0 \\ (\boldsymbol{\tau}, v, \lambda) \neq 0}} \frac{A((\boldsymbol{\sigma} - \boldsymbol{\sigma}_h, u - u_h, \xi - \xi_h), (\boldsymbol{\tau}, v, \lambda))}{\|(\boldsymbol{\tau}, v, \lambda)\|_{\mathbf{H}}} \\
& \leq C \left\{ \sum_{T \in \mathcal{T}_h} \hat{\theta}^2_T + \|g - \boldsymbol{\sigma}_h \cdot \boldsymbol{\nu}\|^2_{H^{-1/2}(\Gamma)} + \|\xi_h - u_h\|^2_{H^{1/2}(\Gamma)} \right\}^{1/2}
\end{aligned}$$

where for any triangle $T \in \mathcal{T}_h$ we define

$$\hat{\theta}_T^2 := \|f + \operatorname{div} \boldsymbol{\sigma}_h\|_{L^2(T)}^2 + \|\boldsymbol{\kappa}\,\nabla u_h - \boldsymbol{\sigma}_h\|_{L^2(T)}^2$$

$$+ h_T^2 \,\|\operatorname{curl}(\boldsymbol{\kappa}^{-1}\boldsymbol{\sigma}_h)\|_{L^2(T)}^2 + \sum_{e \in E(T) \cap E_h(\Omega)} h_e \,\|J[(\nabla u_h - \boldsymbol{\kappa}^{-1}\boldsymbol{\sigma}_h)\cdot \mathbf{t}_T]\|_{L^2(e)}^2$$

$$+ \sum_{e \in E(T) \cap E_h(\Gamma)} h_e \,\|(\nabla u_h - \boldsymbol{\kappa}^{-1}\boldsymbol{\sigma}_h)\cdot \mathbf{t}_T\|_{L^2(e)}^2 + \sum_{e \in E(T) \cap E_h(\Gamma)} h_e \left\| \frac{du_h}{d\mathbf{t}_T} - \frac{d\xi_h}{d\mathbf{t}_T} \right\|_{L^2(e)}^2 . \tag{3.31}$$

Proof. Let $(\boldsymbol{\tau}, v, \lambda) \in \mathbf{H}_0$ such that $(\boldsymbol{\tau}, v, \lambda) \neq 0$. Since $\operatorname{div}(\boldsymbol{\tau}) = 0$ in Ω and Ω is connected, there exists $\varphi \in H^1(\Omega)$ such that $\int_\Omega \varphi = 0$ and $\boldsymbol{\tau} = \mathbf{curl}(\varphi) := \begin{pmatrix} -\frac{\partial \varphi}{\partial x_2} \\ \frac{\partial \varphi}{\partial x_1} \end{pmatrix}$. Then, denoting by φ_h the Clément interpolant of φ and defining $\boldsymbol{\tau}_h := \mathbf{curl}\,\varphi_h$, we get that $\boldsymbol{\tau}_h \in H_h^{\boldsymbol{\sigma}}$, $\operatorname{div} \boldsymbol{\tau}_h = 0$ in Ω, and $\boldsymbol{\tau} - \boldsymbol{\tau}_h = \mathbf{curl}(\varphi - \varphi_h)$.

Next, from the first equations of (3.10) and (3.19) we find that

$$A((\boldsymbol{\sigma}, u, \xi), (\boldsymbol{\tau} - \boldsymbol{\tau}_h, v, \lambda)) = F(\boldsymbol{\tau} - \boldsymbol{\tau}_h, v, \lambda)\,,$$

and

$$A((\boldsymbol{\sigma} - \boldsymbol{\sigma}_h, u - u_h, \xi - \xi_h), (\boldsymbol{\tau}_h, 0, 0)) = 0\,,$$

which gives

$$A((\boldsymbol{\sigma} - \boldsymbol{\sigma}_h, u - u_h, \xi - \xi_h), (\boldsymbol{\tau}, v, \lambda)) = A((\boldsymbol{\sigma} - \boldsymbol{\sigma}_h, u - u_h, \xi - \xi_h), (\boldsymbol{\tau} - \boldsymbol{\tau}_h, v, \lambda))$$

$$= F(\boldsymbol{\tau} - \boldsymbol{\tau}_h, v, \lambda) - A((\boldsymbol{\sigma}_h, u_h, \xi_h), (\boldsymbol{\tau} - \boldsymbol{\tau}_h, v, \lambda))\,.$$

Then, employing the definition of F (cf. (3.12)), developing $A((\boldsymbol{\sigma}_h, u_h, \xi_h), (\boldsymbol{\tau} - \boldsymbol{\tau}_h, v, \lambda))$, integrating by parts in Ω, using that $\operatorname{div}(\boldsymbol{\tau} - \boldsymbol{\tau}_h) = 0$ in Ω and that $\boldsymbol{\tau} - \boldsymbol{\tau}_h = \mathbf{curl}(\varphi - \varphi_h)$ in Ω, and reordering the resulting terms, we arrive at

$$A((\boldsymbol{\sigma} - \boldsymbol{\sigma}_h, u - u_h, \xi - \xi_h), (\boldsymbol{\tau}, v, \lambda)) = \int_\Omega (f + \operatorname{div} \boldsymbol{\sigma}_h)\, v + \langle g - \boldsymbol{\sigma}_h \cdot \boldsymbol{\nu}, \lambda \rangle$$

$$+ (1 + \delta_2) \int_\Omega (\nabla u_h - \boldsymbol{\kappa}^{-1}\boldsymbol{\sigma}_h) \cdot \mathbf{curl}(\varphi - \varphi_h) - \langle \mathbf{curl}(\varphi - \varphi_h) \cdot \boldsymbol{\nu}, u_h - \xi_h \rangle$$

$$- \delta_2 \int_\Omega \nabla v \cdot (\boldsymbol{\kappa} \nabla u_h - \boldsymbol{\sigma}_h) - \delta_1 (\xi_h - u_h, \lambda - v)_{1/2}\,. \tag{3.32}$$

On the other hand, using that $\int_\Omega = \sum_{T\in\mathcal{T}_h}\int_T$, integrating by parts on each triangle $T \in \mathcal{T}_h$, and noting that $\mathrm{curl}(\nabla u_h) = 0$ in T, we deduce that

$$\int_\Omega (\nabla u_h - \boldsymbol{\kappa}^{-1}\boldsymbol{\sigma}_h)\cdot \mathbf{curl}(\varphi-\varphi_h) \;=\; \sum_{T\in\mathcal{T}_h}\int_T (\nabla u_h - \boldsymbol{\kappa}^{-1}\boldsymbol{\sigma}_h)\cdot \mathbf{curl}(\varphi-\varphi_h)$$

$$= \sum_{T\in\mathcal{T}_h}\left\{ \int_T \mathrm{curl}(\boldsymbol{\kappa}^{-1}\boldsymbol{\sigma}_h)(\varphi-\varphi_h) \;+\; \frac{1}{2}\sum_{e\in E(T)\cap E_h(\Omega)} \langle J[\nabla u_h - \boldsymbol{\kappa}^{-1}\boldsymbol{\sigma}_h]\cdot \mathbf{t}_T, \varphi-\varphi_h\rangle_{L^2(e)} \right.$$

$$\left. + \sum_{e\in E(T)\cap E_h(\Gamma)} \langle (\nabla u_h - \boldsymbol{\kappa}^{-1}\boldsymbol{\sigma}_h)\cdot \mathbf{t}_T, \varphi-\varphi_h\rangle_{L^2(e)} \right\}. \tag{3.33}$$

Then, applying the Cauchy-Schwarz inequality, the estimates from Lemma 2.4.1, and the fact that the number of triangles in $\Delta(T)$ and $\Delta(e)$ are bounded, we find that the terms of (3.33) are bounded as follows

$$\left| \sum_{T\in\mathcal{T}_h}\int_T \mathrm{curl}(\boldsymbol{\kappa}^{-1}\boldsymbol{\sigma}_h)\,(\varphi-\varphi_h) \right|$$

$$\leq\; C\left\{ \sum_{T\in\mathcal{T}_h} h_T^2 \,\|\,\mathrm{curl}(\boldsymbol{\kappa}^{-1}\boldsymbol{\sigma}_h)\|^2_{L^2(T)} \right\}^{1/2} \|\varphi\|_{H^1(\Omega)}\,, \tag{3.34}$$

$$\left| \sum_{T\in\mathcal{T}_h}\sum_{e\in E(T)\cap E_h(\Omega)} \langle J[\nabla u_h - \boldsymbol{\kappa}^{-1}\boldsymbol{\sigma}_h]\cdot \mathbf{t}_T, \varphi-\varphi_h\rangle_{L^2(e)} \right|$$

$$\leq C\left\{ \sum_{T\in\mathcal{T}_h}\sum_{e\in E(T)\cap E_h(\Omega)} h_e \,\|J[\nabla u_h - \boldsymbol{\kappa}^{-1}\boldsymbol{\sigma}_h]\cdot \mathbf{t}_T\|^2_{L^2(e)} \right\}^{1/2} \|\varphi\|_{H^1(\Omega)}\,, \tag{3.35}$$

and

$$\left| \sum_{T\in\mathcal{T}_h}\sum_{e\in E(T)\cap E_h(\Gamma)} \langle (\nabla u_h - \boldsymbol{\kappa}^{-1}\boldsymbol{\sigma}_h)\cdot \mathbf{t}_T, \varphi-\varphi_h\rangle_{L^2(e)} \right|$$

$$\leq C\left\{ \sum_{T\in\mathcal{T}_h}\sum_{e\in E(T)\cap E_h(\Gamma)} h_e \,\|(\nabla u_h - \boldsymbol{\kappa}^{-1}\boldsymbol{\sigma}_h)\cdot \mathbf{t}_T\|^2_{L^2(e)} \right\}^{1/2} \|\varphi\|_{H^1(\Omega)}\,. \tag{3.36}$$

On the other hand, observing that $\mathbf{curl}(\varphi-\varphi_h)\cdot\boldsymbol{\nu} = -\frac{d(\varphi-\varphi_h)}{d\mathbf{t}_T}$, we deduce that

$$|\langle \mathbf{curl}(\varphi-\varphi_h)\cdot\boldsymbol{\nu}, u_h-\xi_h\rangle| \;=\; \left| \left\langle \varphi-\varphi_h, \frac{du_h}{d\mathbf{t}_T} - \frac{d\xi_h}{d\mathbf{t}_T} \right\rangle \right|$$

$$= \left| \sum_{T\in\mathcal{T}_h} \sum_{e\in E(T)\cap E_h(\Gamma)} \left\langle \varphi - \varphi_h, \frac{du_h}{d\mathbf{t}_T} - \frac{d\xi_h}{d\mathbf{t}_T} \right\rangle_{L^2(e)} \right|$$

$$\leq C \left\{ \sum_{T\in\mathcal{T}_h} \sum_{e\in E(T)\cap E_h(\Gamma)} h_e \left\| \frac{du_h}{d\mathbf{t}_T} - \frac{d\xi_h}{d\mathbf{t}_T} \right\|^2_{L^2(e)} \right\}^{1/2} \|\varphi\|_{H^1(\Omega)} \,. \tag{3.37}$$

Moreover, since $(\cdot,\cdot)_{1/2,\Gamma}$ is a scalar product on $H^{1/2}(\Gamma)$, using the Cauchy-Schwarz inequality, (3.9), and the trace theorem, we obtain

$$|(\xi_h - u_h, \lambda - v)_{1/2}| \,\leq\, C\, \|\xi_h - u_h\|_{H^{1/2}(\Gamma)}\, \|(\boldsymbol{\tau}, v, \lambda)\|_{\mathbf{H}} \,. \tag{3.38}$$

Now, since $\int_\Omega \varphi = 0$ and $\mathbf{curl}(\varphi) = \boldsymbol{\tau}$, we have that

$$\|\varphi\|_{H^1(\Omega)} \,\leq\, C\, |\varphi|_{H^1(\Omega)} \,=\, C\, \|\boldsymbol{\tau}\|_{L^2(\Omega)} \,=\, C\, \|\boldsymbol{\tau}\|_{H(\mathrm{div};\Omega)} \,. \tag{3.39}$$

Therefore, by replacing (3.34) up to (3.38) back into (3.33) and (3.32), using Lemma 3.4.1, the estimate (3.39), and applying the Cauchy-Schwarz inequality to the first, second, and fifth terms of (3.32), we conclude the proof. □

The next lemma bounds the global expression $\|g - \boldsymbol{\sigma}_h\cdot\boldsymbol{\nu}\|^2_{H^{-1/2}(\Gamma)}$.

Lemma 3.4.3 *Assume that the Neumann data $g \in L^2(\Gamma)$. Then there holds*

$$\|g \,-\, \boldsymbol{\sigma}_h\cdot\boldsymbol{\nu}\|^2_{H^{-1/2}(\Gamma)}$$

$$\leq\, C \left\{ \log[1 + C_h(\Gamma)]\, h \sum_{j=1}^{m} \|g \,-\, \boldsymbol{\sigma}_h\cdot\boldsymbol{\nu}\|^2_{L^2(\Gamma_j)} \,+\, \|\xi_h - u_h\|^2_{H^{1/2}(\Gamma)} \right\} , \tag{3.40}$$

where $C_h(\Gamma) := \max\left\{ \frac{|\Gamma_i|}{|\Gamma_j|} : \quad |i-j| = 1\,,\ i,j \in \{1,...,m\} \right\}$.

Proof. Let $P_h : L^2(\Gamma) \to H_h^\xi$ be the orthogonal projection with respect to the $L^2(\Gamma)$-inner product $\langle\cdot,\cdot\rangle_{L^2(\Gamma)}$. Then, we have

$$\|g - \boldsymbol{\sigma}_h\cdot\boldsymbol{\nu}\|_{H^{-1/2}(\Gamma)} \leq \|P_h(g - \boldsymbol{\sigma}_h\cdot\boldsymbol{\nu})\|_{H^{-1/2}(\Gamma)} + \|(I - P_h)(g - \boldsymbol{\sigma}_h\cdot\boldsymbol{\nu})\|_{H^{-1/2}(\Gamma)} \,.$$

Now, since $(I - P_h)(g - \boldsymbol{\sigma}_h\cdot\boldsymbol{\nu})$ is $L^2(\Gamma)$-orthogonal to the finite element subspace H_h^ξ (cf. (3.16)), a straightforward application of Theorem 2 in [23] yields

$$\|(I - P_h)(g - \boldsymbol{\sigma}_h\cdot\boldsymbol{\nu})\|^2_{H^{-1/2}(\Gamma)} \leq \log[1 + C_h(\Gamma)] \sum_{j=1}^{m} h_j\, \|(I - P_h)(g \,-\, \boldsymbol{\sigma}_h\cdot\boldsymbol{\nu})\|^2_{L^2(\Gamma_j)}$$

$$\leq \log[1 + C_h(\Gamma)]\, h \sum_{j=1}^{m} \|g \,-\, \boldsymbol{\sigma}_h \cdot \boldsymbol{\nu}\|^2_{L^2(\Gamma_j)}\,.$$

On the other hand, using the properties of P_h, we find that

$$\|P_h(g - \boldsymbol{\sigma}_h \cdot \boldsymbol{\nu})\|_{H^{-1/2}(\Gamma)} \,=\, \sup_{\substack{\lambda \in H^{1/2}(\Gamma) \\ \lambda \neq 0}} \frac{\langle P_h(g - \boldsymbol{\sigma}_h \cdot \boldsymbol{\nu})\,,\, \lambda \rangle_{L^2(\Gamma)}}{\|\lambda\|_{H^{1/2}(\Gamma)}}$$

$$= \sup_{\substack{\lambda \in H^{1/2}(\Gamma) \\ \lambda \neq 0}} \frac{\langle P_h(g - \boldsymbol{\sigma}_h \cdot \boldsymbol{\nu})\,,\, P_h(\lambda) \rangle_{L^2(\Gamma)}}{\|\lambda\|_{H^{1/2}(\Gamma)}} \,=\, \sup_{\substack{\lambda \in H^{1/2}(\Gamma) \\ \lambda \neq 0}} \frac{\langle g - \boldsymbol{\sigma}_h \cdot \boldsymbol{\nu}\,,\, P_h(\lambda) \rangle_{L^2(\Gamma)}}{\|\lambda\|_{H^{1/2}(\Gamma)}}\,. \quad (3.41)$$

Furthermore, taking $\boldsymbol{\tau}_h \,=\, v_h \,=0$ in (3.19), we arrive at

$$\langle g - \boldsymbol{\sigma}_h \cdot \boldsymbol{\nu}\,,\, \lambda_h \rangle_{L^2(\Gamma)} \,=\, \delta_1\, \langle u_h - \xi_h\,,\, \lambda_h \rangle_{1/2,N(h)} \qquad \forall\, \lambda_h \,\in\, H^{\xi}_h\,,$$

which replaced back into (3.41), together with the fact that the norm induced by $\langle \cdot\,,\, \cdot \rangle_{1/2,N(h)}$ is equivalent to the usual norm of $H^{1/2}(\Gamma)$, yields

$$\sup_{\substack{\lambda \in H^{1/2}(\Gamma) \\ \lambda \neq 0}} \frac{\langle g - \boldsymbol{\sigma}_h \cdot \boldsymbol{\nu}\,,\, P_h(\lambda) \rangle_{L^2(\Gamma)}}{\|\lambda\|_{H^{1/2}(\Gamma)}} \,=\, \sup_{\substack{\lambda \in H^{1/2}(\Gamma) \\ \lambda \neq 0}} \frac{\delta_1\, \langle u_h - \xi_h\,,\, P_h(\lambda) \rangle_{1/2,N(h)}}{\|\lambda\|_{H^{1/2}(\Gamma)}}$$

$$\leq\, \|\xi_h - u_h\|_{H^{1/2}(\Gamma)} \sup_{\substack{\lambda \in H^{1/2}(\Gamma) \\ \lambda \neq 0}} \frac{\|P_h(\lambda)\|_{H^{1/2}(\Gamma)}}{\|\lambda\|_{H^{1/2}(\Gamma)}}\,.$$

Finally, using a suitable orthogonal projector form $H^{1/2}(\Gamma)$ into H^{ξ}_h, and employing classical duality arguments (see [40]), one can prove that $\|P_h(\lambda)\|_{H^{1/2}(\Gamma)} \leq C\, \|\lambda\|_{H^{1/2}(\Gamma)}$. $\square$

Consequently, the reliability of the a posteriori error estimate, which is given by the upper bound in (3.26), follows directly from Lemmas 3.4.1, 3.4.2 and 3.4.3.

3.4.2 Efficiency of the a posteriori error estimate $\tilde{\boldsymbol{\theta}}$

In this subsection we follow the approach from [35] and [38] (see also [7]) to derive the lower bound in (3.26), which shows the efficiency of the a posteriori error estimator $\tilde{\boldsymbol{\theta}}$. We first recall from [49] that given $k \in \mathbb{N}$, $T \in \mathcal{T}_h$, and $e \in E(T)$, there exists an extension operator $L : C(e) \to C(T)$ that satisfies $L(p) \in \mathbf{P}_k(T)$ and $L(p)|_e \,=\, p \;\forall p \in \mathbf{P}_k(e)$. In addition, we define $w_e := \cup\{T' \in \mathcal{T}_h : \quad e \in E(T')\}$ and let ψ_T and ψ_e be te usual triangle-bubble and edge-bubble functions, respectively (see (1.5) and (1.6) in [50]), which satisfy $\mathrm{supp}(\psi_T) \subseteq T$, $\psi_T \in \mathbf{P}_3(T)$, $\psi_T = 0$ on ∂T, $0 \leq \psi_T \leq 1$ in T, $\mathrm{supp}(\psi_e) \subseteq w_e$,

$\psi_e|_T \in \mathbf{P}_2(T)\ \forall T \subseteq w_e$, $\psi_e = 0$ on $\partial T \backslash e$, and $0 \leq \psi_e \leq 1$ in w_e. Additional properties of ψ_T, ψ_e, and L are collected in Lemma 2.4.4.

We first use that $u = \xi$ on Γ and apply the trace theorem to obtain that

$$\|\xi_h - u_h\|^2_{H^{1/2}(\Gamma)} \leq C \left\{ \|u - u_h\|^2_{H^1(\Gamma)} + \|\xi - \xi_h\|^2_{H^{1/2}(\Gamma)} \right\} . \tag{3.42}$$

Also, since $\operatorname{div} \boldsymbol{\sigma} = -f$ in Ω, we easily have

$$\sum_{T \in \mathcal{T}_h} \|f + \operatorname{div} \boldsymbol{\sigma}_h\|^2_{L^2(T)} = \|\operatorname{div} (\boldsymbol{\sigma} - \boldsymbol{\sigma}_h)\|^2_{L^2(\Omega)} . \tag{3.43}$$

The corresponding estimate for the second term in (3.27) is also easily obtained. In fact, adding and substracting $\boldsymbol{\sigma} = \boldsymbol{\kappa} \nabla u$, we get

$$\|\boldsymbol{\kappa} \nabla u_h - \boldsymbol{\sigma}_h\|^2_{[L^2(T)]^2} \leq C \left\{ |u - u_h|^2_{H^1(T)} + \|\boldsymbol{\sigma} - \boldsymbol{\sigma}_h\|^2_{[L^2(T)]^2} \right\} . \tag{3.44}$$

The third term in (3.27) is bounded next.

Lemma 3.4.4 *There exists $C > 0$, independent of h, such that*

$$\sum_{e \in E_h(\Gamma)} h_e \left\| \frac{du_h}{d\mathbf{t}_T} - \frac{d\xi_h}{d\mathbf{t}_T} \right\|^2_{L^2(e)} \leq C \left\{ \|\xi - \xi_h\|^2_{H^{1/2}(\Gamma)} + \|u - u_h\|^2_{H^1(\Omega)} \right\} . \tag{3.45}$$

Proof. See Lemma 5.7 in [35] or Lemma 4.5 in [7]. □

The following technical lemma is needed to bound the fourth and fifth terms in (3.27).

Lemma 3.4.5 *There exists $c > 0$, independent of h, such that for each $e \in E_h$ there holds*

$$h_e \|\hat{J}_e[(\nabla u_h - \boldsymbol{\kappa}^{-1} \boldsymbol{\sigma}_h) \cdot \mathbf{t}_T]\|^2_{L^2(e)} \leq c \|\nabla u_h - \boldsymbol{\kappa}^{-1} \boldsymbol{\sigma}_h\|^2_{[L^2(w_e)]^2} , \tag{3.46}$$

where $\hat{J}_e[(\nabla u_h - \boldsymbol{\kappa}^{-1} \boldsymbol{\sigma}_h) \cdot \mathbf{t}_T] := \begin{cases} J[(\nabla u_h - \boldsymbol{\kappa}^{-1} \boldsymbol{\sigma}_h) \cdot \mathbf{t}_T] & \text{if } e \in E_h(\Omega) \\ (\nabla u_h - \boldsymbol{\kappa}^{-1} \boldsymbol{\sigma}_h) \cdot \mathbf{t}_T & \text{if } e \in E_h(\Gamma) \end{cases} .$

Proof. See Lemma 4.6 in [7] or Lemma 6.2 in [24]. □

As a direct consequence of Lemma 3.4.5, noting that the number of triangles of each w_e is at most 2, and adding and substracting $\boldsymbol{\kappa}^{-1} \boldsymbol{\sigma} = \nabla u$ on the right hand side of (3.46), we deduce, using also (3.3), that there exists $C > 0$, independent of h, such that

$$\sum_{e \in E_h(\Omega)} h_e \|J[(\nabla u_h - \boldsymbol{\kappa}^{-1} \boldsymbol{\sigma}_h) \cdot \mathbf{t}_T]\|^2_{L^2(e)} \leq C \left\{ \|\boldsymbol{\sigma} - \boldsymbol{\sigma}_h\|^2_{[L^2(\Omega)]^2} + |u - u_h|^2_{H^1(\Omega)} \right\} \tag{3.47}$$

and

$$\sum_{e\in E_h(\Gamma)} h_e \,\|(\nabla u_h - \boldsymbol{\kappa}^{-1}\boldsymbol{\sigma}_h)\cdot \mathbf{t}_T\|^2_{L^2(e)} \,\leq\, C\left\{\|\boldsymbol{\sigma}-\boldsymbol{\sigma}_h\|^2_{[L^2(\Omega)]^2} \,+\, |u-u_h|^2_{H^1(\Omega)}\right\}. \quad (3.48)$$

The estimate required for the term in (3.27) involving the curl operator is provided in the next lemma

Lemma 3.4.6 *There exists $c>0$, independent of h , such that*

$$\sum_{T\in\mathcal{T}} h_T^2 \,\|\,\mathrm{curl}(\boldsymbol{\kappa}^{-1}\boldsymbol{\sigma}_h)\|^2_{L^2(T)} \,\leq\, c\,\|\boldsymbol{\sigma}-\boldsymbol{\sigma}_h\|^2_{[L^2(\Omega)]^2}\,. \quad (3.49)$$

Proof. See Lemma 5.3 and equation (5.12) in [35]. □

In order to bound the last term in (3.27) we recall the following result from [35].

Lemma 3.4.7 *There exists $c>0$, independent of h , such that*

$$\log[1+C_h(\Gamma)]\,h \sum_{e\in E_h(\Gamma)} \|g-\boldsymbol{\sigma}_h\cdot\boldsymbol{\nu}\|^2_{L^2(e)} \leq\; c\left\{\|\boldsymbol{\sigma}-\boldsymbol{\sigma}_h\|^2_{[L^2(\Omega)]^2} + h^2\,\|\mathrm{div}\,(\boldsymbol{\sigma}-\boldsymbol{\sigma}_h)\|^2_{L^2(\Omega)}\right\}.$$

Proof. It follows by adapting the proof of Lemma 6.5 in [25] (see also Lemma 5.9 and equation (5.25) in [35]). □

It follows easily from the previous lemma that

$$\log[1+C_h(\Gamma)]\,h \sum_{e\in E_h(\Gamma)} \|g-\boldsymbol{\sigma}_h\cdot\boldsymbol{\nu}\|^2_{L^2(e)} \leq\; C\,\|\boldsymbol{\sigma}-\boldsymbol{\sigma}_h\|^2_{H(\mathrm{div};\Omega)}\,. \quad (3.50)$$

Finally, the lower bound in (3.26) follows from (3.42), (3.43), (3.44), (3.45), (3.47), (3.48), (3.49) and (3.50).

3.4.3 A fully local a posteriori error estimate

The non-local character of the expression $\|\xi_h-u_h\|^2_{H^{1/2}(\Gamma)}$ defining $\tilde{\boldsymbol{\theta}}^2$, can be avoided applying the arguments of Section 5 in [7], that is, introducing an auxiliary function. To this end, we let $\bar{u}_h$ be the unique function in H^u_h such that $\bar{u}_h(\mathbf{x}) = u_h(\mathbf{x})$ for each node $\mathbf{x}\in\Omega$, and $\bar{u}_h(\mathbf{x}) = \xi_h(\mathbf{x})$ for each node $\mathbf{x}\in\Gamma$. It follows that $\overline{u}_h = \xi_h$ on Γ. Furthermore, since $u_h = \bar{u}_h$ on each $T\in\mathcal{T}_h$ not touching the Neumann boundary Γ, we

see that $\|u_h-\bar{u}_h\|_{H^1(T)}$ vanishes on these triangles. This property of the auxiliary function $\bar{u}_h$ induces the definition of the following parameter associated to each $T \in \mathcal{T}_h$:

$$\chi(T) := \begin{cases} 1 & \text{if} \quad \partial T \cap \bar{\Gamma} \neq \phi\,, \\ 0 & \text{otherwise}\,. \end{cases} \tag{3.51}$$

We are now in a position to establish a reliable and *quasi-efficient* fully local a posteriori error estimate. Here, the *quasi-efficiency* refers to the extra term appearing below on the right hand side of (3.53).

Theorem 3.4.2 *Assume that $\boldsymbol{\kappa} \in C^1(\Omega)$. Then there exist positive constants $C_{\mathtt{rel}}$, $C_{\mathtt{eff}}$, independent of h, such that*

$$\|(\boldsymbol{\sigma}-\boldsymbol{\sigma}_h, u-u_h, \xi-\xi_h)\|^2_{\mathbf{H}} \leq C_{\mathtt{rel}}\, \boldsymbol{\theta}^2\,, \tag{3.52}$$

and

$$C_{\mathtt{eff}}\, \boldsymbol{\theta}^2 \leq \|(\boldsymbol{\sigma}-\boldsymbol{\sigma}_h, u-u_h, \xi-\xi_h)\|^2_{\mathbf{H}} + \sum_{T\in\mathcal{T}_h} \chi(T)\, \|u-\bar{u}_h\|^2_{H^1(T)}\,, \tag{3.53}$$

where $\boldsymbol{\theta}^2 := \sum_{T\in\mathcal{T}_h} \theta^2_T$, *and for each $T \in \mathcal{T}_h$ we define*

$$\theta^2_T := \|f+\operatorname{div}\boldsymbol{\sigma}_h\|^2_{L^2(T)} + \|\boldsymbol{\kappa}\nabla u_h - \boldsymbol{\sigma}_h\|^2_{L^2(T)} + \sum_{e\in E(T)\cap E_h(\Gamma)} h_e \left\| \frac{du_h}{d\mathbf{t}_T} - \frac{d\xi_h}{d\mathbf{t}_T} \right\|^2_{L^2(e)}$$

$$+ \sum_{e\in E(T)\cap E_h(\Omega)} h_e \|J[(\nabla u_h - \boldsymbol{\kappa}^{-1}\boldsymbol{\sigma}_h)\cdot\mathbf{t}_T]\|^2_{L^2(e)} + \sum_{e\in E(T)\cap E_h(\Gamma)} h_e \|(\nabla u_h - \boldsymbol{\kappa}^{-1}\boldsymbol{\sigma}_h)\cdot\mathbf{t}_T\|^2_{L^2(e)}$$

$$+ h^2_T \quad \|\operatorname{curl}(\boldsymbol{\kappa}^{-1}\boldsymbol{\sigma}_h)\|^2_{L^2(T)} + \chi(T)\, \|\bar{u}_h - u_h\|^2_{H^1(T)}$$

$$+ \quad \log[1+C_h(\Gamma)]\, h \sum_{e\in E(T)\cap E_h(\Gamma)} \|g - \boldsymbol{\sigma}_h\cdot\boldsymbol{\nu}\|^2_{L^2(e)}\,, \tag{3.54}$$

where $C_h(\Gamma) := \max\left\{ \frac{|\Gamma_i|}{|\Gamma_j|} : \quad |i-j|=1\,,\ i,j\in\{1,...,m\} \right\}$.

Proof. Using that $\bar{u}_h = \xi_h$ on Γ, in the term $(\xi_h-u_h, \lambda-v)_{1/2}$ appearing in (3.32), and then applying trace theorem, we arrive to

$$|(\xi_h-u_h, \lambda-v)_{1/2}| \leq C\, \|\bar{u}_h-u_h\|_{H^1(\Omega)}\, \|(\boldsymbol{\tau}, v, \lambda)\|_{\mathbf{H}}\,.$$

Thus, proceeding as in Lemma 3.4.2, we obtain that there exists $C > 0$, independent of h, such that

$$\sup_{\substack{(\boldsymbol{\tau},v,\lambda)\in\mathbf{H}_0\\(\boldsymbol{\tau},v,\lambda)\neq 0}} \frac{A((\boldsymbol{\sigma}-\boldsymbol{\sigma}_h,u-u_h,\xi-\xi_h),(\boldsymbol{\tau},v,\lambda))}{\|(\boldsymbol{\tau},v,\lambda)\|_{\mathbf{H}}} \leq C \left\{ \sum_{T\in\mathcal{T}_h} \hat{\theta}_T^2 + \|g-\boldsymbol{\sigma}_h\cdot\boldsymbol{\nu}\|^2_{H^{-1/2}(\Gamma)} \right\}^{1/2}$$

where for any triangle $T \in \mathcal{T}$ we define

$$\hat{\theta}_T^2 := \|f+\operatorname{div}\boldsymbol{\sigma}_h\|^2_{L^2(T)} + \|\boldsymbol{\kappa}\nabla u_h - \boldsymbol{\sigma}_h\|^2_{L^2(T)} + h_T^2\|\operatorname{curl}(\boldsymbol{\kappa}^{-1}\boldsymbol{\sigma}_h)\|^2_{L^2(T)}$$

$$+ \sum_{e\in E(T)\cap E_h(\Omega)} h_e\|J[(\nabla u_h-\boldsymbol{\kappa}^{-1}\boldsymbol{\sigma}_h)\cdot\mathbf{t}_T]\|^2_{L^2(e)} + \chi(T)\,\|\bar{u}_h-u_h\|^2_{H^1(T)}$$

$$+ \sum_{e\in E(T)\cap E_h(\Gamma)} h_e\|(\nabla u_h-\boldsymbol{\kappa}^{-1}\boldsymbol{\sigma}_h)\cdot\mathbf{t}_T\|^2_{L^2(e)} + \sum_{e\in E(T)\cap E_h(\Gamma)} h_e\left\|\frac{du_h}{d\mathbf{t}_T}-\frac{d\xi_h}{d\mathbf{t}_T}\right\|^2_{L^2(e)} . \tag{3.55}$$

Thus (3.52) is consequence of Lemma 3.4.1, (3.55), and Lemma 3.4.3. For the quasi-efficiency of $\boldsymbol{\theta}$ (cf. (3.53)) we just observe, adding and substrating u, that

$$\sum_{T\in\mathcal{T}_h}\chi(T)\,\|\bar{u}_h-u_h\|^2_{H^1(T)} \leq C\left\{\|u-u_h\|^2_{H^1(\Omega)} + \|u-\bar{u}_h\|^2_{H^1(\Omega)}\right\} .$$

The rest follows from the estimates given in Section 3.4.2. □

We end this chapter by mentioning that further developments, including computational aspects of (3.19), adaptivity based on $\boldsymbol{\theta}$, and corresponding numerical results, will be reported in a separate work.

Chapter 4

A residual based a posteriori error estimator for an augmented mixed finite element method in linear elasticity

In this chapter we develop a residual based a posteriori error analysis for an augmented mixed finite element method applied to the problem of linear elasticity in the plane. More precisely, we derive a reliable and efficient a posteriori error estimator for the case of pure Dirichlet boundary conditions. In addition, several numerical experiments confirming the theoretical properties of the estimator, and illustrating the capability of the corresponding adaptive algorithm to localize the singularities and the large stress regions of the solution, are also reported.

4.1 Introduction

A new stabilized mixed finite element method for plane linear elasticity was presented and analyzed recently in [36]. The approach there is based on the introduction of suitable Galerkin least-squares terms arising from the constitutive and equilibrium equations, and from the relation defining the rotation in terms of the displacement. The resulting augmented method, which is easily generalized to 3D, can be viewed as an extension to the elasticity problem of the non-symmetric procedures utilized in [30] and [44]. It is

shown in [36] that the continuous and discrete augmented formulations are well-posed, and that the latter becomes locking-free and asymptotically locking-free for Dirichlet and mixed boundary conditions, respectively. In particular, the discrete scheme allows the utilization of Raviart-Thomas spaces of lowest order for the stress tensor, piecewise linear elements for the displacement, and piecewise constants for the rotation. In the case of mixed boundary conditions, the essential one (Neumann) is imposed weakly, which yields the introduction of the trace of the displacement as a suitable Lagrange multiplier. This trace is then approximated by piecewise linear elements on an independent partition of the Neumann boundary whose mesh size needs to satisfy a compatibility condition with the mesh size associated with the triangulation of the domain.

The purpose of this chapter is to develop an a posteriori error analysis for the augmented scheme from [36] in the case of pure Dirichlet boundary conditions. The rest of the chapter is organized as follows. In Section 4.2 we recall from [36] the continuous and discrete augmented formulations of the corresponding boundary value problem, state the well-posedness of both schemes, and provide the associated a priori error estimate. The kernel of the present work is given by Sections 4.3 and 4.4, where we develop the residual based a posteriori error analysis. More precisely, in Section 4.3 we employ a suitable auxiliary problem and apply the local approximation properties of the Clément interpolant to derive a reliable a posteriori error estimator. Next, in Section 4.4 we make use of inverse inequalities and the localization technique based on triangle-bubble and edge-bubble functions to show the efficiency of the estimator. Finally, several numerical results confirming these properties and also the robustness of the estimator with respect to the Poisson ratio, are provided in Section 4.5. In addition, the capability of the corresponding adaptive algorithm to localize the singularities and the large stress regions of the solution is also illustrated here.

We end this section with some notations to be used below. Given any Hilbert space U, U^2 and $U^{2\times 2}$ denote, respectively, the space of vectors and square matrices of order 2 with entries in U. In addition, $\mathbf{I}$ is the identity matrix of $\mathbb{R}^{2\times 2}$, and given $\boldsymbol{\tau} := (\tau_{ij})$, $\boldsymbol{\zeta} := (\zeta_{ij}) \in \mathbb{R}^{2\times 2}$, we write as usual $\boldsymbol{\tau}^{\mathtt{t}} := (\tau_{ji})$, $\mathrm{tr}(\boldsymbol{\tau}) := \sum_{i=1}^{2} \tau_{ii}$, $\boldsymbol{\tau}^{\mathtt{d}} := \boldsymbol{\tau} - \frac{1}{2}\mathrm{tr}(\boldsymbol{\tau})\,\mathbf{I}$, and $\boldsymbol{\tau} : \boldsymbol{\zeta} := \sum_{i,j=1}^{2} \tau_{ij}\,\zeta_{ij}$. Also, in what follows we utilize the standard terminology for Sobolev spaces and norms, employ $\mathbf{0}$ to denote a generic null vector, and use C and c, with or without subscripts, bars, tildes or hats, to denote generic constants independent of the discretization parameters, which may take different values at different

places.

4.2 The augmented formulations

First we let Ω be a simply connected domain in $\mathbb{R}^2$ with polygonal boundary $\Gamma := \partial\Omega$. Our goal is to determine the displacement $\mathbf{u}$ and stress tensor $\boldsymbol{\sigma}$ of a linear elastic material occupying the region Ω. In other words, given a volume force $\mathbf{f} \in [L^2(\Omega)]^2$, we seek a symmetric tensor field $\boldsymbol{\sigma}$ and a vector field $\mathbf{u}$ such that

$$\boldsymbol{\sigma} = \mathcal{C}\,\mathbf{e}(\mathbf{u})\,, \quad \mathbf{div}\,(\boldsymbol{\sigma}) = -\,\mathbf{f} \quad \text{in} \quad \Omega\,, \quad \text{and} \quad \mathbf{u} = \mathbf{0} \quad \text{on} \quad \Gamma\,. \tag{4.1}$$

Hereafter, $\mathbf{e}(\mathbf{u}) := \frac{1}{2}\,(\nabla\mathbf{u} + (\nabla\mathbf{u})^{\mathtt{t}})$ is the strain tensor of small deformations and $\mathcal{C}$ is the elasticity tensor determined by Hooke's law, that is

$$\mathcal{C}\,\boldsymbol{\zeta} \;:=\; \lambda\,\mathrm{tr}(\boldsymbol{\zeta})\,\mathbf{I} \;+\; 2\,\mu\,\boldsymbol{\zeta} \qquad \forall\,\boldsymbol{\zeta} \,\in\, [L^2(\Omega)]^{2\times 2}\,, \tag{4.2}$$

where λ, $\mu > 0$ denote the corresponding Lamé constants. It is easy to see from (4.2) that the inverse tensor $\mathcal{C}^{-1}$ reduces to

$$\mathcal{C}^{-1}\,\boldsymbol{\zeta} \,:=\, \frac{1}{2\,\mu}\,\boldsymbol{\zeta} \,-\, \frac{\lambda}{4\,\mu\,(\lambda+\mu)}\,\mathrm{tr}(\boldsymbol{\zeta})\,\mathbf{I} \qquad \forall\,\boldsymbol{\zeta} \,\in\, [L^2(\Omega)]^{2\times 2}\,. \tag{4.3}$$

We now define the spaces $H = H(\mathbf{div}\,;\Omega) := \{\boldsymbol{\tau} \in [L^2(\Omega)]^{2\times 2} : \quad \mathbf{div}\,(\boldsymbol{\tau}) \in [L^2(\Omega)]^2\,\}$, $H_0 := \{\boldsymbol{\tau} \in H : \quad \int_\Omega \mathrm{tr}(\boldsymbol{\tau}) = 0\}$, and note that $H = H_0 \oplus \mathbb{R}\,\mathbf{I}$, that is for any $\boldsymbol{\tau} \in H$ there exist unique $\boldsymbol{\tau}_0 \in H_0$ and $d := \frac{1}{2|\Omega|}\int_\Omega \mathrm{tr}(\boldsymbol{\tau}) \in \mathbb{R}$ such that $\boldsymbol{\tau} = \boldsymbol{\tau}_0 + d\,\mathbf{I}$. In addition, we define the space of skew-symmetric tensors $[L^2(\Omega)]^{2\times 2}_{\mathtt{skew}} := \{\,\boldsymbol{\eta} \in [L^2(\Omega)]^{2\times 2} : \boldsymbol{\eta} + \boldsymbol{\eta}^{\mathtt{t}} = \mathbf{0}\}$ and introduce the rotation $\boldsymbol{\gamma} := \frac{1}{2}(\nabla\mathbf{u} - (\nabla u)^{\mathtt{t}})) \in [L^2(\Omega)]^{2\times 2}_{\mathtt{skew}}$ as an auxiliary unknown. Then, given positive parameters κ_1, κ_2, and κ_3, independent of λ, we consider from [36] the following augmented variational formulation for (4.1): Find $(\boldsymbol{\sigma}, \mathbf{u}, \boldsymbol{\gamma}) \in \mathbf{H}_0 := H_0 \times [H^1_0(\Omega)]^2 \times [L^2(\Omega)]^{2\times 2}_{\mathtt{skew}}$ such that

$$A((\boldsymbol{\sigma}, \mathbf{u}, \boldsymbol{\gamma}), (\boldsymbol{\tau}, \mathbf{v}, \boldsymbol{\eta})) \;=\; F(\boldsymbol{\tau}, \mathbf{v}, \boldsymbol{\eta}) \qquad \forall\,(\boldsymbol{\tau}, \mathbf{v}, \boldsymbol{\eta}) \in \mathbf{H}_0\,, \tag{4.4}$$

where the bilinear form $A : \mathbf{H}_0 \times \mathbf{H}_0 \to \mathbb{R}$ and the functional $F : \mathbf{H}_0 \to \mathbb{R}$ are defined by

$$A((\boldsymbol{\sigma}, \mathbf{u}, \boldsymbol{\gamma}), (\boldsymbol{\tau}, \mathbf{v}, \boldsymbol{\eta})) := \int_\Omega \mathcal{C}^{-1}\boldsymbol{\sigma} : \boldsymbol{\tau} + \int_\Omega \mathbf{u}\cdot\mathbf{div}\,(\boldsymbol{\tau}) + \int_\Omega \boldsymbol{\gamma} : \boldsymbol{\tau} - \int_\Omega \mathbf{v}\cdot\mathbf{div}\,(\boldsymbol{\sigma}) - \int_\Omega \boldsymbol{\eta} : \boldsymbol{\sigma}$$

$$+ \;\; \kappa_1 \int_\Omega \big(\,\mathbf{e}(\mathbf{u}) - \mathcal{C}^{-1}\,\boldsymbol{\sigma}\,\big) : \big(\,\mathbf{e}(\mathbf{v}) + \mathcal{C}^{-1}\,\boldsymbol{\tau}\,\big) \;+\; \kappa_2 \int_\Omega \mathbf{div}\,(\boldsymbol{\sigma})\cdot\mathbf{div}\,(\boldsymbol{\tau})$$

$$+ \ \kappa_3 \ \int_\Omega \left(\boldsymbol{\gamma} - \frac{1}{2}(\nabla \mathbf{u} - (\nabla \mathbf{u})^{\mathtt{t}}) \right) : \left(\boldsymbol{\eta} + \frac{1}{2}(\nabla \mathbf{v} - (\nabla \mathbf{v})^{\mathtt{t}}) \right) , \tag{4.5}$$

and

$$F(\boldsymbol{\tau}, \mathbf{v}, \boldsymbol{\eta}) \ := \ \int_\Omega \mathbf{f} \cdot (\, \mathbf{v} \ - \ \kappa_2 \ \mathbf{div} \, (\boldsymbol{\tau}) \,) \ . \tag{4.6}$$

The well-posedness of (4.4) was proved in [36]. More precisely, we have the following result.

Theorem 4.2.1 *Assume that* $(\kappa_1, \kappa_2, \kappa_3)$ *is independent of* λ *and such that* $0 < \kappa_1 < 2\,\mu$, $0 < \kappa_2$, *and* $0 < \kappa_3 < \kappa_1$. *Then, there exist positive constants* M, α, *independent of* λ, *such that*

$$| \, A((\boldsymbol{\sigma}, \mathbf{u}, \boldsymbol{\gamma}), (\boldsymbol{\tau}, \mathbf{v}, \boldsymbol{\eta})) \, | \ \leq \ M \ \|(\boldsymbol{\sigma}, \mathbf{u}, \boldsymbol{\gamma})\|_{\mathbf{H}_0} \, \|(\boldsymbol{\tau}, \mathbf{v}, \boldsymbol{\eta})\|_{\mathbf{H}_0} \tag{4.7}$$

and

$$A((\boldsymbol{\tau}, \mathbf{v}, \boldsymbol{\eta}), (\boldsymbol{\tau}, \mathbf{v}, \boldsymbol{\eta})) \ \geq \ \alpha \ \|(\boldsymbol{\tau}, \mathbf{v}, \boldsymbol{\eta})\|^2_{\mathbf{H}_0} \tag{4.8}$$

for all $(\boldsymbol{\sigma}, \mathbf{u}, \boldsymbol{\gamma})$, $(\boldsymbol{\tau}, \mathbf{v}, \boldsymbol{\eta}) \in \mathbf{H}_0$. *In particular, taking*

$$\kappa_1 \ = \ \tilde{C}_1 \, \mu \, , \qquad \kappa_2 = \frac{1}{\mu} \left(1 - \frac{\kappa_1}{2\,\mu} \right) , \qquad \textit{and} \qquad \kappa_3 \ = \ \tilde{C}_3 \, \kappa_1 \, , \tag{4.9}$$

with any $\tilde{C}_1 \ \in]0, 2[$ *and any* $\tilde{C}_3 \ \in]0, 1[$, *this yields* M *and* α *depending only on* μ, $\dfrac{1}{\mu}$, *and* Ω. *Therefore, the augmented variational formulation* (4.4) *has a unique solution* $(\boldsymbol{\sigma}, \mathbf{u}, \boldsymbol{\gamma}) \in \mathbf{H}_0$, *and there exists a positive constant* C, *independent of* λ, *such that*

$$\|(\boldsymbol{\sigma}, \mathbf{u}, \boldsymbol{\gamma})\|_{\mathbf{H}_0} \ \leq \ C \, \|F\| \ \leq \ C \, \|\mathbf{f}\|_{[L^2(\Omega)]^2} \, .$$

Proof. See Theorems 3.1 and 3.2 in [36]. □

Now, given a finite element subspace $\mathbf{H}_{0,h} \subseteq \mathbf{H}_0$, the Galerkin scheme associated to (4.4) reads: Find $(\boldsymbol{\sigma}_h, \mathbf{u}_h, \boldsymbol{\gamma}_h) \in \mathbf{H}_{0,h}$ such that

$$A((\boldsymbol{\sigma}_h, \mathbf{u}_h, \boldsymbol{\gamma}_h), (\boldsymbol{\tau}_h, \mathbf{v}_h, \boldsymbol{\eta}_h)) \ = \ F(\boldsymbol{\tau}_h, \mathbf{v}_h, \boldsymbol{\eta}_h) \qquad \forall \, (\boldsymbol{\tau}_h, \mathbf{v}_h, \boldsymbol{\eta}_h) \in \mathbf{H}_{0,h} \, , \tag{4.10}$$

where κ_1, κ_2, and κ_3, being the same parameters employed in the formulation (4.4), satisfy the assumptions of Theorem 4.2.1. Since A becomes bounded and strongly coercive on the whole space $\mathbf{H}_0$, we remark that the well-posedness of (4.10) is guaranteed for any arbitrary choice of the subspace $\mathbf{H}_{0,h}$. In fact, the following result is also established in [36].

Theorem 4.2.2 *Assume that the parameters κ_1, κ_2, and κ_3 satisfy the assumptions of Theorem* 4.2.1 *and let $\mathbf{H}_{0,h}$ be any finite element subspace of $\mathbf{H}_0$. Then, the Galerkin scheme* (4.10) *has a unique solution $(\boldsymbol{\sigma}_h, \mathbf{u}_h, \boldsymbol{\gamma}_h) \in \mathbf{H}_{0,h}$, and there exist positive constants C, $\tilde{C}$, independent of h and λ, such that*

$$\|(\boldsymbol{\sigma}_h, \mathbf{u}_h, \boldsymbol{\gamma}_h)\|_{\mathbf{H}_0} \;\leq\; C \sup_{\substack{(\boldsymbol{\tau}_h, \mathbf{v}_h, \boldsymbol{\eta}_h) \in \mathbf{H}_{0,h} \\ (\boldsymbol{\tau}_h, \mathbf{v}_h, \boldsymbol{\eta}_h) \neq \mathbf{0}}} \frac{|\, F(\boldsymbol{\tau}_h, \mathbf{v}_h, \boldsymbol{\eta}_h)\,|}{\|(\boldsymbol{\tau}_h, \mathbf{v}_h, \boldsymbol{\eta}_h)\|_{\mathbf{H}_0}} \;\leq\; C\, \|\mathbf{f}\|_{[L^2(\Omega)]^2}\,,$$

and

$$\|(\boldsymbol{\sigma}, \mathbf{u}, \boldsymbol{\gamma}) - (\boldsymbol{\sigma}_h, \mathbf{u}_h, \boldsymbol{\gamma}_h)\|_{\mathbf{H}_0} \;\leq\; \tilde{C} \inf_{(\boldsymbol{\tau}_h, \mathbf{v}_h, \boldsymbol{\eta}_h) \in \mathbf{H}_{0,h}} \|(\boldsymbol{\sigma}, \mathbf{u}, \boldsymbol{\gamma}) - (\boldsymbol{\tau}_h, \mathbf{v}_h, \boldsymbol{\eta}_h)\|_{\mathbf{H}_0}\,. \quad (4.11)$$

Proof. It follows from Theorem 4.2.1, Lax-Milgram's Lemma, and Céa's estimate. □

An immediate consequence of the definition of the continuous and discrete augmented formulations is the Galerkin orthogonality

$$A((\boldsymbol{\sigma} - \boldsymbol{\sigma}_h, \mathbf{u} - \mathbf{u}_h, \boldsymbol{\gamma} - \boldsymbol{\gamma}_h), (\boldsymbol{\tau}_h, \mathbf{v}_h, \boldsymbol{\eta}_h)) = 0 \qquad \forall\, (\boldsymbol{\tau}_h, \mathbf{v}_h, \boldsymbol{\eta}_h) \in \mathbf{H}_{0,h}\,. \quad (4.12)$$

Next, we recall the specific space $\mathbf{H}_{0,h}$ introduced in [36], which is the simplest finite element subspace of $\mathbf{H}_0$. To this end, we first let $\{\mathcal{T}_h\}_{h>0}$ be a regular family of triangulations of the polygonal region $\bar{\Omega}$ by triangles T of diameter h_T with mesh size $h := \max\{\, h_T : \quad T \in \mathcal{T}_h \,\}$, and such that there holds $\bar{\Omega} = \cup\{\, T : \quad T \in \mathcal{T}_h \,\}$. In addition, given an integer $\ell \geq 0$ and a subset S of $\mathbb{R}^2$, we denote by $\mathbf{P}_\ell(S)$ the space of polynomials in two variables defined in S of total degree at most ℓ, and for each $T \in \mathcal{T}_h$ we introduce $\mathbb{RT}_0(T)$ as the local Raviart-Thomas space of order zero (cf. Section 2.3, [17], [47]). Then, defining

$$H_h^{\boldsymbol{\sigma}} := \left\{ \boldsymbol{\tau}_h \in H(\mathbf{div}\,;\Omega) : \quad \boldsymbol{\tau}_h|_T \in [\mathbb{RT}_0(T)^{\mathtt{t}}]^2 \qquad \forall\, T \in \mathcal{T}_h \right\}, \quad (4.13)$$

$$X_h := \left\{ v_h \in C(\bar{\Omega}) : \quad v_h|_T \in \mathbf{P}_1(T) \quad \forall\, T \in \mathcal{T}_h \right\}, \quad (4.14)$$

and

$$H_h^{\mathbf{u}} := X_h \times X_h\,, \quad (4.15)$$

we take

$$\mathbf{H}_{0,h} := H_{0,h}^{\boldsymbol{\sigma}} \times H_{0,h}^{\mathbf{u}} \times H_h^{\boldsymbol{\gamma}}\,, \quad (4.16)$$

where

$$H_{0,h}^{\boldsymbol{\sigma}} := \left\{ \boldsymbol{\tau}_h \in H_h^{\boldsymbol{\sigma}} : \quad \int_\Omega \mathrm{tr}(\boldsymbol{\tau}_h) = 0 \right\}, \quad (4.17)$$

$$H^{\mathbf{u}}_{0,h} := \{ \mathbf{v}_h \in H^{\mathbf{u}}_h : \quad \mathbf{v}_h = \mathbf{0} \quad \text{on} \quad \Gamma \} , \tag{4.18}$$

and

$$H^{\boldsymbol{\gamma}}_h := \left\{ \boldsymbol{\eta}_h \in [L^2(\Omega)]^{2\times 2}_{\mathtt{skew}} : \quad \boldsymbol{\eta}_h|_T \in [\mathbf{P}_0(T)]^{2\times 2} \quad \forall T \in \mathcal{T}_h \right\} . \tag{4.19}$$

The following theorem provides the rate of convergence of (4.10) when the specific finite element subspace (4.16) is utilized.

Theorem 4.2.3 *Let* $(\boldsymbol{\sigma}, \mathbf{u}, \boldsymbol{\gamma}) \in \mathbf{H}_0$ *and* $(\boldsymbol{\sigma}_h, \mathbf{u}_h, \boldsymbol{\gamma}_h) \in \mathbf{H}_{0,h} := H^{\boldsymbol{\sigma}}_{0,h} \times H^{\mathbf{u}}_{0,h} \times H^{\boldsymbol{\gamma}}_h$ *be the unique solutions of the continuous and discrete augmented mixed formulations* (4.4) *and* (4.10)*, respectively. Assume that* $\mathbf{u} \in [H^{r+1}(\Omega)]^2$ *and* $\mathbf{f} = \mathbf{div}\,(\boldsymbol{\sigma}) \in [H^r(\Omega)]^2$*, for some* $r \in (0, 1]$*. Then there exists* $C > 0$*, independent of* h *and* λ*, such that*

$$\|(\boldsymbol{\sigma}, \mathbf{u}, \boldsymbol{\gamma}) - (\boldsymbol{\sigma}_h, \mathbf{u}_h, \boldsymbol{\gamma}_h)\|_{\mathbf{H}_0}$$

$$\leq C\, h^r \left\{ \|\boldsymbol{\sigma}\|_{[H^r(\Omega)]^{2\times 2}} + \|\,\mathbf{div}\,(\boldsymbol{\sigma})\|_{[H^r(\Omega)]^2} + \|\mathbf{u}\|_{[H^{r+1}(\Omega)]^2} + \|\boldsymbol{\gamma}\|_{[H^r(\Omega)]^{2\times 2}} \right\} .$$

Proof. It is a consequence of Céa's estimate, the approximation properties of the subspaces defining $\mathbf{H}_{0,h}$, and suitable interpolation theorems in the corresponding function spaces. See Section 4.1 in [36] for more details. □

4.3 A residual based a posteriori error estimator

In this section we derive a residual based a posteriori error estimator for (4.10). First we introduce several notations. Given $T \in \mathcal{T}_h$, we let $E(T)$ be the set of its edges, and let E_h be the set of all edges of the triangulation $\mathcal{T}_h$. Then we write $E_h = E_h(\Omega) \cup E_h(\Gamma)$, where $E_h(\Omega) := \{e \in E_h : \quad e \subseteq \Omega\}$ and $E_h(\Gamma) := \{e \in E_h : \quad e \subseteq \Gamma\}$. In what follows, h_e stands for the length of edge $e \in E_h$. Further, given $\boldsymbol{\tau} \in [L^2(\Omega)]^{2\times 2}$ (such that $\boldsymbol{\tau}|_T \in C(T)$ on each $T \in \mathcal{T}_h$), an edge $e \in E(T) \cap E_h(\Omega)$, and the unit tangential vector $\mathbf{t}_T$ along e, we let $J[\boldsymbol{\tau}\mathbf{t}_T]$ be the corresponding jump across e, that is, $J[\boldsymbol{\tau}\mathbf{t}_T] := (\boldsymbol{\tau}|_T - \boldsymbol{\tau}|_{T'})|_e \mathbf{t}_T$, where T' is the other triangle of $\mathcal{T}_h$ having e as an edge. Abusing notation, when $e \in E_h(\Gamma)$, we also write $J[\boldsymbol{\tau}\mathbf{t}_T] := \boldsymbol{\tau}|_e \mathbf{t}_T$. We recall here that $\mathbf{t}_T := (-\nu_2, \nu_1)^{\mathtt{t}}$ where $\boldsymbol{\nu}_T := (\nu_1, \nu_2)^{\mathtt{t}}$ is the unit outward normal to ∂T. Analogously, we define the normal jumps $J[\boldsymbol{\tau}\boldsymbol{\nu}_T]$. In addition, given scalar, vector, and tensor valued fields v, $\boldsymbol{\varphi} := (\varphi_1, \varphi_2)$, and $\boldsymbol{\tau} := (\tau_{ij})$, respectively, we let

$$\mathbf{curl}(v) := \begin{pmatrix} -\frac{\partial v}{\partial x_2} \\ \frac{\partial v}{\partial x_1} \end{pmatrix} , \ \underline{\mathbf{curl}}(\boldsymbol{\varphi}) := \begin{pmatrix} \mathbf{curl}(\varphi_1)^{\mathtt{t}} \\ \mathbf{curl}(\varphi_2)^{\mathtt{t}} \end{pmatrix} , \text{ and } \mathrm{curl}(\boldsymbol{\tau}) := \begin{pmatrix} \frac{\partial \tau_{12}}{\partial x_1} - \frac{\partial \tau_{11}}{\partial x_2} \\ \frac{\partial \tau_{22}}{\partial x_1} - \frac{\partial \tau_{21}}{\partial x_2} \end{pmatrix} .$$

Then, for $(\boldsymbol{\sigma},\mathbf{u},\boldsymbol{\gamma}) \in \mathbf{H}_0$ and $(\boldsymbol{\sigma}_h,\mathbf{u}_h,\boldsymbol{\gamma}_h) \in \mathbf{H}_{0,h}$ being the solutions of the continuous and discrete formulations (4.4) and (4.10), respectively, we define an error indicator θ_T as follows:

$$
\begin{aligned}
\theta_T^2 \;:=\; & \|\mathbf{f}+\mathbf{div}\,(\boldsymbol{\sigma}_h)\|^2_{[L^2(T)]^2} \,+\, \|\boldsymbol{\sigma}_h-\boldsymbol{\sigma}_h^{\mathtt{t}}\|^2_{[L^2(T)]^{2\times 2}} \,+\, \|\boldsymbol{\gamma}_h-\frac{1}{2}(\nabla\mathbf{u}_h-(\nabla\mathbf{u}_h)^{\mathtt{t}})\|^2_{[L^2(T)]^{2\times 2}} \\
& + \; h_T^2\left\{\|\operatorname{curl}(\mathcal{C}^{-1}\boldsymbol{\sigma}_h+\boldsymbol{\gamma}_h)\|^2_{[L^2(T)]^2} \,+\, \|\operatorname{curl}(\mathcal{C}^{-1}(\mathbf{e}(\mathbf{u}_h)-\mathcal{C}^{-1}\boldsymbol{\sigma}_h))\|^2_{[L^2(T)]^2}\right\} \\
& + \sum_{e\in E(T)} h_e\left\{\|J[(\mathcal{C}^{-1}\boldsymbol{\sigma}_h-\nabla\mathbf{u}_h+\boldsymbol{\gamma}_h)\mathbf{t}_T]\|^2_{[L^2(e)]^2} \,+\, \|J[(\mathcal{C}^{-1}(\mathbf{e}(\mathbf{u}_h)-\mathcal{C}^{-1}\boldsymbol{\sigma}_h))\mathbf{t}_T]\|^2_{[L^2(e)]^2}\right\} \\
& + \; h_T^2\,\|\mathbf{div}\,(\mathbf{e}(\mathbf{u}_h)-\frac{1}{2}(\mathcal{C}^{-1}\boldsymbol{\sigma}_h+(\mathcal{C}^{-1}\boldsymbol{\sigma}_h)^{\mathtt{t}}))\|^2_{[L^2(T)]^2} \\
& + \; h_T^2\,\|\mathbf{div}\,(\boldsymbol{\gamma}_h-\frac{1}{2}(\nabla\mathbf{u}_h-(\nabla\mathbf{u}_h)^{\mathtt{t}}))\|^2_{[L^2(T)]^2} \\
& + \sum_{e\in E(T)\cap E_h(\Omega)} h_e\,\|J[(\mathbf{e}(\mathbf{u}_h)-\frac{1}{2}(\mathcal{C}^{-1}\boldsymbol{\sigma}_h+(\mathcal{C}^{-1}\boldsymbol{\sigma}_h)^{\mathtt{t}}))\boldsymbol{\nu}_T]\|^2_{[L^2(e)]^2} \\
& + \sum_{e\in E(T)\cap E_h(\Omega)} h_e\,\|J[(\boldsymbol{\gamma}_h-\frac{1}{2}(\nabla\mathbf{u}_h-(\nabla\mathbf{u}_h)^{\mathtt{t}}))\boldsymbol{\nu}_T]\|^2_{[L^2(e)]^2}\,. \qquad (4.20)
\end{aligned}
$$

The residual character of each term on the right hand side of (4.20) is quite clear. We omit further comments and just mention that, as usual, the expression $\boldsymbol{\theta} := \Big\{\sum_{T\in\mathcal{T}_h}\theta_T^2\Big\}^{1/2}$ is employed as the global residual error estimator.

The following theorem is the main result of this chapter.

Theorem 4.3.1 *Let $(\boldsymbol{\sigma},\mathbf{u},\boldsymbol{\gamma}) \in \mathbf{H}_0$ and $(\boldsymbol{\sigma}_h,\mathbf{u}_h,\boldsymbol{\gamma}_h) \in \mathbf{H}_{0,h}$ be the unique solutions of (4.4) and (4.10), respectively. Then there exist $C_{\mathtt{eff}}, C_{\mathtt{rel}} > 0$, independent of h and λ, such that*

$$
C_{\mathtt{eff}}\,\boldsymbol{\theta} \;\le\; \|(\boldsymbol{\sigma}-\boldsymbol{\sigma}_h,\mathbf{u}-\mathbf{u}_h,\boldsymbol{\gamma}-\boldsymbol{\gamma}_h)\|_{\mathbf{H}_0} \;\le\; C_{\mathtt{rel}}\,\boldsymbol{\theta}\,. \qquad (4.21)
$$

The so-called efficiency (lower bound in (4.21)) is proved below in Section 4.4 and the reliability estimate (upper bound in (4.21)) is derived throughout the rest of the present section. We begin with the following preliminary estimate.

Lemma 4.3.1 *There exists $C > 0$, independent of h and λ, such that*

$$
\begin{aligned}
& C\;\|(\boldsymbol{\sigma}-\boldsymbol{\sigma}_h,\mathbf{u}-\mathbf{u}_h,\boldsymbol{\gamma}-\boldsymbol{\gamma}_h)\|_{\mathbf{H}_0} \\
& \le \sup_{\substack{\mathbf{0}\neq(\boldsymbol{\tau},\mathbf{v},\boldsymbol{\eta})\in\mathbf{H}_0\\ \mathbf{div}\,(\boldsymbol{\tau})=\mathbf{0}}} \frac{A((\boldsymbol{\sigma}-\boldsymbol{\sigma}_h,\mathbf{u}-\mathbf{u}_h,\boldsymbol{\gamma}-\boldsymbol{\gamma}_h),(\boldsymbol{\tau},\mathbf{v},\boldsymbol{\eta}))}{\|(\boldsymbol{\tau},\mathbf{v},\boldsymbol{\eta})\|_{\mathbf{H}_0}} \,+\, \|\mathbf{f}+\mathbf{div}\,(\boldsymbol{\sigma}_h)\|_{[L^2(\Omega)]^2}\,.
\end{aligned} \qquad (4.22)
$$

Proof. Let us define $\boldsymbol{\sigma}^* = \mathbf{e}(\mathbf{z})$, where $\mathbf{z} \in [H_0^1(\Omega)]^2$ is the unique solution of the boundary value problem: $-\mathbf{div}\,(\mathbf{e}(\mathbf{z})) = \mathbf{f} + \mathbf{div}\,(\boldsymbol{\sigma}_h)$ in Ω, $\mathbf{z} = \mathbf{0}$ on Γ. It follows that $\boldsymbol{\sigma}^* \in H_0$, and the corresponding continuous dependence result establishes the existence of $c > 0$ such that

$$\|\boldsymbol{\sigma}^*\|_{H(\mathbf{div};\Omega)} \leq c \, \|\mathbf{f} + \mathbf{div}\,(\boldsymbol{\sigma}_h)\|_{[L^2(\Omega)]^2} . \tag{4.23}$$

In addition, it is easy to see that $\mathbf{div}\,(\boldsymbol{\sigma} - \boldsymbol{\sigma}_h - \boldsymbol{\sigma}^*) = \mathbf{0}$ in Ω. Then, using the coercivity of A (cf. (4.8)), we find that

$$\begin{aligned}
&\alpha \, \|(\boldsymbol{\sigma} - \boldsymbol{\sigma}_h - \boldsymbol{\sigma}^*, \mathbf{u} - \mathbf{u}_h, \boldsymbol{\gamma} - \boldsymbol{\gamma}_h)\|^2_{\mathbf{H}_0} \\
&\quad \leq \; A((\boldsymbol{\sigma} - \boldsymbol{\sigma}_h - \boldsymbol{\sigma}^*, \mathbf{u} - \mathbf{u}_h, \boldsymbol{\gamma} - \boldsymbol{\gamma}_h), (\boldsymbol{\sigma} - \boldsymbol{\sigma}_h - \boldsymbol{\sigma}^*, \mathbf{u} - \mathbf{u}_h, \boldsymbol{\gamma} - \boldsymbol{\gamma}_h)) \\
&\quad = \; A((\boldsymbol{\sigma} - \boldsymbol{\sigma}_h, \mathbf{u} - \mathbf{u}_h, \boldsymbol{\gamma} - \boldsymbol{\gamma}_h), (\boldsymbol{\sigma} - \boldsymbol{\sigma}_h - \boldsymbol{\sigma}^*, \mathbf{u} - \mathbf{u}_h, \boldsymbol{\gamma} - \boldsymbol{\gamma}_h)) \\
&\qquad -A((\boldsymbol{\sigma}^*, \mathbf{0}, \mathbf{0}), (\boldsymbol{\sigma} - \boldsymbol{\sigma}_h - \boldsymbol{\sigma}^*, \mathbf{u} - \mathbf{u}_h, \boldsymbol{\gamma} - \boldsymbol{\gamma}_h)) ,
\end{aligned}$$

which, employing the boundedness of A (cf. (4.7)), yields

$$\begin{aligned}
&\alpha \, \|(\boldsymbol{\sigma} - \boldsymbol{\sigma}_h - \boldsymbol{\sigma}^*, \mathbf{u} - \mathbf{u}_h, \boldsymbol{\gamma} - \boldsymbol{\gamma}_h)\|_{\mathbf{H}_0} \\
&\quad \leq \sup_{\substack{\mathbf{0} \neq (\boldsymbol{\tau}, \mathbf{v}, \boldsymbol{\eta}) \in \mathbf{H}_0 \\ \mathbf{div}\,(\boldsymbol{\tau}) = \mathbf{0}}} \frac{A((\boldsymbol{\sigma} - \boldsymbol{\sigma}_h, \mathbf{u} - \mathbf{u}_h, \boldsymbol{\gamma} - \boldsymbol{\gamma}_h), (\boldsymbol{\tau}, \mathbf{v}, \boldsymbol{\eta}))}{\|(\boldsymbol{\tau}, \mathbf{v}, \boldsymbol{\eta})\|_{\mathbf{H}_0}} \; + \; M \, \|\boldsymbol{\sigma}^*\|_{H(\mathbf{div};\Omega)}
\end{aligned} \tag{4.24}$$

Hence, (4.22) follows straightforwardly from the triangle inequality, (4.23), and (4.24). □

It remains to bound the first term on the right hand side of (4.22). To this end, we will make use of the well known Clément interpolation operator $I_h : H^1(\Omega) \to X_h$ (cf. [27]), with X_h given by (4.14), which satisfies the standard local approximation properties stated in Lemma 2.4.1. It is important to remark that I_h is defined in [27] so that $I_h(v) \in X_h \cap H_0^1(\Omega)$ for all $v \in H_0^1(\Omega)$.

We now let $(\boldsymbol{\tau}, \mathbf{v}, \boldsymbol{\eta}) \in \mathbf{H}_0$, $(\boldsymbol{\tau}, \mathbf{v}, \boldsymbol{\eta}) \neq \mathbf{0}$, such that $\mathbf{div}\,(\boldsymbol{\tau}) = \mathbf{0}$ in Ω. Since Ω is connected, there exists a stream function $\boldsymbol{\varphi} := (\varphi_1, \varphi_2) \in [H^1(\Omega)]^2$ such that $\displaystyle\int_\Omega \varphi_1 = \int_\Omega \varphi_2 = 0$ and $\boldsymbol{\tau} = \underline{\mathbf{curl}}(\boldsymbol{\varphi})$. Then, denoting $\boldsymbol{\varphi}_h := (\varphi_{1,h}, \varphi_{2,h})$, with $\varphi_{i,h} := I_h(\varphi_i)$, $i \in \{1, 2\}$, the Clément interpolant of φ_i, we define $\boldsymbol{\tau}_h := \underline{\mathbf{curl}}(\boldsymbol{\varphi}_h)$. Note that there holds the decomposition $\boldsymbol{\tau}_h = \boldsymbol{\tau}_{h,0} + d_h \, \mathbf{I}$, where $\boldsymbol{\tau}_{h,0} \in H_{0,h}^{\boldsymbol{\sigma}}$ and $d_h = \frac{\int_\Omega tr(\boldsymbol{\tau}_h)}{2|\Omega|} \in \mathbb{R}$. From the orthogonality relation (4.12) it follows that

$$A((\boldsymbol{\sigma} - \boldsymbol{\sigma}_h, \mathbf{u} - \mathbf{u}_h, \boldsymbol{\gamma} - \boldsymbol{\gamma}_h), (\boldsymbol{\tau}, \mathbf{v}, \boldsymbol{\eta}))$$

$$= A((\boldsymbol{\sigma}-\boldsymbol{\sigma}_h, \mathbf{u}-\mathbf{u}_h, \boldsymbol{\gamma}-\boldsymbol{\gamma}_h), (\boldsymbol{\tau}-\boldsymbol{\tau}_{h,0}, \mathbf{v}-\mathbf{v}_h, \boldsymbol{\eta}))\,, \tag{4.25}$$

where $\mathbf{v}_h := (I_h(v_1), I_h(v_2)) \in H^{\mathbf{u}}_{0,h}$ is the vector Clément interpolant of $\mathbf{v} := (v_1, v_2) \in [H^1_0(\Omega)]^2$. Since $\int_\Omega tr(\boldsymbol{\sigma}-\boldsymbol{\sigma}_h) = 0$ and $\mathbf{u}-\mathbf{u}_h = \mathbf{0}$ on Γ, we deduce, using the orthogonality between symmetric and skew-symmetric tensors, that

$$A((\boldsymbol{\sigma}-\boldsymbol{\sigma}_h, \mathbf{u}-\mathbf{u}_h, \boldsymbol{\gamma}-\boldsymbol{\gamma}_h), (d_h\mathbf{I}, \mathbf{0}, \mathbf{0})) = 0\,.$$

Hence, (4.25) and (4.4) give

$$\begin{aligned} & A((\boldsymbol{\sigma}-\boldsymbol{\sigma}_h, \mathbf{u}-\mathbf{u}_h, \boldsymbol{\gamma}-\boldsymbol{\gamma}_h), (\boldsymbol{\tau}, \mathbf{v}, \boldsymbol{\eta})) \\ = \; & A((\boldsymbol{\sigma}-\boldsymbol{\sigma}_h, \mathbf{u}-\mathbf{u}_h, \boldsymbol{\gamma}-\boldsymbol{\gamma}_h), (\boldsymbol{\tau}-\boldsymbol{\tau}_h, \mathbf{v}-\mathbf{v}_h, \boldsymbol{\eta})) \\ = \; & F(\boldsymbol{\tau}-\boldsymbol{\tau}_h, \mathbf{v}-\mathbf{v}_h, \boldsymbol{\eta}) \;-\; A((\boldsymbol{\sigma}_h, \mathbf{u}_h, \boldsymbol{\gamma}_h), (\boldsymbol{\tau}-\boldsymbol{\tau}_h, \mathbf{v}-\mathbf{v}_h, \boldsymbol{\eta}))\,. \end{aligned}$$

According to the definitions of the forms A and F (cf. (4.5), (4.6)), noting that $\mathbf{div}\,(\boldsymbol{\tau}-\boldsymbol{\tau}_h) = \mathbf{div}\;\underline{\mathbf{curl}}(\boldsymbol{\varphi}-\boldsymbol{\varphi}_h) = \mathbf{0}$, and using again the above mentioned orthogonality, we find, after some algebraic manipulations, that

$$\begin{aligned} A((\boldsymbol{\sigma}-\boldsymbol{\sigma}_h, \mathbf{u}-\mathbf{u}_h, \boldsymbol{\gamma}-\boldsymbol{\gamma}_h), (\boldsymbol{\tau}, \mathbf{v}, \boldsymbol{\eta})) \;=\; & \int_\Omega (\mathbf{f} + \mathbf{div}\,(\boldsymbol{\sigma}_h)) \cdot (\mathbf{v}-\mathbf{v}_h) \\ + \quad & \int_\Omega \left\{ \frac{1}{2}(\boldsymbol{\sigma}_h - \boldsymbol{\sigma}_h^{\mathtt{t}}) \;-\; \kappa_3 \left(\boldsymbol{\gamma}_h - \frac{1}{2}(\nabla \mathbf{u}_h - (\nabla \mathbf{u}_h)^{\mathtt{t}}) \right) \right\} : \boldsymbol{\eta} \\ - \quad & \int_\Omega \left\{ (\mathcal{C}^{-1}\boldsymbol{\sigma}_h - \nabla \mathbf{u}_h + \boldsymbol{\gamma}_h) \;+\; \kappa_1\, \mathcal{C}^{-1}(\mathbf{e}(\mathbf{u}_h) - \mathcal{C}^{-1}\boldsymbol{\sigma}_h) \right\} : (\boldsymbol{\tau}-\boldsymbol{\tau}_h) \\ - \int_\Omega \left\{ \kappa_1 \left(\mathbf{e}(\mathbf{u}_h) - \frac{1}{2}(\mathcal{C}^{-1}\boldsymbol{\sigma}_h + (\mathcal{C}^{-1}\boldsymbol{\sigma}_h)^{\mathtt{t}}) \right) \;+\; \kappa_3 \left(\boldsymbol{\gamma}_h - \frac{1}{2}(\nabla \mathbf{u}_h - (\nabla \mathbf{u}_h)^{\mathtt{t}}) \right) \right\} & : \nabla(\mathbf{v}-\mathbf{v}_h)\,. \end{aligned} \tag{4.26}$$

The rest of the proof of reliability consists in deriving suitable upper bounds for each one of the terms appearing on the right hand side of (4.26). We begin by noticing that direct applications of the Cauchy-Schwarz inequality give

$$\left| \int_\Omega \frac{1}{2}(\boldsymbol{\sigma}_h - \boldsymbol{\sigma}_h^{\mathtt{t}}) : \boldsymbol{\eta} \right| \leq \|\boldsymbol{\sigma}_h - \boldsymbol{\sigma}_h^{\mathtt{t}}\|_{[L^2(\Omega)]^{2\times 2}} \;\|\boldsymbol{\eta}\|_{[L^2(\Omega)]^{2\times 2}}\,, \tag{4.27}$$

and

$$\left| \int_\Omega (\boldsymbol{\gamma}_h - \frac{1}{2}(\nabla \mathbf{u}_h - (\nabla \mathbf{u}_h)^{\mathtt{t}})) : \boldsymbol{\eta} \right| \leq \|\boldsymbol{\gamma}_h - \frac{1}{2}(\nabla \mathbf{u}_h - (\nabla \mathbf{u}_h)^{\mathtt{t}})\|_{[L^2(\Omega)]^{2\times 2}} \;\|\boldsymbol{\eta}\|_{[L^2(\Omega)]^{2\times 2}}\,. \tag{4.28}$$

The decomposition $\Omega = \cup_{T\in\mathcal{T}_h} T$ and the integration by parts formula on each element are employed next to handle the terms from the third and fourth rows of (4.26). We first replace $(\boldsymbol{\tau} - \boldsymbol{\tau}_h)$ by $\underline{\mathbf{curl}}(\boldsymbol{\varphi} - \boldsymbol{\varphi}_h)$ and use that $\mathrm{curl}(\nabla \mathbf{u}_h) = \mathbf{0}$ in each triangle $T \in \mathcal{T}_h$, to obtain

$$\begin{aligned}\int_\Omega (\mathcal{C}^{-1}\boldsymbol{\sigma}_h - \nabla \mathbf{u}_h + \boldsymbol{\gamma}_h) : (\boldsymbol{\tau} - \boldsymbol{\tau}_h) &= \sum_{T\in\mathcal{T}_h} \int_T (\mathcal{C}^{-1}\boldsymbol{\sigma}_h - \nabla \mathbf{u}_h + \boldsymbol{\gamma}_h) : \underline{\mathbf{curl}}(\boldsymbol{\varphi} - \boldsymbol{\varphi}_h) \\ &= \sum_{T\in\mathcal{T}_h} \int_T \mathrm{curl}(\mathcal{C}^{-1}\boldsymbol{\sigma}_h + \boldsymbol{\gamma}_h) \cdot (\boldsymbol{\varphi} - \boldsymbol{\varphi}_h) \\ &- \sum_{e\in E_h} \langle J[(\mathcal{C}^{-1}\boldsymbol{\sigma}_h - \nabla \mathbf{u}_h + \boldsymbol{\gamma}_h)\mathbf{t}_T], \boldsymbol{\varphi} - \boldsymbol{\varphi}_h\rangle_{[L^2(e)]^2}\,, \end{aligned} \tag{4.29}$$

and

$$\begin{aligned}\int_\Omega \mathcal{C}^{-1}(\mathbf{e}(\mathbf{u}_h) - \mathcal{C}^{-1}\boldsymbol{\sigma}_h) : (\boldsymbol{\tau} - \boldsymbol{\tau}_h) &= \sum_{T\in\mathcal{T}_h} \int_T \mathcal{C}^{-1}(\mathbf{e}(\mathbf{u}_h) - \mathcal{C}^{-1}\boldsymbol{\sigma}_h) : \underline{\mathbf{curl}}(\boldsymbol{\varphi} - \boldsymbol{\varphi}_h) \\ &= \sum_{T\in\mathcal{T}_h} \int_T \mathrm{curl}(\mathcal{C}^{-1}(\mathbf{e}(\mathbf{u}_h) - \mathcal{C}^{-1}\boldsymbol{\sigma}_h)) \cdot (\boldsymbol{\varphi} - \boldsymbol{\varphi}_h) \\ &- \sum_{e\in E_h} \langle J[(\mathcal{C}^{-1}(\mathbf{e}(\mathbf{u}_h) - \mathcal{C}^{-1}\boldsymbol{\sigma}_h))\mathbf{t}_T], \boldsymbol{\varphi} - \boldsymbol{\varphi}_h\rangle_{[L^2(e)]^2}\,. \end{aligned} \tag{4.30}$$

On the other hand, using that $\mathbf{v} - \mathbf{v}_h = \mathbf{0}$ on Γ, we easily get

$$\begin{aligned}&\int_\Omega (\mathbf{e}(\mathbf{u}_h) - \frac{1}{2}(\mathcal{C}^{-1}\boldsymbol{\sigma}_h + (\mathcal{C}^{-1}\boldsymbol{\sigma}_h)^{\mathtt{t}})) : \nabla(\mathbf{v} - \mathbf{v}_h) \\ = &- \sum_{T\in\mathcal{T}_h} \int_T \mathbf{div}\,(\mathbf{e}(\mathbf{u}_h) - \frac{1}{2}(\mathcal{C}^{-1}\boldsymbol{\sigma}_h + (\mathcal{C}^{-1}\boldsymbol{\sigma}_h)^{\mathtt{t}})) \cdot (\mathbf{v} - \mathbf{v}_h) \\ + &\sum_{e\in E_h(\Omega)} \langle J[(\mathbf{e}(\mathbf{u}_h) - \frac{1}{2}(\mathcal{C}^{-1}\boldsymbol{\sigma}_h + (\mathcal{C}^{-1}\boldsymbol{\sigma}_h)^{\mathtt{t}}))\boldsymbol{\nu}_T], \mathbf{v} - \mathbf{v}_h\rangle_{[L^2(e)]^2}\,, \end{aligned} \tag{4.31}$$

and

$$\begin{aligned}&\int_\Omega (\boldsymbol{\gamma}_h - \frac{1}{2}(\nabla \mathbf{u}_h - (\nabla \mathbf{u}_h)^{\mathtt{t}})) : \nabla(\mathbf{v} - \mathbf{v}_h) \\ = &- \sum_{T\in\mathcal{T}_h} \int_T \mathbf{div}\,(\boldsymbol{\gamma}_h - \frac{1}{2}(\nabla \mathbf{u}_h - (\nabla \mathbf{u}_h)^{\mathtt{t}})) \cdot (\mathbf{v} - \mathbf{v}_h) \\ + &\sum_{e\in E_h(\Omega)} \langle J[(\boldsymbol{\gamma}_h - \frac{1}{2}(\nabla \mathbf{u}_h - (\nabla \mathbf{u}_h)^{\mathtt{t}}))\boldsymbol{\nu}_T], \mathbf{v} - \mathbf{v}_h\rangle_{[L^2(e)]^2}\,. \end{aligned} \tag{4.32}$$

In what follows, we apply again the Cauchy-Schwarz inequality, Lemma 2.4.1, and the fact that the numbers of triangles in $\Delta(T)$ and $\Delta(e)$ are bounded, independently of h, to

derive the estimates for the expression $\int_\Omega (\mathbf{f} + \mathbf{div}\ \boldsymbol{\sigma}_h)\cdot(\mathbf{v}-\mathbf{v}_h)$ in (4.26) and the right hand sides of (4.29), (4.30), (4.31), and (4.32), with constants C independent of h and λ. Indeed, we easily have

$$\left|\int_\Omega (\mathbf{f} + \mathbf{div}\ \boldsymbol{\sigma}_h)\cdot(\mathbf{v}-\mathbf{v}_h)\right| \ \le\ C\left\{\sum_{T\in\mathcal{T}_h} h_T^2\,\|\mathbf{f} + \mathbf{div}\ \boldsymbol{\sigma}_h\|^2_{[L^2(T)]^2}\right\}^{1/2} \|\mathbf{v}\|_{[H^1(\Omega)]^2}\,, \quad (4.33)$$

In addition, for the terms containing the stream function $\boldsymbol{\varphi}$ (cf. (4.29), (4.30)), we get

$$\begin{aligned}&\left|\sum_{T\in\mathcal{T}_h}\int_T \operatorname{curl}(\mathcal{C}^{-1}\boldsymbol{\sigma}_h+\boldsymbol{\gamma}_h)\cdot(\boldsymbol{\varphi}-\boldsymbol{\varphi}_h)\right|\\ &\quad\le\ C\left\{\sum_{T\in\mathcal{T}_h} h_T^2\,\|\operatorname{curl}(\mathcal{C}^{-1}\boldsymbol{\sigma}_h+\boldsymbol{\gamma}_h)\|^2_{[L^2(T)]^2}\right\}^{1/2}\|\boldsymbol{\varphi}\|_{[H^1(\Omega)]^2}\,, \quad (4.34)\end{aligned}$$

$$\begin{aligned}&\left|\sum_{T\in\mathcal{T}_h}\int_T \operatorname{curl}(\mathcal{C}^{-1}(\mathbf{e}(\mathbf{u}_h)-\mathcal{C}^{-1}\boldsymbol{\sigma}_h))\cdot(\boldsymbol{\varphi}-\boldsymbol{\varphi}_h)\right|\\ &\quad\le\ C\left\{\sum_{T\in\mathcal{T}_h} h_T^2\,\|\operatorname{curl}(\mathcal{C}^{-1}(\mathbf{e}(\mathbf{u}_h)-\mathcal{C}^{-1}\boldsymbol{\sigma}_h))\|^2_{[L^2(T)]^2}\right\}^{1/2}\|\boldsymbol{\varphi}\|_{[H^1(\Omega)]^2}\,, \quad (4.35)\end{aligned}$$

$$\begin{aligned}&\left|\sum_{e\in E_h}\langle J[(\mathcal{C}^{-1}\boldsymbol{\sigma}_h-\nabla\mathbf{u}_h+\boldsymbol{\gamma}_h)\mathbf{t}_T],\boldsymbol{\varphi}-\boldsymbol{\varphi}_h\rangle_{[L^2(e)]^2}\right|\\ &\quad\le\ C\left\{\sum_{e\in E_h} h_e\,\|J[(\mathcal{C}^{-1}\boldsymbol{\sigma}_h-\nabla\mathbf{u}_h+\boldsymbol{\gamma}_h)\mathbf{t}_T]\|^2_{[L^2(e)]^2}\right\}^{1/2}\|\boldsymbol{\varphi}\|_{[H^1(\Omega)]^2}\,, \quad (4.36)\end{aligned}$$

and

$$\begin{aligned}&\left|\sum_{e\in E_h}\langle J[(\mathcal{C}^{-1}(\mathbf{e}(\mathbf{u}_h)-\mathcal{C}^{-1}\boldsymbol{\sigma}_h))\mathbf{t}_T],\boldsymbol{\varphi}-\boldsymbol{\varphi}_h\rangle_{[L^2(e)]^2}\right|\\ &\quad\le\ C\left\{\sum_{e\in E_h} h_e\,\|J[(\mathcal{C}^{-1}(\mathbf{e}(\mathbf{u}_h)-\mathcal{C}^{-1}\boldsymbol{\sigma}_h))\mathbf{t}_T]\|^2_{[L^2(e)]^2}\right\}^{1/2}\|\boldsymbol{\varphi}\|_{[H^1(\Omega)]^2}\,. \quad (4.37)\end{aligned}$$

We observe here, thanks to the equivalence between $\|\boldsymbol{\varphi}\|_{[H^1(\Omega)]^2}$ and $|\boldsymbol{\varphi}|_{[H^1(\Omega)]^2}$, that

$$\|\boldsymbol{\varphi}\|_{[H^1(\Omega)]^2}\ \le\ C\,|\boldsymbol{\varphi}|_{[H^1(\Omega)]^2}\ =\ C\,\|\underline{\mathbf{curl}}(\boldsymbol{\varphi})\|_{[L^2(\Omega)]^2}\ =\ C\,\|\boldsymbol{\tau}\|_{H(\mathbf{div};\Omega)}\,, \quad (4.38)$$

which allows to replace $\|\boldsymbol{\varphi}\|_{[H^1(\Omega)]^2}$ by $\|\boldsymbol{\tau}\|_{H(\mathbf{div};\Omega)}$ in the above estimates (4.34) - (4.37).

Similarly, for the terms on the right hand side of (4.31) and (4.32), we find that

$$\left|\sum_{T\in\mathcal{T}_h}\int_T \mathbf{div}\,(\mathbf{e}(\mathbf{u}_h)-\frac{1}{2}(\mathcal{C}^{-1}\boldsymbol{\sigma}_h+(\mathcal{C}^{-1}\boldsymbol{\sigma}_h)^{\mathtt{t}}))\cdot(\mathbf{v}-\mathbf{v}_h)\right|$$
$$\leq\ C\left\{\sum_{T\in\mathcal{T}_h} h_T^2\,\|\,\mathbf{div}\,(\mathbf{e}(\mathbf{u}_h)-\frac{1}{2}(\mathcal{C}^{-1}\boldsymbol{\sigma}_h+(\mathcal{C}^{-1}\boldsymbol{\sigma}_h)^{\mathtt{t}}))\|^2_{[L^2(T)]^2}\right\}^{1/2}\|\mathbf{v}\|_{[H^1(\Omega)]^2}, \tag{4.39}$$

$$\left|\sum_{T\in\mathcal{T}_h}\int_T \mathbf{div}\,(\boldsymbol{\gamma}_h-\frac{1}{2}(\nabla\mathbf{u}_h-(\nabla\mathbf{u}_h)^{\mathtt{t}}))\cdot(\mathbf{v}-\mathbf{v}_h)\right|$$
$$\leq\ C\left\{\sum_{T\in\mathcal{T}_h} h_T^2\,\|\,\mathbf{div}\,(\boldsymbol{\gamma}_h-\frac{1}{2}(\nabla\mathbf{u}_h-(\nabla\mathbf{u}_h)^{\mathtt{t}}))\|^2_{[L^2(T)]^2}\right\}^{1/2}\|\mathbf{v}\|_{[H^1(\Omega)]^2}\,, \tag{4.40}$$

$$\left|\sum_{e\in E_h(\Omega)}\langle J[(\mathbf{e}(\mathbf{u}_h)-\frac{1}{2}(\mathcal{C}^{-1}\boldsymbol{\sigma}_h+(\mathcal{C}^{-1}\boldsymbol{\sigma}_h)^{\mathtt{t}}))\boldsymbol{\nu}_T],\mathbf{v}-\mathbf{v}_h\rangle_{[L^2(e)]^2}\right|$$
$$\leq\ C\left\{\sum_{e\in E_h(\Omega)} h_e\,\|J[(\mathbf{e}(\mathbf{u}_h)-\frac{1}{2}(\mathcal{C}^{-1}\boldsymbol{\sigma}_h+(\mathcal{C}^{-1}\boldsymbol{\sigma}_h)^{\mathtt{t}}))\boldsymbol{\nu}_T]\|^2_{[L^2(e)]^2}\right\}^{1/2}\|\mathbf{v}\|_{[H^1(\Omega)]^2}, \tag{4.41}$$

and

$$\left|\sum_{e\in E_h(\Omega)}\langle J[(\boldsymbol{\gamma}_h-\frac{1}{2}(\nabla\mathbf{u}_h-(\nabla\mathbf{u}_h)^{\mathtt{t}}))\boldsymbol{\nu}_T],\mathbf{v}-\mathbf{v}_h\rangle_{[L^2(e)]^2}\right|$$
$$\leq\ C\left\{\sum_{e\in E_h(\Omega)} h_e\,\|J[(\boldsymbol{\gamma}_h-\frac{1}{2}(\nabla\mathbf{u}_h-(\nabla\mathbf{u}_h)^{\mathtt{t}}))\boldsymbol{\nu}_T]\|^2_{[L^2(e)]^2}\right\}^{1/2}\|\mathbf{v}\|_{[H^1(\Omega)]^2}\,. \tag{4.42}$$

Therefore, placing (4.34) - (4.37) (resp. (4.39) - (4.42)) back into (4.29) and (4.30) (resp. (4.31) and (4.32)), employing the estimates (4.27), (4.28), and (4.33), and using the identities

$$\sum_{e\in E_h(\Omega)}\int_e = \frac{1}{2}\sum_{T\in\mathcal{T}_h}\sum_{e\in E(T)\cap E_h(\Omega)}\int_e$$

and

$$\sum_{e\in E_h}\int_e = \sum_{e\in E_h(\Omega)}\int_e \;+\; \sum_{T\in\mathcal{T}_h}\sum_{e\in E(T)\cap E_h(\Gamma)}\int_e,$$

we conclude from (4.26) that

$$\sup_{\substack{\mathbf{0}\neq(\boldsymbol{\tau},\mathbf{v},\boldsymbol{\eta})\in\mathbf{H}_0\\ \mathbf{div}\,(\boldsymbol{\tau})=\mathbf{0}}} \frac{A((\boldsymbol{\sigma}-\boldsymbol{\sigma}_h,\mathbf{u}-\mathbf{u}_h,\boldsymbol{\gamma}-\boldsymbol{\gamma}_h),(\boldsymbol{\tau},\mathbf{v},\boldsymbol{\eta}))}{\|(\boldsymbol{\tau},\mathbf{v},\boldsymbol{\eta})\|_{\mathbf{H}_0}} \leq C\,\boldsymbol{\theta}\,.$$

This inequality and Lemma 4.3.1 complete the proof of reliability of $\boldsymbol{\theta}$.

We end this section by remarking that when the finite element subspace $\mathbf{H}_{0,h}$ is given by (4.16), that is when $\boldsymbol{\sigma}_h|_T \in [\mathbb{R}\mathbb{T}_0(T)^{\mathtt{t}}]^2$, $\mathbf{u}_h|_T \in [\mathbf{P}_1(T)]^2$ and $\boldsymbol{\gamma}_h|_T \in [\mathbf{P}_0(T)]^{2\times 2}$, then the expression (4.20) for θ_T^2 simplifies to

$$\begin{aligned}
\theta_T^2 \;:=\; & \|\mathbf{f}+\mathbf{div}\,(\boldsymbol{\sigma}_h)\|^2_{[L^2(T)]^2} \,+\, \|\boldsymbol{\sigma}_h-\boldsymbol{\sigma}_h^{\mathtt{t}}\|^2_{[L^2(T)]^{2\times 2}} \,+\, \|\boldsymbol{\gamma}_h-\frac{1}{2}(\nabla\mathbf{u}_h-(\nabla\mathbf{u}_h)^{\mathtt{t}})\|^2_{[L^2(T)]^{2\times 2}} \\
& + \; h_T^2\left\{\|\,\mathrm{curl}(\mathcal{C}^{-1}\boldsymbol{\sigma}_h)\|^2_{[L^2(T)]^2} \,+\, \|\,\mathrm{curl}(\mathcal{C}^{-1}(\mathcal{C}^{-1}\boldsymbol{\sigma}_h))\|^2_{[L^2(T)]^2}\right\} \\
& + \sum_{e\in E(T)} h_e\left\{\|J[(\mathcal{C}^{-1}\boldsymbol{\sigma}_h-\nabla\mathbf{u}_h+\boldsymbol{\gamma}_h)\mathbf{t}_T]\|^2_{[L^2(e)]^2} \,+\, \|J[(\mathcal{C}^{-1}(\mathbf{e}(\mathbf{u}_h)-\mathcal{C}^{-1}\boldsymbol{\sigma}_h))\mathbf{t}_T]\|^2_{[L^2(e)]^2}\right\} \\
& + \; h_T^2\,\|\,\mathbf{div}\,(\frac{1}{2}(\mathcal{C}^{-1}\boldsymbol{\sigma}_h+(\mathcal{C}^{-1}\boldsymbol{\sigma}_h)^{\mathtt{t}}))\|^2_{[L^2(T)]^2} \\
& + \sum_{e\in E(T)\cap E_h(\Omega)} h_e\,\|J[(\mathbf{e}(\mathbf{u}_h)-\frac{1}{2}(\mathcal{C}^{-1}\boldsymbol{\sigma}_h+(\mathcal{C}^{-1}\boldsymbol{\sigma}_h)^{\mathtt{t}}))\boldsymbol{\nu}_T]\|^2_{[L^2(e)]^2} \\
& + \sum_{e\in E(T)\cap E_h(\Omega)} h_e\,\|J[(\boldsymbol{\gamma}_h-\frac{1}{2}(\nabla\mathbf{u}_h-(\nabla\mathbf{u}_h)^{\mathtt{t}}))\boldsymbol{\nu}_T]\|^2_{[L^2(e)]^2}\,. \qquad (4.43)
\end{aligned}$$

4.4 Efficiency of the a posteriori error estimator

In this section we proceed as in [24] and [25] (see also [35]) and apply inverse inequalities (see [26]) and the localization technique introduced in [50], which is based on triangle-bubble and edge-bubble functions, to prove the efficiency of our a posteriori error estimator $\boldsymbol{\theta}$ (lower bound of the estimate (4.21)).

4.4.1 Preliminaries

We begin with some notations and preliminary results. Given $T \in \mathcal{T}_h$ and $e \in E(T)$, we let ψ_T and ψ_e be the usual triangle-bubble and edge-bubble functions, respectively (see (1.5) and (1.6) in [50]). In particular, ψ_T satisfies $\psi_T \in \mathbf{P}_3(T)$, $\mathrm{supp}(\psi_T) \subseteq T$, $\psi_T = 0$ on ∂T, and $0 \leq \psi_T \leq 1$ in T. Similarly, $\psi_e|_T \in \mathbf{P}_2(T)$, $\mathrm{supp}(\psi_e) \subseteq w_e := \cup\{T' \in \mathcal{T}_h : e \in E(T')\}$, $\psi_e = 0$ on $\partial T\backslash e$, and $0 \leq \psi_e \leq 1$ in w_e. We also recall from [49] that,

given $k \in \mathbb{N} \cup \{0\}$, there exists an extension operator $L : C(e) \to C(T)$ that satisfies $L(p) \in \mathbf{P}_k(T)$ and $L(p)|_e = p \ \forall p \in \mathbf{P}_k(e)$. Additional properties of ψ_T, ψ_e, and L are collected in Lemma 2.4.4.

The following inverse estimate will also be used.

Lemma 4.4.1 *Let $l, m \in \mathbb{N} \cup \{0\}$ such that $l \leq m$. Then, for any triangle T, there exists $c > 0$, depending only on k, l, m and the shape of T, such that*

$$|q|_{H^m(T)} \ \leq \ c\, h_T^{l-m}\, |q|_{H^l(T)} \quad \forall\, q \ \in \ \mathbf{P}_k(T)\,. \tag{4.44}$$

Proof.ing-mat.udec See Theorem 3.2.6 in [26]. □

Our goal is to estimate the 11 terms defining the error indicator θ_T^2 (cf. (4.20)). Using $\mathbf{f} \ = \ -\ \mathbf{div}\ \boldsymbol{\sigma}$, the symmetry of $\boldsymbol{\sigma}$, and $\boldsymbol{\gamma} = \frac{1}{2}(\nabla \mathbf{u} - (\nabla \mathbf{u})^{\mathtt{t}})$, we first observe that there hold

$$\|\mathbf{f} + \mathbf{div}\,(\boldsymbol{\sigma}_h)\|^2_{[L^2(T)]^2} \ = \ \|\,\mathbf{div}\,(\boldsymbol{\sigma} - \boldsymbol{\sigma}_h)\|^2_{[L^2(T)]^2}\,, \tag{4.45}$$

$$\|\boldsymbol{\sigma}_h - \boldsymbol{\sigma}_h^{\mathtt{t}}\|^2_{[L^2(T)]^{2\times 2}} \ \leq \ 4\,\|\boldsymbol{\sigma} - \boldsymbol{\sigma}_h\|^2_{[L^2(T)]^{2\times 2}}\,, \tag{4.46}$$

and

$$\|\boldsymbol{\gamma}_h - \frac{1}{2}(\nabla \mathbf{u}_h - (\nabla \mathbf{u}_h)^{\mathtt{t}})\|^2_{[L^2(T)]^{2\times 2}} \ \leq \ 2\left\{\|\boldsymbol{\gamma} - \boldsymbol{\gamma}_h\|^2_{[L^2(T)]^{2\times 2}} \ + \ |\mathbf{u} - \mathbf{u}_h|^2_{[H^1(T)]^2}\right\}. \tag{4.47}$$

The upper bounds of the remaining 8 terms, which depend on the mesh parameters h_T and h_e, will be derived in Section 4.4.2 below. To this end we prove four lemmata. The result required for the terms involving the curl operator is given first.

Lemma 4.4.2 *Let $\boldsymbol{\rho}_h \in [L^2(\Omega)]^{2\times 2}$ be a piecewise polynomial of degree $k \geq 0$ on each $T \in \mathcal{T}_h$. In addition, let $\boldsymbol{\rho} \in [L^2(\Omega)]^{2\times 2}$ such that $\mathrm{curl}(\boldsymbol{\rho}) = \mathbf{0}$ on each $T \in \mathcal{T}_h$. Then, there exists $c > 0$, independent of h, such that for any $T \in \mathcal{T}_h$*

$$\|\,\mathrm{curl}(\boldsymbol{\rho}_h)\|_{[L^2(T)]^2} \ \leq \ c\, h_T^{-1}\, \|\boldsymbol{\rho} - \boldsymbol{\rho}_h\|_{[L^2(T)]^{2\times 2}}\,. \tag{4.48}$$

Proof. We proceed as in the proof of Lemma 6.3 in [25]. Applying (2.37), integrating by parts, observing that $\psi_T \ = \ 0$ on ∂T, and using the Cauchy-Schwarz inequality, we obtain

$$c_1^{-1}\,\|\,\mathrm{curl}(\boldsymbol{\rho}_h)\|^2_{[L^2(T)]^2} \ \leq \ \|\psi_T^{1/2}\ \mathrm{curl}(\boldsymbol{\rho}_h)\|^2_{[L^2(T)]^2} \ = \ \int_T \psi_T\, \mathrm{curl}(\boldsymbol{\rho}_h) \cdot \mathrm{curl}(\boldsymbol{\rho}_h - \boldsymbol{\rho})$$

$$= \ \int_T (\boldsymbol{\rho} - \boldsymbol{\rho}_h) : \underline{\mathbf{curl}}(\psi_T\, \mathrm{curl}(\boldsymbol{\rho}_h)) \ \leq \ \|\boldsymbol{\rho} - \boldsymbol{\rho}_h\|_{[L^2(T)]^{2\times 2}}\ \|\underline{\mathbf{curl}}(\psi_T\, \mathrm{curl}(\boldsymbol{\rho}_h))\|_{[L^2(T)]^{2\times 2}}\,. \tag{4.49}$$

Next, the inverse inequality (4.44) and the fact that $0 \leq \psi_T \leq 1$ give

$$\|\underline{\mathbf{curl}}(\psi_T \operatorname{curl}(\boldsymbol{\rho}_h))\|_{[L^2(T)]^{2\times 2}} \leq c\, h_T^{-1} \|\psi_T \operatorname{curl}(\boldsymbol{\rho}_h)\|_{[L^2(T)]^2} \leq c\, h_T^{-1} \|\operatorname{curl}(\boldsymbol{\rho}_h)\|_{[L^2(T)]^2},$$

which, together with (4.49), yields (4.48). □

The tangential jumps across the edges of the triangulation will be handled by employing the following estimate.

Lemma 4.4.3 *Let $\boldsymbol{\rho}_h \in [L^2(\Omega)]^{2\times 2}$ be a piecewise polynomial of degree $k \geq 0$ on each $T \in \mathcal{T}_h$. Then, there exists $c > 0$, independent of h, such that for any $e \in E_h$*

$$\|J[\boldsymbol{\rho}_h \mathbf{t}_T]\|_{[L^2(e)]^2} \leq c\, h_e^{-1/2} \|\boldsymbol{\rho}_h\|_{[L^2(w_e)]^{2\times 2}}. \tag{4.50}$$

Proof. Given an edge $e \in E_h$, we first denote by $\mathbf{w}_h := J[\boldsymbol{\rho}_h \mathbf{t}_T]$ the corresponding tangential jump of $\boldsymbol{\rho}_h$. Then, employing (2.38) and integrating by parts on each triangle of w_e, we obtain

$$c_2^{-1} \|\mathbf{w}_h\|^2_{[L^2(e)]^2} \leq \|\psi_e^{1/2} \mathbf{w}_h\|^2_{[L^2(e)]^2} = \|\psi_e^{1/2} L(\mathbf{w}_h)\|^2_{[L^2(e)]^2}$$

$$= \int_e \psi_e\, L(\mathbf{w}_h) \cdot J[\boldsymbol{\rho}_h \mathbf{t}_T] = \int_{w_e} \operatorname{curl}(\boldsymbol{\rho}_h) \cdot \psi_e\, L(\mathbf{w}_h) + \int_{w_e} \boldsymbol{\rho}_h : \underline{\mathbf{curl}}(\psi_e L(\mathbf{w}_h)), \tag{4.51}$$

which, using the Cauchy-Schwarz inequality, yields

$$\begin{aligned} c_2^{-1} \|\mathbf{w}_h\|^2_{[L^2(e)]^2} &\leq \|\operatorname{curl}(\boldsymbol{\rho}_h)\|_{[L^2(w_e)]^2} \|\psi_e\, L(\mathbf{w}_h)\|_{[L^2(w_e)]^2} \\ &+ \|\boldsymbol{\rho}_h\|_{[L^2(w_e)]^{2\times 2}} \|\underline{\mathbf{curl}}(\psi_e\, L(\mathbf{w}_h))\|_{[L^2(w_e)]^{2\times 2}}. \end{aligned} \tag{4.52}$$

Now, applying Lemma 4.4.2 with $\boldsymbol{\rho} = \mathbf{0}$ and using that $h_T^{-1} \leq h_e^{-1}$, we find that

$$\|\operatorname{curl}(\boldsymbol{\rho}_h)\|_{[L^2(w_e)]^2} \leq C\, h_e^{-1} \|\boldsymbol{\rho}_h\|_{[L^2(w_e)]^{2\times 2}}. \tag{4.53}$$

On the other hand, employing (2.39) and the fact that $0 \leq \psi_e \leq 1$, we deduce that

$$\|\psi_e L(\mathbf{w}_h)\|_{[L^2(w_e)]^2} \leq C\, h_e^{1/2} \|\mathbf{w}_h\|_{[L^2(e)]^2}, \tag{4.54}$$

whereas the inverse estimate (4.44) and (2.39) yield

$$\|\underline{\mathbf{curl}}(\psi_e L(\mathbf{w}_h))\|_{[L^2(w_e)]^{2\times 2}} \leq C\, h_e^{-1/2} \|\mathbf{w}_h\|_{[L^2(e)]^2}. \tag{4.55}$$

Finally, (4.50) follows easily from (4.52)–(4.55), which completes the proof. □

The estimate required for the terms involving the **div** operator is provided next.

Lemma 4.4.4 *Let $\boldsymbol{\rho}_h \in [L^2(\Omega)]^{2\times 2}$ be a piecewise polynomial of degree $k \geq 0$ on each $T \in \mathcal{T}_h$. Then, there exists $c > 0$, independent of h, such that for any $T \in \mathcal{T}_h$*

$$\|\,\mathbf{div}\,(\boldsymbol{\rho}_h)\|_{[L^2(T)]^2} \;\leq\; c\,h_T^{-1}\,\|\boldsymbol{\rho}_h\|_{[L^2(T)]^{2\times 2}}\,. \tag{4.56}$$

Proof. Applying (2.37), integrating by parts, and then employing the Cauchy-Schwarz inequality, we find that

$$\begin{aligned} c_1^{-1}\|\,\mathbf{div}\,(\boldsymbol{\rho}_h)\|^2_{[L^2(T)]^2} \;\leq\; \|\psi_T^{1/2}\,\mathbf{div}\,(\boldsymbol{\rho}_h)\|^2_{[L^2(T)]^2} \;=\; \int_T \psi_T\,\mathbf{div}\,(\boldsymbol{\rho}_h)\cdot\mathbf{div}\,(\boldsymbol{\rho}_h) \\ =\; -\int_T \boldsymbol{\rho}_h : \nabla(\psi_T\,\mathbf{div}\,(\boldsymbol{\rho}_h)) \;\leq\; \|\boldsymbol{\rho}_h\|_{[L^2(T)]^{2\times 2}}\,\|\nabla(\psi_T\,\mathbf{div}\,(\boldsymbol{\rho}_h))\|_{[L^2(T)]^{2\times 2}}\,. \end{aligned} \tag{4.57}$$

Next, the inverse estimate (4.44) and the fact that $0 \leq \psi_T \leq 1$ in T imply that

$$\|\nabla(\psi_T\,\mathbf{div}\,(\boldsymbol{\rho}_h))\|_{[L^2(T)]^{2\times 2}} \;\leq\; c\,h_T^{-1}\,\|\psi_T\,\mathbf{div}\,(\boldsymbol{\rho}_h)\|_{[L^2(T)]^2} \;\leq\; c\,h_T^{-1}\,\|\,\mathbf{div}\,(\boldsymbol{\rho}_h)\|_{[L^2(T)]^2}\,,$$

which, together with (4.57), yields (4.56). □

Finally, the estimate required for the normal jumps across the edges of the triangulation is established as follows.

Lemma 4.4.5 *Let $\boldsymbol{\rho}_h \in [L^2(\Omega)]^{2\times 2}$ be a piecewise polynomial of degree $k \geq 0$ on each $T \in \mathcal{T}_h$. Then, there exists $c > 0$, independent of h, such that for any $e \in E_h$*

$$\|J[\boldsymbol{\rho}_h\boldsymbol{\nu}_T]\|_{[L^2(e)]^2} \;\leq\; c\,h_e^{-1/2}\,\|\boldsymbol{\rho}_h\|_{[L^2(w_e)]^{2\times 2}}\,. \tag{4.58}$$

Proof. We proceed similarly as in the proof of Lemma 4.4.3. Given an edge $e \in E_h$, we now denote by $\mathbf{w}_h := J[\boldsymbol{\rho}_h\boldsymbol{\nu}_T]$ the corresponding normal jump of $\boldsymbol{\rho}_h$. Then, employing (2.38) and integrating by parts on each triangle of w_e, we obtain

$$\begin{aligned} c_2^{-1}\,\|\mathbf{w}_h\|^2_{[L^2(e)]^2} \;\leq\; \|\psi_e^{1/2}\,\mathbf{w}_h\|^2_{[L^2(e)]^2} \;=\; \|\psi_e^{1/2}\,L(\mathbf{w}_h)\|^2_{[L^2(e)]^2} \\ =\; \int_e \psi_e\,L(\mathbf{w}_h)\cdot J[\boldsymbol{\rho}_h\boldsymbol{\nu}_T] \;=\; \int_{w_e}\mathbf{div}\,(\boldsymbol{\rho}_h)\cdot\psi_e\,L(\mathbf{w}_h) \;+\; \int_{w_e}\boldsymbol{\rho}_h : \nabla(\psi_e L(\mathbf{w}_h))\,, \end{aligned} \tag{4.59}$$

which, using the Cauchy-Schwarz inequality, yields

$$\begin{aligned} c_2^{-1}\;\|\mathbf{w}_h\|^2_{[L^2(e)]^2} \;\leq\; \|\,\mathbf{div}\,(\boldsymbol{\rho}_h)\|_{[L^2(w_e)]^2}\;\|\psi_e\,L(\mathbf{w}_h)\|_{[L^2(w_e)]^2} \\ +\quad \|\boldsymbol{\rho}_h\|_{[L^2(w_e)]^{2\times 2}}\;\|\nabla(\psi_e\,L(\mathbf{w}_h))\|_{[L^2(w_e)]^{2\times 2}}\,. \end{aligned} \tag{4.60}$$

Now, applying Lemma 4.4.4 and using that $h_T^{-1} \leq h_e^{-1}$, we deduce that

$$\|\operatorname{\mathbf{div}}(\boldsymbol{\rho}_h)\|_{[L^2(w_e)]^2} \leq C\, h_e^{-1}\, \|\boldsymbol{\rho}_h\|_{[L^2(w_e)]^{2\times 2}}\,. \tag{4.61}$$

On the other hand, employing (2.39) and the fact that $0 \leq \psi_e \leq 1$, we deduce that

$$\|\psi_e L(\mathbf{w}_h)\|_{[L^2(w_e)]^2} \leq C\, h_e^{1/2} \|\mathbf{w}_h\|_{[L^2(e)]^2}\,, \tag{4.62}$$

whereas the inverse estimate (4.44) and (2.39) yield

$$\|\nabla(\psi_e L(\mathbf{w}_h))\|_{[L^2(w_e)]^{2\times 2}} \leq C\, h_e^{-1/2}\, \|\mathbf{w}_h\|_{[L^2(e)]^2}\,. \tag{4.63}$$

Finally, (4.58) follows easily from (4.60)–(4.63), which completes the proof. □

4.4.2 The main efficiency estimates

As already announced, we now complete the proof of efficiency of $\boldsymbol{\theta}$ by conveniently applying Lemmata 4.4.2 - 4.4.5 to the corresponding terms defining θ_T^2.

Lemma 4.4.6 *There exist C_1, $C_2 > 0$, independent of h and λ, such that for any $T \in \mathcal{T}_h$*

$$h_T^2\, \|\operatorname{curl}(\mathcal{C}^{-1}\boldsymbol{\sigma}_h + \boldsymbol{\gamma}_h)\|^2_{[L^2(T)]^2} \leq C_1 \left\{ \|\boldsymbol{\sigma} - \boldsymbol{\sigma}_h\|^2_{[L^2(T)]^{2\times 2}} + \|\boldsymbol{\gamma} - \boldsymbol{\gamma}_h\|^2_{[L^2(T)]^{2\times 2}} \right\} \tag{4.64}$$

and

$$h_T^2\, \|\operatorname{curl}(\mathcal{C}^{-1}(\mathbf{e}(\mathbf{u}_h) - \mathcal{C}^{-1}\boldsymbol{\sigma}_h))\|^2_{[L^2(T)]^2} \leq C_2 \left\{ |\mathbf{u} - \mathbf{u}_h|^2_{[H^1(T)]^2} + \|\boldsymbol{\sigma} - \boldsymbol{\sigma}_h\|^2_{[L^2(T)]^{2\times 2}} \right\}. \tag{4.65}$$

Proof. Applying Lemma 4.4.2 with $\boldsymbol{\rho}_h := \mathcal{C}^{-1}\boldsymbol{\sigma}_h + \boldsymbol{\gamma}_h$ and $\boldsymbol{\rho} := \nabla \mathbf{u} = \mathcal{C}^{-1}\boldsymbol{\sigma} + \boldsymbol{\gamma}$, and then using the triangle inequality and the continuity of $\mathcal{C}^{-1}$, we obtain (4.64). Similarly, (4.65) follows from Lemma 4.4.2 with $\boldsymbol{\rho}_h := \mathcal{C}^{-1}(\mathbf{e}(\mathbf{u}_h) - \mathcal{C}^{-1}\boldsymbol{\sigma}_h)$ and $\boldsymbol{\rho} := \mathcal{C}^{-1}(\mathbf{e}(\mathbf{u}) - \mathcal{C}^{-1}\boldsymbol{\sigma}) = \mathbf{0}$. □

Lemma 4.4.7 *There exist C_3, $C_4 > 0$, independent of h and λ, such that for any $e \in E_h$*

$$\begin{aligned} &h_e\, J[(\mathcal{C}^{-1}\boldsymbol{\sigma}_h - \nabla \mathbf{u}_h + \boldsymbol{\gamma}_h)\mathbf{t}_T]\|^2_{[L^2(e)]^2} \\ &\qquad \leq C_3 \left\{ \|\boldsymbol{\sigma} - \boldsymbol{\sigma}_h\|^2_{[L^2(w_e)]^{2\times 2}} + |\mathbf{u} - \mathbf{u}_h|^2_{[H^1(w_e)]^2} + \|\boldsymbol{\gamma} - \boldsymbol{\gamma}_h\|^2_{[L^2(w_e)]^{2\times 2}} \right\} \end{aligned} \tag{4.66}$$

and

$$h_e\, \|J[(\mathcal{C}^{-1}(\mathbf{e}(\mathbf{u}_h) - \mathcal{C}^{-1}\boldsymbol{\sigma}_h))\mathbf{t}_T]\|^2_{[L^2(e)]^2} \leq C_4 \left\{ |\mathbf{u} - \mathbf{u}_h|^2_{[H^1(w_e)]^2} + \|\boldsymbol{\sigma} - \boldsymbol{\sigma}_h\|^2_{[L^2(w_e)]^{2\times 2}} \right\}. \tag{4.67}$$

Proof. The inequality (4.66) follows from Lemma 4.4.3 with $\boldsymbol{\rho}_h := \mathcal{C}^{-1}\boldsymbol{\sigma}_h - \nabla \mathbf{u}_h + \boldsymbol{\gamma}_h$, introducing $\mathbf{0} = \mathcal{C}^{-1}\boldsymbol{\sigma} - \nabla \mathbf{u} + \boldsymbol{\gamma}$ in the resulting estimate, and then applying the triangle inequality and the continuity of $\mathcal{C}^{-1}$. Analogously, the estimate (4.67) is obtained from Lemma 4.4.3 defining $\boldsymbol{\rho}_h := \mathcal{C}^{-1}(\mathbf{e}(\mathbf{u}_h) - \mathcal{C}^{-1}\boldsymbol{\sigma}_h)$ and then introducing $\mathbf{0} = \mathcal{C}^{-1}(\mathbf{e}(\mathbf{u}) - \mathcal{C}^{-1}\boldsymbol{\sigma})$. □

Lemma 4.4.8 *There exist C_5, $C_6 > 0$, independent of h and λ, such that for any $T \in \mathcal{T}_h$*

$$h_T^2 \, \| \, \mathbf{div} \, (\mathbf{e}(\mathbf{u}_h) - \frac{1}{2}(\mathcal{C}^{-1}\boldsymbol{\sigma}_h + (\mathcal{C}^{-1}\boldsymbol{\sigma}_h)^{\mathtt{t}}))\|^2_{[L^2(T)]^2} \, \leq \, C_5 \left\{ |\mathbf{u} - \mathbf{u}_h|^2_{[H^1(T)]^2} + \|\boldsymbol{\sigma} - \boldsymbol{\sigma}_h\|^2_{[L^2(T)]^2} \right\} \tag{4.68}$$

and

$$h_T^2 \, \| \, \mathbf{div} \, (\boldsymbol{\gamma}_h - \frac{1}{2}(\nabla \mathbf{u}_h - (\nabla \mathbf{u}_h)^{\mathtt{t}}))\|^2_{[L^2(T)]^2} \, \leq \, C_6 \left\{ \|\boldsymbol{\gamma} - \boldsymbol{\gamma}_h\|^2_{[L^2(T)]^2} + |\mathbf{u} - \mathbf{u}_h|^2_{[H^1(T)]^2} \right\}. \tag{4.69}$$

Proof. The upper bound given by (4.68) follows from Lemma 4.4.4 defining $\boldsymbol{\rho}_h := \mathbf{e}(\mathbf{u}_h) - \frac{1}{2}(\mathcal{C}^{-1}\boldsymbol{\sigma}_h + (\mathcal{C}^{-1}\boldsymbol{\sigma}_h)^{\mathtt{t}})$, introducing $\mathbf{0} = \mathbf{e}(\mathbf{u}) - \frac{1}{2}(\mathcal{C}^{-1}\boldsymbol{\sigma} + (\mathcal{C}^{-1}\boldsymbol{\sigma})^{\mathtt{t}})$ in the resulting estimate, and then using the triangle inequality and the continuity of the operators $\mathbf{e}$ and $\mathcal{C}^{-1}$. Similarly, applying Lemma 4.4.4 with $\boldsymbol{\rho}_h := \boldsymbol{\gamma}_h - \frac{1}{2}(\nabla \mathbf{u}_h - (\nabla \mathbf{u}_h)^{\mathtt{t}})$ and introducing $\mathbf{0} = \boldsymbol{\gamma} - \frac{1}{2}(\nabla \mathbf{u} - (\nabla \mathbf{u})^{\mathtt{t}})$, we obtain (4.69). □

Lemma 4.4.9 *There exist C_7, $C_8 > 0$, independent of h and λ, such that for any $e \in E_h$*

$$h_e \, \|J[(\mathbf{e}(\mathbf{u}_h) - \frac{1}{2}(\mathcal{C}^{-1}\boldsymbol{\sigma}_h + (\mathcal{C}^{-1}\boldsymbol{\sigma}_h)^{\mathtt{t}}))\boldsymbol{\nu}_T]\|^2_{[L^2(e)]^2} \, \leq \, C_7 \left\{ |\mathbf{u} - \mathbf{u}_h|^2_{[H^1(w_e)]^2} + \|\boldsymbol{\sigma} - \boldsymbol{\sigma}_h\|^2_{[L^2(w_e)]^{2\times 2}} \right\} \tag{4.70}$$

and

$$h_e \, \|J[(\boldsymbol{\gamma}_h - \frac{1}{2}(\nabla \mathbf{u}_h - (\nabla \mathbf{u}_h)^{\mathtt{t}}))\boldsymbol{\nu}_T]\|^2_{[L^2(e)]^2} \, \leq \, C_8 \left\{ \|\boldsymbol{\gamma} - \boldsymbol{\gamma}_h\|^2_{[L^2(w_e)]^{2\times 2}} + |\mathbf{u} - \mathbf{u}_h|^2_{[H^1(w_e)]^2} \right\}. \tag{4.71}$$

Proof. The estimate (4.70) follows from Lemma 4.4.5 with $\boldsymbol{\rho}_h := \mathbf{e}(\mathbf{u}_h) - \frac{1}{2}(\mathcal{C}^{-1}\boldsymbol{\sigma}_h + (\mathcal{C}^{-1}\boldsymbol{\sigma}_h)^{\mathtt{t}})$, introducing $\mathbf{0} := \mathbf{e}(\mathbf{u}) - \frac{1}{2}(\mathcal{C}^{-1}\boldsymbol{\sigma} + (\mathcal{C}^{-1}\boldsymbol{\sigma})^{\mathtt{t}})$, and then employing again the triangle inequality and the continuity of the operators $\mathbf{e}$ and $\mathcal{C}^{-1}$. Analogously, the estimate (4.71) follows from Lemma 4.4.5 defining $\boldsymbol{\rho}_h := \boldsymbol{\gamma}_h - \frac{1}{2}(\nabla \mathbf{u}_h + (\nabla \mathbf{u}_h)^{\mathtt{t}})$ and then introducing $\mathbf{0} = \boldsymbol{\gamma} - \frac{1}{2}(\nabla \mathbf{u} + (\nabla \mathbf{u})^{\mathtt{t}})$. □

Finally, the efficiency of $\boldsymbol{\theta}$ (lower bound of (4.21)) follows straightforwardly from the estimates (4.45) - (4.47), (4.64), (4.65) (cf. Lemma 4.4.6), (4.66), (4.67) (cf. Lemma 4.4.7), (4.68), (4.69) (cf. Lemma 4.4.8), and (4.70), (4.71) (cf. Lemma 4.4.9), after summing over all $T \in \mathcal{T}_h$ and using that the number of triangles in each domain w_e is bounded by two.

4.5 Numerical results

In this section we present several numerical results illustrating the performance of the augmented mixed finite element scheme (4.10) and the a posteriori error estimator $\boldsymbol{\theta}$ analyzed in this paper, using the specific finite element subspaces defined at the end of Section 4.2 (see (4.13) - (4.19)). We recall that in this case the local indicator θ_T^2 reduces to (4.43). Now, in order to implement the integral mean zero condition for functions of the space $H_{0,h}^{\boldsymbol{\sigma}} = \left\{ \boldsymbol{\tau}_h \in H_h^{\boldsymbol{\sigma}} : \quad \int_\Omega tr(\boldsymbol{\tau}_h) = 0 \right\}$ we introduce, as described in [36], a Lagrange multiplier ($\varphi_h \in \mathbb{R}$ below). That is, instead of (4.10), we consider the equivalent problem: *Find* $(\boldsymbol{\sigma}_h, \mathbf{u}_h, \boldsymbol{\gamma}_h, \varphi_h) \in H_h^{\boldsymbol{\sigma}} \times H_{0,h}^{\mathbf{u}} \times H_h^{\boldsymbol{\gamma}} \times \mathbb{R}$ *such that*

$$\begin{aligned} A((\boldsymbol{\sigma}_h, \mathbf{u}_h, \boldsymbol{\gamma}_h), (\boldsymbol{\tau}_h, \mathbf{v}_h, \boldsymbol{\eta}_h)) + \varphi_h \int_\Omega tr(\boldsymbol{\tau}_h) &= F(\boldsymbol{\tau}_h, \mathbf{v}_h, \boldsymbol{\eta}_h)\,, \\ \psi_h \int_\Omega tr(\boldsymbol{\sigma}_h) &= 0\,, \end{aligned} \tag{4.72}$$

for all $(\boldsymbol{\tau}_h, \mathbf{v}_h, \boldsymbol{\eta}_h, \psi_h) \in H_h^{\boldsymbol{\sigma}} \times H_{0,h}^{\mathbf{u}} \times H_h^{\boldsymbol{\gamma}} \times \mathbb{R}$. In fact, we recall from [36] the following theorem establishing the equivalence between (4.10) and (4.72).

Theorem 4.5.1

a) *Let* $(\boldsymbol{\sigma}_h, \mathbf{u}_h, \boldsymbol{\gamma}_h) \in \mathbf{H}_{0,h}$ *be the solution of* (4.10). *Then* $(\boldsymbol{\sigma}_h, \mathbf{u}_h, \boldsymbol{\gamma}_h, 0)$ *is a solution of* (4.72).

b) *Let* $(\boldsymbol{\sigma}_h, \mathbf{u}_h, \boldsymbol{\gamma}_h, \varphi_h) \in H_h^{\boldsymbol{\sigma}} \times H_{0,h}^{\mathbf{u}} \times H_h^{\boldsymbol{\gamma}} \times \mathbb{R}$ *be a solution of* (4.72). *Then* $\varphi_h = 0$ *and* $(\boldsymbol{\sigma}_h, \mathbf{u}_h, \boldsymbol{\gamma}_h)$ *is the solution of* (4.10).

Proof. See Theorem 3.3.4 or Theorem 4.3 in [36]. □

In what follows, N stands for the total number of degrees of freedom (unknowns) of (4.72), which, at least for uniform refinements, behaves asymptotically as five times the number of elements of each triangulation (see [36]). Also, the individual and total errors are denoted by

$$e(\boldsymbol{\sigma}) := \|\boldsymbol{\sigma} - \boldsymbol{\sigma}_h\|_{H(\mathbf{div};\Omega)}\,, \quad e(\mathbf{u}) := |\mathbf{u} - \mathbf{u}_h|_{[H^1(\Omega)]^2}\,, \quad e(\boldsymbol{\gamma}) := \|\boldsymbol{\gamma} - \boldsymbol{\gamma}_h\|_{[L^2(\Omega)]^{2\times 2}}\,,$$

and

$$e(\boldsymbol{\sigma}, \mathbf{u}, \boldsymbol{\gamma}) := \left\{ [e(\boldsymbol{\sigma})]^2 + [e(\mathbf{u})]^2 + [e(\boldsymbol{\gamma})]^2 \right\}^{1/2}\,,$$

respectively, whereas the effectivity index with respect to $\boldsymbol{\theta}$ is defined by $e(\boldsymbol{\sigma}, \mathbf{u}, \boldsymbol{\gamma})/\boldsymbol{\theta}$.

On the other hand, we recall that given the Young modulus E and the Poisson ratio ν of a linear elastic material, the corresponding Lamé constants are defined by $\mu := \frac{E}{2(1+\nu)}$ and $\lambda := \frac{E\,\nu}{(1+\nu)\,(1-2\,\nu)}$. Then, in order to emphasize the robustness of the a posteriori error estimator $\boldsymbol{\theta}$ with respect to the Poisson ratio, in the examples below we fix $E = 1$ and consider $\nu = 0.4900$, $\nu = 0.4999$, or both, which yield the following values of μ and λ :

ν	μ	λ
0.4900	0.3356	16.4430
0.4999	0.3333	1666.4444

In addition, since the augmented method was already shown in [36] to be robust with respect to the parameters κ_1, κ_2, and κ_3, we simply consider for all the examples $(\kappa_1, \kappa_2, \kappa_3) = \Big(\mu, \frac{1}{2\,\mu}, \frac{\mu}{2}\Big)$, which corresponds to the feasible choice described in Theorem 4.2.1 with $\tilde{C}_1 = 1$ and $\tilde{C}_3 = \frac{1}{2}$.

We now specify the data of the five examples to be presented here. We take Ω as either the square $]0,1[^2$ or the L-shaped domain $]-0.5,0.5[^2 \setminus [0,0.5]^2$, and choose the datum $\mathbf{f}$ so that ν and the exact solution $\mathbf{u}(x_1,x_2) := (u_1(x_1,x_2), u_2(x_1,x_2))^{\mathtt{t}}$ are given in the table below. Actually, according to (4.1) and (4.2) we have $\boldsymbol{\sigma} = \lambda\,\mathbf{div}\,(\mathbf{u})\,\mathbf{I} + 2\,\mu\,\mathbf{e}(\mathbf{u})$, and hence simple computations show that $\mathbf{f} := -\,\mathbf{div}\,(\boldsymbol{\sigma}) = -\,(\lambda+\mu)\,\nabla(\mathbf{div}\ \mathbf{u}) - \mu\,\Delta\,\mathbf{u}$. We also recall that the rotation $\boldsymbol{\gamma}$ is defined as $\frac{1}{2}\,(\nabla\mathbf{u} - (\nabla\mathbf{u})^{\mathtt{t}})$.

Example	Ω	ν	$u_1(x_1,x_2) = u_2(x_1,x_2)$
1	$]0,1[^2$	0.4900 0.4999	$\dfrac{x_1\,(x_1-1)\,x_2\,(x_2-1)}{(x_1-1)^2+(x_2-1)^2+0.01}$
2	$]0,1[^2$	0.4900 0.4999	$x_1\,(x_1-1)\,x_2\,(x_2-1)\,(x_1^2+x_2^2)^{1/3}$
3	$]-0.5,0.5[^2 \setminus [0,0.5]^2$	0.4900	$x_1\,x_2\,(x_1^2-0.25)\,(x_2^2-0.25)\,(x_1^2+x_2^2)^{-1/3}$
4	$]0,1[^2$	0.4900	$\dfrac{\sin(\pi\,x_1)\,\sin(\pi\,x_2)}{1000\,(x_1-1/2)^2+1000\,(x_2-1/2)^2+10}$
5	$]-0.5,0.5[^2 \setminus [0,0.5]^2$	0.4900	$x_1\,x_2\,(x_1^2-0.25)\,(x_2^2-0.25)\,(x_1^2+0.0001)^{-1/3}$

We observe that the solution of Example 3 is singular at the boundary point $(0,0)$. In fact, the behaviour of $\mathbf{u}$ in a neighborhood of the origin implies that $\mathbf{div}\,(\boldsymbol{\sigma}) \in [H^{1/3}(\Omega)]^2$ only, which, according to Theorem 4.2.3, yields $1/3$ as the expected rate of convergence for the uniform refinement. On the other hand, the solutions of Examples 1, 4, and 5 show large stress regions in a neighborhood of the boundary point $(1,1)$, in a neighborhood of the interior point $(1/2,1/2)$, and around the line $x_1 = 0$, respectively.

The numerical results given below were obtained using a *Compaq Alpha ES40 Parallel Computer* and a Fortran code. The linear system arising from the augmented mixed scheme (4.72) is implemented as explained in Section 4.3 of [36], and the individual errors are computed on each triangle using a Gaussian quadrature rule.

We first utilize Examples 1 and 2 to illustrate the good behaviour of the a posteriori error estimator $\boldsymbol{\theta}$ in a sequence of uniform meshes generated by equally spaced partitions on the sides of the square $]0,1[^2$. In Tables 5.1 through 5.4 we present the individual and total errors, the a posteriori error estimators, and the effectivity indexes for these examples, with $\nu = 0.4900$ and $\nu = 0.4999$, for this sequence of uniform meshes. We remark that in both cases, and independently of how large the errors could become, there are practically no differences between the effectivity indexes obtained with the two values of ν, which numerically shows the robustness of $\boldsymbol{\theta}$ with respect to the Poisson ratio (and hence with respect to the Lamé constant λ). Moreover, this index remains always in a neighborhood of 0.89 in Example 1 (resp. 0.46 in Example 2), which confirms the reliability and efficiency of $\boldsymbol{\theta}$.

Next, we consider Examples 3, 4, and 5, to illustrate the performance of the adaptive algorithm based on $\boldsymbol{\theta}$ for the computation of the solutions of (4.72). The adaptive algorithm corresponds to one described in Section 2.6 with parameter $\gamma = \frac{1}{2}$

At this point we introduce the experimental rate of convergence, which, given two consecutive triangulations with degrees of freedom N and N' and corresponding total errors e and e', is defined by

$$r(e) := -2\,\frac{\log(e/e')}{\log(N/N')}\,.$$

In Tables 5.5 through 5.10 we provide the individual and total errors, the experimental rates of convergence, the a posteriori error estimators, and the effectivity indexes for the uniform and adaptive refinements as applied to Examples 3, 4, and 5. In this case, uniform

refinement means that, given a uniform initial triangulation, each subsequent mesh is obtained from the previous one by dividing each triangle into the four ones arising when connecting the midpoints of its sides. We observe from these tables that the errors of the adaptive procedure decrease much faster than those obtained by the uniform one, which is confirmed by the experimental rates of convergence provided there. This fact can also be seen in Figures 5.1 through 5.3 where we display the total error $e(\boldsymbol{\sigma}, \mathbf{u}, \boldsymbol{\gamma})$ vs. the degrees of freedom N for both refinements. As shown by the values of $r(e)$, particularly in Example 3 (where $r(e)$ approaches $1/3$ for the uniform refinement), the adaptive method is able to recover, at least approximately, the quasi-optimal rate of convergence $O(h)$ for the total error. Furthermore, the effectivity indexes remain again bounded from above and below, which confirms the reliability and efficiency of $\boldsymbol{\theta}$ for the adaptive algorithm. On the other hand, some intermediate meshes obtained with the adaptive refinement are displayed in Figures 5.4 through 5.6. Note that the method is able to recognize the singularities and the large stress regions of the solutions. In particular, this fact is observed in Example 3 (see Figure 5.4) where the adapted meshes are highly refined around the singular point $(0, 0)$. Similarly, the adapted meshes obtained in Examples 4 and 5 (see Figures 5.5 and 5.6) concentrate the refinements around the interior point $(1/2, 1/2)$ and the segment $x_1 = 0$, respectively, where the largest stresses occur.

Summarizing, the numerical results presented in this section underline the reliability and efficiency of $\boldsymbol{\theta}$ and strongly demonstrate that the associated adaptive algorithm is much more suitable than a uniform discretization procedure when solving problems with non-smooth solutions.

Table 5.1: Mesh sizes, individual and total errors, a posteriori error estimators, and effectivity indexes for a sequence of uniform meshes (EXAMPLE 1, $\nu = 0.4900$).

N	h	$e(\boldsymbol{\sigma})$	$e(\mathbf{u})$	$e(\boldsymbol{\gamma})$	$e(\boldsymbol{\sigma},\mathbf{u},\boldsymbol{\gamma})$	$\boldsymbol{\theta}$	$e(\boldsymbol{\sigma},\mathbf{u},\boldsymbol{\gamma})/\boldsymbol{\theta}$
163	0.25000	0.9067E+2	0.2756E+1	0.1899E+1	0.9073E+2	0.1277E+3	0.7102
363	0.16667	0.9112E+2	0.2576E+1	0.2452E+1	0.9118E+2	0.1085E+3	0.8397
643	0.12500	0.7570E+2	0.2050E+1	0.2458E+1	0.7577E+2	0.8784E+2	0.8625
1003	0.10000	0.6100E+2	0.1673E+1	0.2321E+1	0.6107E+2	0.7070E+2	0.8637
1443	0.08333	0.5047E+2	0.1422E+1	0.2168E+1	0.5054E+2	0.5854E+2	0.8633
1963	0.07143	0.4348E+2	0.1227E+1	0.2026E+1	0.4355E+2	0.5026E+2	0.8663
2563	0.06250	0.3859E+2	0.1060E+1	0.1899E+1	0.3865E+2	0.4435E+2	0.8714
3243	0.05556	0.3483E+2	0.9191E+0	0.1784E+1	0.3489E+2	0.3980E+2	0.8766
4003	0.05000	0.3174E+2	0.8000E+0	0.1681E+1	0.3179E+2	0.3609E+2	0.8810
4843	0.04545	0.2911E+2	0.7009E+0	0.1587E+1	0.2916E+2	0.3297E+2	0.8846
5763	0.04167	0.2685E+2	0.6187E+0	0.1501E+1	0.2690E+2	0.3031E+2	0.8874
6763	0.03846	0.2489E+2	0.5503E+0	0.1423E+1	0.2494E+2	0.2803E+2	0.8898
7843	0.03571	0.2318E+2	0.4930E+0	0.1352E+1	0.2323E+2	0.2605E+2	0.8918
9003	0.03333	0.2169E+2	0.4446E+0	0.1286E+1	0.2173E+2	0.2432E+2	0.8936
10243	0.03125	0.2037E+2	0.4034E+0	0.1226E+1	0.2041E+2	0.2280E+2	0.8951
11563	0.02941	0.1919E+2	0.3681E+0	0.1171E+1	0.1923E+2	0.2145E+2	0.8965
12963	0.02777	0.1815E+2	0.3375E+0	0.1120E+1	0.1818E+2	0.2025E+2	0.8978

Table 5.2: Mesh sizes, individual and total errors, a posteriori error estimators, and effectivity indexes for a sequence of uniform meshes (EXAMPLE 1, $\nu = 0.4999$).

N	h	$e(\boldsymbol{\sigma})$	$e(\mathbf{u})$	$e(\boldsymbol{\gamma})$	$e(\boldsymbol{\sigma},\mathbf{u},\boldsymbol{\gamma})$	$\boldsymbol{\theta}$	$e(\boldsymbol{\sigma},\mathbf{u},\boldsymbol{\gamma})/\boldsymbol{\theta}$
163	0.25000	0.9045E+4	0.2534E+3	0.1713E+3	0.9050E+4	0.1257E+5	0.7198
363	0.16667	0.8986E+4	0.2439E+3	0.2248E+3	0.8992E+4	0.1065E+5	0.8446
643	0.12500	0.7447E+4	0.1962E+3	0.2268E+3	0.7453E+4	0.8609E+4	0.8657
1003	0.10000	0.5991E+4	0.1610E+3	0.2152E+3	0.5997E+4	0.6926E+4	0.8659
1443	0.08333	0.4948E+4	0.1372E+3	0.2019E+3	0.4954E+4	0.5729E+4	0.8647
1963	0.07143	0.4255E+4	0.1183E+3	0.1894E+3	0.4261E+4	0.4914E+4	0.8671
2563	0.06250	0.3771E+4	0.1022E+3	0.1781E+3	0.3777E+4	0.4332E+4	0.8719
3243	0.05556	0.3401E+4	0.8848E+2	0.1677E+3	0.3407E+4	0.3885E+4	0.8769
4003	0.05000	0.3098E+4	0.7688E+2	0.1583E+3	0.3103E+4	0.3521E+4	0.8813
4843	0.04545	0.2841E+4	0.6721E+2	0.1497E+3	0.2846E+4	0.3216E+4	0.8848
5763	0.04167	0.2620E+4	0.5918E+2	0.1418E+3	0.2625E+4	0.2957E+4	0.8877
6763	0.03846	0.2429E+4	0.5249E+2	0.1345E+3	0.2433E+4	0.2733E+4	0.8901
7843	0.03571	0.2262E+4	0.4688E+2	0.1279E+3	0.2266E+4	0.2540E+4	0.8922
9003	0.03333	0.2116E+4	0.4214E+2	0.1218E+3	0.2120E+4	0.2371E+4	0.8940
10243	0.03125	0.1987E+4	0.3810E+2	0.1162E+3	0.1991E+4	0.2223E+4	0.8956
11563	0.02941	0.1873E+4	0.3462E+2	0.1110E+3	0.1876E+4	0.2092E+4	0.8970
12963	0.02777	0.1771E+4	0.3161E+2	0.1062E+3	0.1774E+4	0.1975E+4	0.8983

Table 5.3: Mesh sizes, individual and total errors, a posteriori error estimators, and effectivity indexes for a sequence of uniform meshes (EXAMPLE 2, $\nu = 0.4900$).

N	h	$e(\boldsymbol{\sigma})$	$e(\mathbf{u})$	$e(\boldsymbol{\gamma})$	$e(\boldsymbol{\sigma},\mathbf{u},\boldsymbol{\gamma})$	$\boldsymbol{\theta}$	$e(\boldsymbol{\sigma},\mathbf{u},\boldsymbol{\gamma})/\boldsymbol{\theta}$
163	0.25000	0.2730E+1	0.1483E+0	0.2631E+0	0.2747E+1	0.8203E+1	0.3349
363	0.16666	0.1841E+1	0.1108E+0	0.2492E+0	0.1861E+1	0.5159E+1	0.3607
643	0.12500	0.1386E+1	0.8231E-1	0.2236E+0	0.1406E+1	0.3696E+1	0.3804
1003	0.10000	0.1110E+1	0.6260E-1	0.1978E+0	0.1129E+1	0.2855E+1	0.3955
1443	0.08333	0.9259E+0	0.4904E-1	0.1751E+0	0.9436E+0	0.2315E+1	0.4074
1963	0.07143	0.7939E+0	0.3952E-1	0.1561E+0	0.8101E+0	0.1941E+1	0.4171
2563	0.06250	0.6947E+0	0.3264E-1	0.1403E+0	0.7095E+0	0.1668E+1	0.4252
3243	0.05556	0.6176E+0	0.2753E-1	0.1271E+0	0.6311E+0	0.1460E+1	0.4320
4003	0.05000	0.5558E+0	0.2364E-1	0.1160E+0	0.5683E+0	0.1297E+1	0.4378
4843	0.04545	0.5053E+0	0.2061E-1	0.1066E+0	0.5169E+0	0.1166E+1	0.4429
5763	0.04167	0.4632E+0	0.1820E-1	0.9852E-1	0.4739E+0	0.1059E+1	0.4474
6763	0.03846	0.4276E+0	0.1626E-1	0.9153E-1	0.4376E+0	0.9695E+0	0.4513
7843	0.03571	0.3970E+0	0.1466E-1	0.8543E-1	0.4064E+0	0.8935E+0	0.4548
9003	0.03333	0.3706E+0	0.1333E-1	0.8006E-1	0.3794E+0	0.8284E+0	0.4579
10243	0.03125	0.3474E+0	0.1221E-1	0.7532E-1	0.3557E+0	0.7719E+0	0.4608
11563	0.02941	0.3270E+0	0.1126E-1	0.7109E-1	0.3348E+0	0.7226E+0	0.4633
12963	0.02777	0.3088E+0	0.1044E-1	0.6730E-1	0.3162E+0	0.6791E+0	0.4657

Table 5.4: Mesh sizes, individual and total errors, a posteriori error estimators, and effectivity indexes for a sequence of uniform meshes (EXAMPLE 2, $\nu = 0.4999$).

N	h	$e(\boldsymbol{\sigma})$	$e(\mathbf{u})$	$e(\boldsymbol{\gamma})$	$e(\boldsymbol{\sigma},\mathbf{u},\boldsymbol{\gamma})$	$\boldsymbol{\theta}$	$e(\boldsymbol{\sigma},\mathbf{u},\boldsymbol{\gamma})/\boldsymbol{\theta}$
163	0.25000	0.2707E+3	0.1356E+2	0.2536E+2	0.2722E+3	0.8067E+3	0.3374
363	0.16666	0.1825E+3	0.1053E+2	0.2375E+2	0.1843E+3	0.5070E+3	0.3635
643	0.12500	0.1373E+3	0.7847E+1	0.2126E+2	0.1392E+3	0.3628E+3	0.3837
1003	0.10000	0.1100E+3	0.5913E+1	0.1879E+2	0.1118E+3	0.2801E+3	0.3990
1443	0.08333	0.9176E+2	0.4558E+1	0.1665E+2	0.9337E+2	0.2270E+3	0.4112
1963	0.07143	0.7867E+2	0.3599E+1	0.1484E+2	0.8014E+2	0.1903E+3	0.4211
2563	0.06250	0.6884E+2	0.2903E+1	0.1334E+2	0.7018E+2	0.1634E+3	0.4293
3243	0.05556	0.6119E+2	0.2386E+1	0.1209E+2	0.6242E+2	0.1430E+3	0.4362
4003	0.05000	0.5507E+2	0.1993E+1	0.1104E+2	0.5620E+2	0.1270E+3	0.4422
4843	0.04545	0.5007E+2	0.1689E+1	0.1014E+2	0.5111E+2	0.1142E+3	0.4474
5763	0.04167	0.4589E+2	0.1449E+1	0.9377E+1	0.4686E+2	0.1036E+3	0.4519
6763	0.03846	0.4236E+2	0.1256E+1	0.8712E+1	0.4327E+2	0.9490E+2	0.4559
7843	0.03571	0.3934E+2	0.1099E+1	0.8132E+1	0.4018E+2	0.8745E+2	0.4595
9003	0.03333	0.3671E+2	0.9697E+0	0.7622E+1	0.3751E+2	0.8106E+2	0.4627
10243	0.03125	0.3442E+2	0.8617E+0	0.7171E+1	0.3517E+2	0.7553E+2	0.4656
11563	0.02941	0.3239E+2	0.7708E+0	0.6768E+1	0.3310E+2	0.7070E+2	0.4682
12963	0.02777	0.3059E+2	0.6935E+0	0.6408E+1	0.3126E+2	0.6644E+2	0.4706

Table 5.5: Individual and total errors, experimental rates of convergence, a posteriori error estimators, and effectivity indexes for the uniform refinement (EXAMPLE 3).

N	$e(\boldsymbol{\sigma})$	$e(\mathbf{u})$	$e(\boldsymbol{\gamma})$	$e(\boldsymbol{\sigma},\mathbf{u},\boldsymbol{\gamma})$	$r(e)$	$\boldsymbol{\theta}$	$e(\boldsymbol{\sigma},\mathbf{u},\boldsymbol{\gamma})/\boldsymbol{\theta}$
123	0.2182E+1	0.1994E+0	0.9131E-1	0.2193E+1	—	0.2898E+1	0.7567
483	0.1525E+1	0.9385E-1	0.9919E-1	0.1531E+1	0.5254	0.1840E+1	0.8323
1923	0.1122E+1	0.4040E-1	0.7723E-1	0.1125E+1	0.4455	0.1242E+1	0.9058
7683	0.8585E+0	0.2246E-1	0.4795E-1	0.8601E+0	0.3885	0.8996E+0	0.9561

Table 5.6: Individual and total errors, experimental rates of convergence, a posteriori error estimators, and effectivity indexes for the adaptive refinement (EXAMPLE 3).

N	$e(\boldsymbol{\sigma})$	$e(\mathbf{u})$	$e(\boldsymbol{\gamma})$	$e(\boldsymbol{\sigma},\mathbf{u},\boldsymbol{\gamma})$	$r(e)$	$\boldsymbol{\theta}$	$e(\boldsymbol{\sigma},\mathbf{u},\boldsymbol{\gamma})/\boldsymbol{\theta}$
123	0.2182E+1	0.1994E+0	0.9131E-1	0.2193E+1	—	0.2898E+1	0.7567
243	0.1795E+1	0.1516E+0	0.7951E-1	0.1803E+1	0.5745	0.2340E+1	0.7707
483	0.1372E+1	0.9211E-1	0.8634E-1	0.1378E+1	0.7839	0.1702E+1	0.8094
543	0.1259E+1	0.9159E-1	0.8658E-1	0.1265E+1	1.4583	0.1609E+1	0.7860
663	0.1137E+1	0.8250E-1	0.8357E-1	0.1143E+1	1.0150	0.1476E+1	0.7746
778	0.1045E+1	0.8113E-1	0.8228E-1	0.1051E+1	1.0454	0.1386E+1	0.7583
1228	0.8540E+0	0.7469E-1	0.6693E-1	0.8599E+0	0.8821	0.1100E+1	0.7814
1518	0.7810E+0	0.7270E-1	0.5604E-1	0.7864E+0	0.8423	0.9562E+0	0.8224
1783	0.7100E+0	0.7233E-1	0.6058E-1	0.7162E+0	1.1622	0.8812E+0	0.8127
2288	0.6381E+0	0.7912E-1	0.6245E-1	0.6460E+0	0.8269	0.7869E+0	0.8209
2533	0.6040E+0	0.7605E-1	0.6008E-1	0.6117E+0	1.0727	0.7569E+0	0.8082
3663	0.5089E+0	0.9206E-1	0.5993E-1	0.5206E+0	0.8745	0.6383E+0	0.8156
4703	0.4449E+0	0.7418E-1	0.5634E-1	0.4546E+0	1.0850	0.5560E+0	0.8175
5698	0.4056E+0	0.7651E-1	0.5628E-1	0.4166E+0	0.9091	0.5052E+0	0.8246
7243	0.3654E+0	0.7278E-1	0.5394E-1	0.3764E+0	0.8448	0.4506E+0	0.8355
8203	0.3428E+0	0.6653E-1	0.5370E-1	0.3533E+0	1.0209	0.4290E+0	0.8234
10818	0.3138E+0	0.8197E-1	0.5696E-1	0.3293E+0	0.5078	0.3865E+0	0.8520

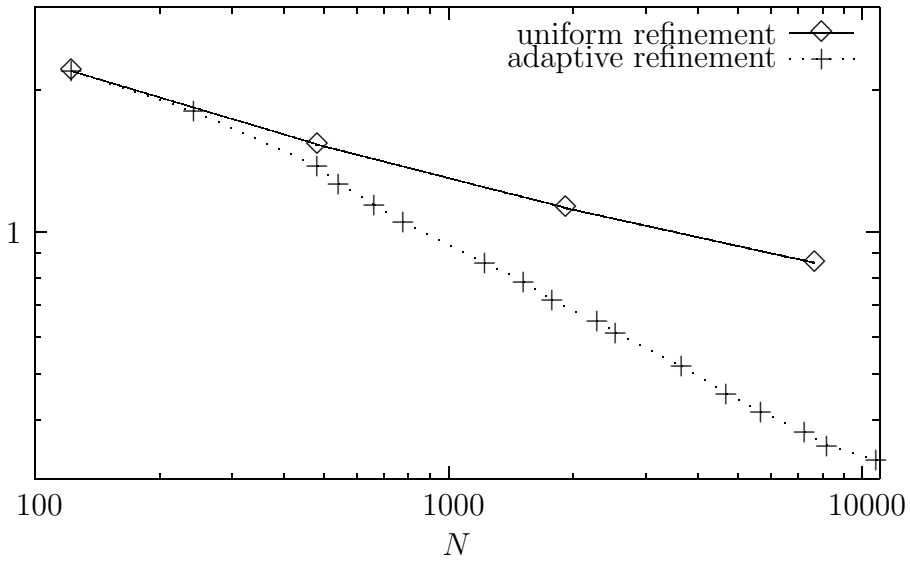

Figure 5.1: Total errors $e(\boldsymbol{\sigma}, \mathbf{u}, \boldsymbol{\gamma})$ vs. degrees of freedom N for the uniform and adaptive refinements (EXAMPLE 3).

Table 5.7: Individual and total errors, experimental rates of convergence, a posteriori error estimators, and effectivity indexes for the uniform refinement (EXAMPLE 4).

N	$e(\boldsymbol{\sigma})$	$e(\mathbf{u})$	$e(\boldsymbol{\gamma})$	$e(\boldsymbol{\sigma}, \mathbf{u}, \boldsymbol{\gamma})$	$r(e)$	$\boldsymbol{\theta}$	$e(\boldsymbol{\sigma}, \mathbf{u}, \boldsymbol{\gamma})/\boldsymbol{\theta}$
163	0.3813E+2	0.5025E+1	0.2685E+1	0.3855E+2	——	0.4070E+2	0.9472
643	0.3593E+2	0.2015E+1	0.1361E+1	0.3601E+2	0.0991	0.3692E+2	0.9755
2563	0.2021E+2	0.1035E+1	0.8087E+0	0.2025E+2	0.8327	0.2093E+2	0.9673
10243	0.9898E+1	0.7493E+0	0.6000E+0	0.9944E+1	1.0267	0.1027E+2	0.9677

Table 5.8: Individual and total errors, experimental rates of convergence, a posteriori error estimators, and effectivity indexes for the adaptive refinement (EXAMPLE 4).

N	$e(\boldsymbol{\sigma})$	$e(\mathbf{u})$	$e(\boldsymbol{\gamma})$	$e(\boldsymbol{\sigma}, \mathbf{u}, \boldsymbol{\gamma})$	$r(e)$	$\boldsymbol{\theta}$	$e(\boldsymbol{\sigma}, \mathbf{u}, \boldsymbol{\gamma})/\boldsymbol{\theta}$
163	0.3813E+2	0.5025E+1	0.2685E+1	0.3855E+2	——	0.4070E+2	0.9472
343	0.3594E+2	0.1913E+1	0.1156E+1	0.3601E+2	0.1827	0.3686E+2	0.9771
643	0.2042E+2	0.1255E+1	0.8721E+0	0.2048E+2	1.7958	0.2122E+2	0.9654
883	0.1174E+2	0.1232E+1	0.6751E+0	0.1183E+2	3.4620	0.1237E+2	0.9559
2583	0.6525E+1	0.1246E+1	0.7400E+0	0.6684E+1	1.0638	0.7092E+1	0.9424
4988	0.4748E+1	0.1109E+1	0.6405E+0	0.4918E+1	0.9324	0.5114E+1	0.9615
9748	0.3540E+1	0.8796E+0	0.5435E+0	0.3688E+1	0.8591	0.3785E+1	0.9743

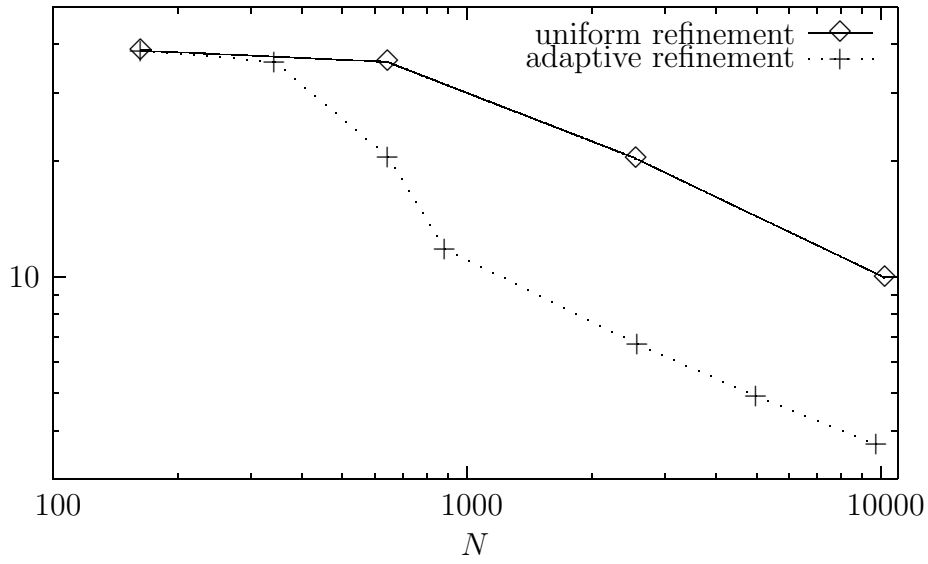

Figure 5.2: Total errors $e(\boldsymbol{\sigma}, \mathbf{u}, \boldsymbol{\gamma})$ vs. degrees of freedom N for the uniform and adaptive refinements (EXAMPLE 4).

Table 5.9: Individual and total errors, experimental rates of convergence, a posteriori error estimators, and effectivity indexes for the uniform refinement (EXAMPLE 5).

N	$e(\boldsymbol{\sigma})$	$e(\mathbf{u})$	$e(\boldsymbol{\gamma})$	$e(\boldsymbol{\sigma}, \mathbf{u}, \boldsymbol{\gamma})$	$r(e)$	$\boldsymbol{\theta}$	$e(\boldsymbol{\sigma}, \mathbf{u}, \boldsymbol{\gamma})/\boldsymbol{\theta}$
123	0.1399E+2	0.4737E+0	0.1629E+0	0.1400E+2	——	0.1436E+2	0.9745
483	0.2522E+2	0.2957E+0	0.1577E+0	0.2522E+2	——	0.2527E+2	0.9980
1923	0.2494E+2	0.1375E+0	0.1454E+0	0.2494E+2	0.0162	0.2496E+2	0.9992
7683	0.1449E+2	0.6395E-1	0.1742E+0	0.1449E+2	0.7834	0.1453E+2	0.9975

Table 5.10: Individual and total errors, experimental rates of convergence, a posteriori error estimators, and effectivity indexes for the adaptive refinement (EXAMPLE 5).

N	$e(\boldsymbol{\sigma})$	$e(\mathbf{u})$	$e(\boldsymbol{\gamma})$	$e(\boldsymbol{\sigma}, \mathbf{u}, \boldsymbol{\gamma})$	$r(e)$	$\boldsymbol{\theta}$	$e(\boldsymbol{\sigma}, \mathbf{u}, \boldsymbol{\gamma})/\boldsymbol{\theta}$
123	0.1399E+2	0.4737E+0	0.1629E+0	0.1400E+2	——	0.1436E+2	0.9745
263	0.2524E+2	0.3215E+0	0.1510E+0	0.2524E+2	——	0.2535E+2	0.9957
513	0.2498E+2	0.2298E+0	0.1420E+0	0.2498E+2	0.0309	0.2507E+2	0.9963
988	0.1507E+2	0.2026E+0	0.1888E+0	0.1507E+2	1.5421	0.1523E+2	0.9894
2383	0.8488E+1	0.1927E+0	0.1773E+0	0.8492E+1	1.3033	0.8603E+1	0.9871
4038	0.6955E+1	0.1424E+0	0.1249E+0	0.6958E+1	0.7556	0.7042E+1	0.9881
7938	0.5361E+1	0.1458E+0	0.1082E+0	0.5364E+1	0.7696	0.5439E+1	0.9862
12743	0.4272E+1	0.1353E+0	0.1044E+0	0.4275E+1	0.9587	0.4331E+1	0.9870

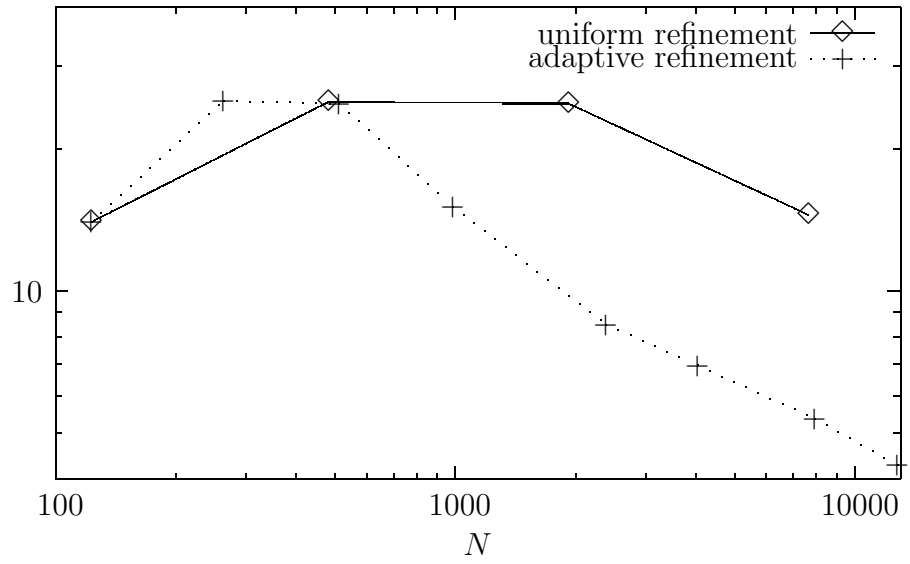

Figure 5.3: Total errors $e(\boldsymbol{\sigma}, \mathbf{u}, \boldsymbol{\gamma})$ vs. degrees of freedom N for the uniform and adaptive refinements (EXAMPLE 5).

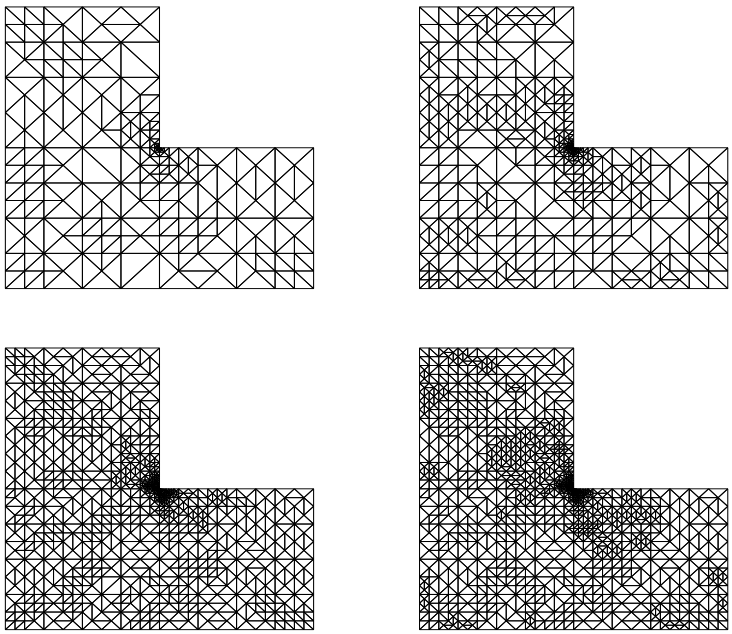

Figure 5.4: Adapted intermediate meshes with 1783, 3663, 8203, and 10818 degrees of freedom (EXAMPLE 3).

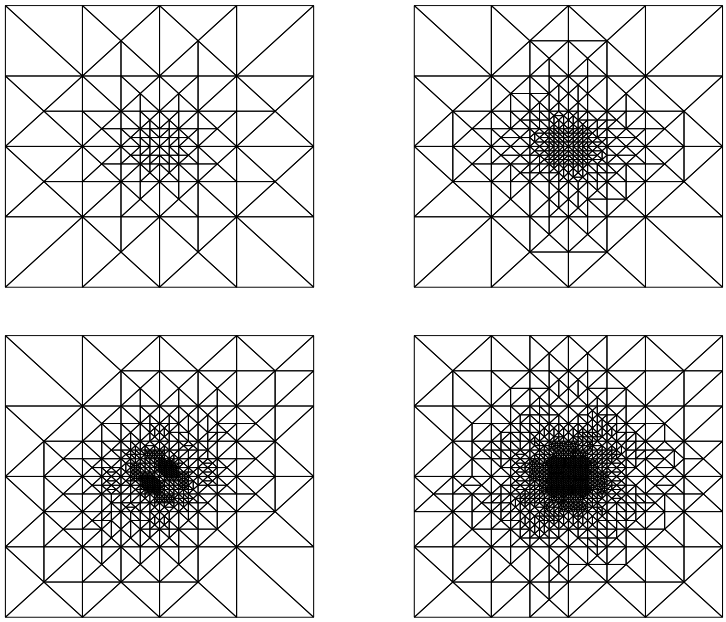

Figure 5.5: Adapted intermediate meshes with 883, 2583, 4988, and 9748 degrees of freedom (EXAMPLE 4).

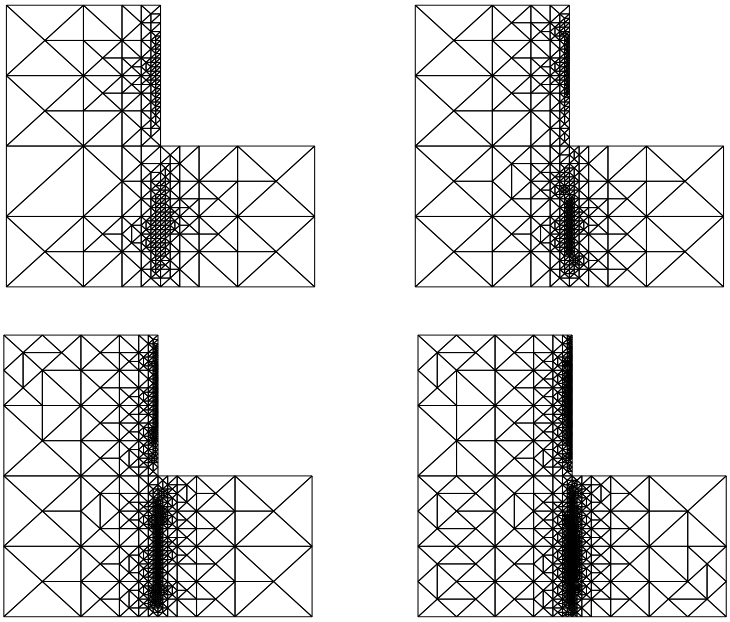

Figure 5.6: Adapted intermediate meshes with 2383, 4038, 7938, and 12743 degrees of freedom (EXAMPLE 5).

Chapter 5

Conclusiones y trabajo futuro

En este capítulo damos un resumen de los principales aportes de esta tesis y una descripción del trabajo futuro a desarrollar.

5.1 Conclusiones

Las contribuciones de esta tesis se clasifican como sigue:

Contribuciones Teóricas

- Análisis de error a-priori y a-posteriori de una nueva formulación mixta aumentada con multiplicadores de Lagrange para un problema de valores de contorno con condiciones mixtas.
- Análisis de error a-priori y a-posteriori de un nuevo método mixto estabilizado, basado en ondelettes, para un problema de valores de contorno con condiciones de Neumann.
- Análisis de error a-posteriori de una nueva formulación mixta aumentada para el problema de elasticidad lineal con condiciones de contorno de Dirichlet.

Contribuciones Numéricas

- Un código en Fortran 90, con adaptación automática de mallas, para la resolución numérica de una ecuación diferencial parcial de segundo orden con condiciones de contorno mixtas.

- Un código en Fortran 90, con adaptación automática de mallas, para la resolución numérica de un problema de elasticidad lineal con condiciones de contorno de Dirichlet.

5.2 Trabajo futuro

Algunas de las líneas de investigación que pueden seguirse a futuro son las siguientes:

- Implementación computacional del algoritmo desarrollado en el Capítulo 3.
- Extensión de los resultados teóricos y numéricos del Capítulo 4 al caso del problema de elasticidad lineal con condiciones de contorno mixtas.
- Análisis numérico y computacional para la aplicación de principios de mínimos cuadrados a la resolución numérica de problemas no lineales.
- Análisis numérico y computacional de métodos mixtos estabilizados para problemas de transmisión en elasticidad lineal y mecánica de fluidos.

Bibliography

[1] M. Ainsworth and J.T. Oden: A Posteriori Error Estimation in Finite Element Analysis. Wiley-Interscience, New York, 2000.

[2] R.A. Araya, T.P. Barrios, G.N. Gatica and N. Heuer: *A-posteriori error estimates for a mixed-FEM formulation of a nonlinear elliptic problem*. Computer Methods in Applied Mechanics and Engineering, vol 191, pp. 2317-2336, (2002).

[3] I. Babuška: *The finite element method with Lagrange multipliers*. Numer. Math., vol 20, pp. 179-192, (1973).

[4] I. Babuška and A.K. Aziz: *Survey lectures on the mathematical foundations of the finite element method*. In: The Mathematical Foundations of the Finite Element Method with Applications to Partial Differential Equations, A.K. Aziz (editor), Academic Press, New York, (1972).

[5] I. Babuška and G.N. Gatica: *On the mixed finite element method with Lagrange multipliers*. Numerical Methods for Partial Differential Equations, vol. 19, 2, pp. 192-210, (2003).

[6] M.A. Barrientos, G.N. Gatica and E.P. Stephan: *A mixed finite element method for nonlinear elasticity: two-fold saddle point approach and a-posteriori error estimate*. Numerische Mathematik, vol. 91, 2, pp. 197-222, (2002).

[7] T.P. Barrios, G.N. Gatica: *An augmented mixed finite element method with Lagrange multipliers: a-priori and a-posteriori error analyses*. Journal of Computational and Applied Mathematics, to appear.

[8] T.P. Barrios, G.N. Gatica and L.F. Gatica: *On the numerical analysis of a nonlinear elliptic problem via mixed-FEM and Lagrange multipliers*. Applied Numerical Mathematics, vol. 48, pp. 135-155, (2004).

[9] T.P. Barrios, G.N. Gatica and F. Paiva: *A wavelet-based stabilization of the mixed finite element method with Lagrange multipliers*. Applied Mathematics Letters, vol. 19, 3, pp. 244-250, (2006).

[10] T.P. Barrios, G.N. Gatica and F. Paiva: *A-priori and a-posteriori error analysis of a wavelet-based stabilization for the mixed finite element*. Preprint 2006-02, Departamento de Ingeniería Matemática. Universidad de Concepción. (2006).

[11] T.P. Barrios, G.N. Gatica, M. González and N. Heuer: *A residual based a posteriori error estimate for an augmented mixed finite element method in linear elasticity*. Submitted. Preprint 2005-20, Departamento de Ingeniería Matemática, Universidad de Concepción. (2005).

[12] S. Bertoluzza: *Wavelet stabilization of the Lagrange multiplier method*. Numerische Mathematik, vol. 86, pp. 1-28, (2000).

[13] P.B. Bochev and M.D. Gunzburger: *Finite element methods of least-squares type*. SIAM Rev, vol. 40, pp. 789-837, (1998).

[14] D. Braess: Finite Elements. Theory, fast solvers, and aplications in solid mechanics. Cambridge University Press, United kingdom, 2001.

[15] S. Brenner and L. Scott: The Mathematical Theory of Finite Elements Methods. Springer-Verlag, 1994.

[16] F. Brezzi: *On the existence, uniqueness, and approximation of saddle-point problems arising from Lagrange multipliers*. RAIRO Anal. Numer., vol. 8, pp. 129-151, (1974).

[17] F. Brezzi and M. Fortin: Mixed and Hybrid Finite Element Methods. Springer-Verlag, 1991.

[18] F. Brezzi and M. Fortin: *A minimal stabilisation procedure for mixed finite element methods*. Numerische Mathematik, vol. 89, 3, pp. 457-491, (2001).

[19] F. Brezzi, M. Fortin and L.D. Marini: *Mixed finite element methods with continuous stresses*. Mathematical Models and Methods in Applied Sciences, vol. 3, 2, pp. 275-287, (1993).

[20] R. Bustinza, G.C. García and G.N. Gatica: *A mixed finite element method with Lagrange multipliers for nonlinear exterior transmission problems*. Numerische Mathematik, vol 96, pp. 481-523, (2004).

[21] R. Bustinza, G.N. Gatica, M. González, S. Meddahi and E.P. Stephan: *Enriched finite element subspaces for dual-dual mixed formulations in fluid mechanics and elasticity*. Computer Methods in Applied Mechanics and Engineering, vol. 194, 2-5, pp. 427-439, (2005).

[22] C. Canuto, A. Tabacco and K. Urban: *The wavelet element method. Part I: Construction and analysis*. Applied and Computational Harmonic Analysis, vol. 6, 1, pp. 1-52, (1999).

[23] C. Carstensen: *An a posteriori error estimate for a first-kind integral equation*. Mathematics of Computation, vol. 66, 217, pp. 139-155, (1997).

[24] C. Carstensen: *A posteriori error estimate for the mixed finite element method*. Mathematics of Computation, vol. 66, 218, pp. 465-476, (1997).

[25] C. Carstensen, G. Dolzmann, *A posteriori error estimates for mixed FEM in elasticity*. Numerische Mathematik, vol. 81, pp. 187-209, (1998).

[26] P.G. Ciarlet: The Finite Element Method for Elliptic Problems. North-Holland, Amsterdam, 1978.

[27] P. Clément: *Approximation by finite element functions using local regularisation*. RAIRO. Analise Numérique, vol. 9, pp. 77-84, (1975).

[28] A. Cohen: *Wavelet Methods in Numerical Analysis*. In: Handbook of Numerical Analysis, edited by P.G. Ciarlet and J.L. Lions, vol. VII, 1999, North-Holland, Amsterdam.

[29] A. Cohen, I. Daubechies and F. Feauveau: *Biorthogonal bases of compactly supported wavelets*. Communications on Pure and Applied Mathematics, vol. 45, pp. 485-560, (1992).

[30] J. Douglas and J. Wan: *An absolutely stabilized finite element method for the Stokes problem*. Mathematics of Computation, vol. 52, 186, pp. 495-508, (1989).

[31] A. Ern and J.-L. Guermond: Theory and Practice of Finite Element. Springer-Verlag, 2004.

[32] L.P. Franca: New Mixed Finite Element Methods. Ph.D. Thesis, Stanford University, 1987.

[33] L.P. Franca and T.J.R. Hughes: *Two classes of finite element methods*. Computer Methods in Applied Mechanics and Engineering, vol. 69, pp. 89-129, (1988).

[34] L.P. Franca and R. Stenberg: *Error analysis of Galerkin least squares methods for the elasticity equations*. SIAM Journal on Numerical Analysis, vol. 28, 6, pp. 1680-1697, (1991).

[35] G.N. Gatica: *A note on the efficiency of residual-based a-posteriori error estimators for some mixed finite element methods*. Electronic Transactions on Numerical Analysis, vol. 17, pp. 218-233, (2004).

[36] G.N. Gatica: *Analysis of a new augmented mixed finite element method for linear elasticity allowing* $\mathbb{R}T_0$-$\mathbb{P}_1$-$\mathbb{P}_0$ *approximations*. Mathematical Modelling and Numerical Analysis, to appear.

[37] G.N. Gatica, L.F. Gatica, E.P. Stephan: *A dual-mixed finite element method for nonlinear incompressible elasticity with mixed boundary conditions*. Submitted, Preprint 2005-06, Departamento de Ingeniería Matemática, Universidad de Concepción, (2005).

[38] G.N. Gatica and M. Maischak: *A-posteriori error estimates for the mixed finite element method with Lagrange multipliers*. Numerical Methods for Partial Differential Equations, vol. 21, 3, pp. 421-450, (2005).

[39] V. Girault, and P.-A. Raviart: Finite Element Methods for Navier-Stokes Equations. Theory and Algorithms. Springer Verlag, 1986.

[40] N. Heuer: Private communication.

[41] B. Jiang: The Least-Squares Finite Element Method. Springer Verlag, 1998.

[42] G. Leborgne: *An optimally consistent stabilization of the inf-sup condition*. Numerische Mathematik, vol. 91, 1, pp. 35-56, (2005).

[43] R. Masson: *Biorthogonal spline wavelets on the interval for the resolution of boundary problems*. Mathematical Models and Methods In Applied Sciences, vol. 6, 6, pp. 749-791, (1996).

[44] A. Masud and T.J.R. Hughes: *A stabilized mixed finite element method for Darcy flow*. Computer Methods in Applied Mechanics and Engineering, vol. 191, pp. 4341-4370, (2002).

[45] P. Oswald: Multilevel Finite Element Approximation, Theory and Applications. B. G. Teubner Stuttgart, 1994.

[46] P.A. Raviart and J.-M. Thomas: Introduction à L'Analyse Numérique des Equations aux Dérivées Partielles. Masson, 1992.

[47] J.E. Roberts and J.-M. Thomas: *Mixed and Hybrid Methods*. In: Handbook of Numerical Analysis, edited by P.G. Ciarlet and J.L. Lions, vol. II, Finite Element Methods (Part 1), 1991, North-Holland, Amsterdam.

[48] A. Stroud: Approximate Calculation of Multiple Integrals. Prentice-Hall, Englewood Cliffs, (1971).

[49] R. Verfürth: *A posteriori error estimation and adaptive mesh-refinement techniques*. Journal of Computational and Applied Mathematics, vol. 50, pp. 67-83, (1994).

[50] R. Verfürth: A Review of A Posteriori Error Estimation and Adaptive Mesh-Refinement Techniques. Wiley-Teubner (Chichester), 1996.